Nuclear Safety
NEA/CSNI/R(2021)13
June 2024
www.oecd-nea.org

NEA Leak-Before-Break Benchmark Phase 1 Final Report

OECD
BETTER POLICIES FOR BETTER LIVES

NEA
NUCLEAR ENERGY AGENCY

Nuclear Energy Agency

NEA/CSNI/R(2021)13

Unclassified English text only

19 June 2024

NUCLEAR ENERGY AGENCY
COMMITTEE ON THE SAFETY OF NUCLEAR INSTALLATIONS

NEA Leak-Before-Break Benchmark Phase 1 Final Report

This document is available in PDF format only.

JT03546478

ORGANISATION FOR ECONOMIC CO-OPERATION AND DEVELOPMENT

The OECD is a unique forum where the governments of 38 democracies work together to address the economic, social and environmental challenges of globalisation. The OECD is also at the forefront of efforts to understand and to help governments respond to new developments and concerns, such as corporate governance, the information economy and the challenges of an ageing population. The Organisation provides a setting where governments can compare policy experiences, seek answers to common problems, identify good practice and work to co-ordinate domestic and international policies.

The OECD member countries are: Australia, Austria, Belgium, Canada, Chile, Colombia, Costa Rica, Czechia, Denmark, Estonia, Finland, France, Germany, Greece, Hungary, Iceland, Ireland, Israel, Italy, Japan, Korea, Latvia, Lithuania, Luxembourg, Mexico, the Netherlands, New Zealand, Norway, Poland, Portugal, the Slovak Republic, Slovenia, Spain, Sweden, Switzerland, Türkiye, the United Kingdom and the United States. The European Commission takes part in the work of the OECD.

OECD Publishing disseminates widely the results of the Organisation's statistics gathering and research on economic, social and environmental issues, as well as the conventions, guidelines and standards agreed by its members.

NUCLEAR ENERGY AGENCY

The OECD Nuclear Energy Agency (NEA) was established on 1 February 1958. Current NEA membership consists of 34 countries: Argentina, Australia, Austria, Belgium, Bulgaria, Canada, Czechia, Denmark, Finland, France, Germany, Greece, Hungary, Iceland, Ireland, Italy, Japan, Korea, Luxembourg, Mexico, the Netherlands, Norway, Poland, Portugal, Romania, Russia (suspended), the Slovak Republic, Slovenia, Spain, Sweden, Switzerland, Türkiye, the United Kingdom and the United States. The European Commission and the International Atomic Energy Agency also take part in the work of the Agency.

The mission of the NEA is:

– to assist its member countries in maintaining and further developing, through international co-operation, the scientific, technological and legal bases required for a safe, environmentally sound and economical use of nuclear energy for peaceful purposes;

– to provide authoritative assessments and to forge common understandings on key issues as input to government decisions on nuclear energy policy and to broader OECD analyses in areas such as energy and the sustainable development of low-carbon economies.

Specific areas of competence of the NEA include the safety and regulation of nuclear activities, radioactive waste management and decommissioning, radiological protection, nuclear science, economic and technical analyses of the nuclear fuel cycle, nuclear law and liability, and public information. The NEA Data Bank provides nuclear data and computer program services for participating countries.

Committee on the Safety of Nuclear Installations

The Committee on the Safety of Nuclear Installations (CSNI) addresses NEA programmes and activities that support maintaining and advancing the scientific and technical knowledge base of the safety of nuclear installations.

The Committee constitutes a forum for the exchange of technical information and for collaboration between organisations, which can contribute, from their respective backgrounds in research, development and engineering, to its activities. It has regard to the exchange of information between member countries and safety R&D programmes of various sizes in order to keep all member countries involved in and abreast of developments in technical safety matters.

The Committee reviews the state of knowledge on important topics of nuclear safety science and techniques and of safety assessments and ensures that operating experience is appropriately accounted for in its activities. It initiates and conducts programmes identified by these reviews and assessments in order to confirm safety, overcome discrepancies, develop improvements and reach consensus on technical issues of common interest. It promotes the co-ordination of work in different member countries that serve to maintain and enhance competence in nuclear safety matters, including the establishment of joint undertakings (e.g. joint research and data projects), and assists in the feedback of the results to participating organisations. The Committee ensures that valuable end-products of the technical reviews and analyses are provided to members in a timely manner, and made publicly available when appropriate, to support broader nuclear safety.

The Committee focuses primarily on the safety aspects of existing power reactors, other nuclear installations and new power reactors; it also considers the safety implications of scientific and technical developments of future reactor technologies and designs. Further, the scope for the Committee includes human and organisational research activities and technical developments that affect nuclear safety.

Acknowledgements

This report would not have been possible without the contributions of the benchmark participants. They helped develop the benchmark problems, conducted the requested analyses, performed additional sensitivity analyses on their own, documented their results, and helped to author and review this manuscript. Their contributions are greatly appreciated.

The benchmark participants thankfully acknowledge the initiative and co-ordination by Robert Tregoning of the NRC, who enabled the thorough comparison of the contributions and the creation of this report. Recognition is also due to Björn Brickstad, formerly of the Swedish Radiation Safety Authority (SSM), for helping in initially conceiving and structuring the benchmark problems. The benchmark would not have been undertaken without his contributions, but unfortunately he retired before he could perform the analyses. A special debt of gratitude is owed to Jay Wallace, who provided an invaluable contribution to understanding trends in the participants' results and was instrumental in elevating the quality of the report through his exhaustive reviews and corresponding edits and suggestions. Finally, Olli Nevander and Diego Escrig Forano are recognised for their contribution as Secretariat for the Nuclear Energy Agency (NEA) Committee on the Safety of Nuclear Installations (CSNI) Working Group on Integrity and Ageing of Components and Structures (WGIAGE). They helped ensure that projects ran smoothly and deliverables were completed on time.

This report was approved by the CSNI on 3 June 2021 and prepared for publication by the NEA Secretariat.

Leading authors

Robert TREGONING	Nuclear Regulatory Commission, United States

Principal benchmark participants

Afaf BOUYDO	Tractebel
Oriol COSTA-GARRIDO	Jozef Stefan Institute (on assignment to the Paul Scherrer Institute [PSI] during the benchmark)
Peter DILLSTRÖM	Kiwa Inspecta Technology (KIWA)
Xinjian DUAN	Candu Energy Inc. (CEI)
B. GHOSH	Bhabha Atomic Research Centre (BARC)
Klaus HECKMANN	Gesellschaft für Anlagen- und Reaktorsicherheit (GRS)
Sun-Yeh KANG	Korea Electric Power Corporation (KEPCO E&C)
Yeji KIM	Korea Institute of Nuclear Safety (KINS)
Yong-Beum KIM	Korea Institute of Nuclear Safety (KINS)
Suranjit KUMAR	Bhabha Atomic Research Centre (BARC)

Elizabeth KURTH	Engineering Mechanics Corporation of Columbus (EMCC)
Juha KUUTTI	VTT Technical Research Centre of Finland (VTT)
Valery LACROIX	Tractebel
Young-Jin OH	Korea Electric Power Corporation (KEPCO E&C)
Akihiro MANO	Japan Atomic Energy Agency (JAEA)
D. MUKHOPADHYAY	Bhabha Atomic Research Centre (BARC)
Pavel SAMOHYL	ÚJV Řež (UJV)
Andrey SHIPSHA	Kiwa Inspecta Technology (KIWA)
P.K. SINGH	Bhabha Atomic Research Centre (BARC)
Antti TIMPERI	VTT Technical Research Centre of Finland (VTT)
Mohammed UDDIN	Engineering Mechanics Corporation of Columbus (EMCC)
Petter VON UNGE	Kiwa Inspecta Technology (KIWA)
Jay WALLACE	US Nuclear Regulatory Commission (NRC)
Songyan YANG	Ontario Power Generation (OPG)

Table of contents

Tables

Figures

List of abbreviations and acronyms

AF	Air fatigue
ASME	American Society of Mechanical Engineers
B	Base metal properties
BARC	Bhabha Atomic Research Centre (India)
CAPS	CSNI Activity Proposal Sheet (NEA)
CBM	Critical bending moment
CCS	Critical crack size
CEI	Candu Energy Inc.
CF	Corrosion fatigue
CFP	Crack face pressure
CNSC	Canadian Nuclear Safety Commission
COA	Crack opening area
COD	Crack opening displacement
CSNI	Committee for the Safety of Nuclear Installations (NEA)
DBE	Design basis earthquake
DLL	Dynamic link library
DMW	Dissimilar metal weld
ECCS	Emergency core cooling system
EMCC	Engineering Mechanics Corporation of Columbus
EPFM	Elastic-plastic fracture mechanics
EPRI	Electric Power Research Institute
FAC	Flow accelerated corrosion
FAD	Failure assessment diagram
FE	Finite element
FEA	Finite element analysis
FF	Friction factor
FULLP	Full pressure
GE/EPRI	General Electric/Electric Power Research Institute
GPM	Gallons per minute
GRS	Gesellschaft für Anlagen- und Reaktorsicherheit (Germany)
ICOD	COD at piping inner diameter
ID	Inner diameter
JAEA	Japan Atomic Energy Agency
JSME	The Japan Society of Mechanical Engineers

KEPCO E&C	Korea Electric Power Corporation Engineering and Construction Company
KINS	Korea Institute of Nuclear Safety
KIWA	Kiwa Inspecta Technology
KSRG	Korean Safety Review Guide
LBB	Leak-before-break
LCS	Leakage crack size
LDC	Loss discharge coefficient
LDL	Leak detection limit
LR	Leak rate
LRDL	Leak rate detection limit
LWR	Light water reactor
M	Mixture base/weld metal properties
MW	Mid-wall
MWCOD	COD at the mid-thickness (or mid-wall) of the pipe
NEA	Nuclear Energy Agency
NDE	Non-destructive examination
NO	Normal operations
NPS	Nominal pipe size
NRC	Nuclear Regulatory Commission (United States)
NSC	Net-section collapse
NUREG	Nuclear Regulatory Commission Nuclear Regulatory Report (United States)
OCOD	COD at piping outer diameter
OD	Outer diameter
OECD	Organisation for Economic Co-operation and Development
OPG	Ontario Power Generation
PICEP	Pipe Crack Evaluation Program
PLL	Plastic limit load
PSI	Paul Scherrer Institute (Switzerland)
PWR	Pressurised water reactors
PWSCC	Primary water stress corrosion cracking
RCS	Reference crack size
REDP	Reduced pressure
RG	Regulatory Guide
RM	Required margin
SAM	Seismic anchor motion
SCC	Stress corrosion cracking
SIC	Strain-induced corrosion

SIF	Stress intensity factor
SLB	Steam line break
SRP	Standard Review Plan
SSE	Safe shutdown earthquake
SSM	Swedish Radiation Safety Authority
STUK	Radiation and Nuclear Safety Authority (Finland)
TWC	Through-wall circumferential crack
UJV	ÚJV Řež, a. s. (Czechia)
VTT	VTT Technical Research Centre of Finland
W	Weld metal properties
w	with
WGIAGE	Working Group on Integrity and Ageing of Components and Structures (NEA CSNI)
wo	without
WRS	Weld residual stress
xFEM	Extended finite element method

Executive summary

The objective of this leak-before-break (LBB) benchmark was to compare the results from different LBB analyses among participating countries using common inputs, and to identify the effects of weld residual stress (WRS) and crack morphology on crack opening displacement (COD) and leak rate (LR) calculations in LBB analyses. The benchmark consisted of a baseline problem that was developed so that it would marginally pass the US Nuclear Regulatory Commission (NRC) NUREG-0800 Standard Review Plan (SRP) 3.6.3 (NRC, 2007) acceptance criteria for the piping configuration, assumptions and inputs considered. Participants were asked to evaluate the baseline problem using their own country's LBB requirements. Four additional tasks evaluating the effects of different crack morphologies and WRS were defined with the same piping configuration and loading conditions as the benchmark problem, but for a prescribed crack length.

Participants from 14 organisations, representing 11 countries, performed the benchmark exercise. Each participant provided a high-level summary of the LBB requirements in their country and documented the computational codes and approaches that they used in their evaluations. The participants determined whether the baseline problem would meet their country's LBB acceptance criteria and provided supporting information. This information included the leak rate detection limit (LRDL), the LR used to determine the leakage crack size (LCS), the LCS value and the critical crack size (CCS).

The high-level summary of the LBB requirements in each of the participating countries revealed that the basic tenets and underlying principles of the LBB philosophy among the countries are generally consistent. Most countries' procedures are rooted in NRC SRP 3.6.3, but virtually every country has modified either the analysis or the acceptance procedure based on additional knowledge that has been gained since the establishment of NRC SRP 3.6.3. Some of the more common modifications include explicitly allowing a lower LRDL, allowing a lower LRDL margin, requiring an additional subcritical cracking analysis to demonstrate that LBB or inspection intervals are not challenged, and requiring that worst-case strength and toughness properties are chosen from the base and weld metal properties. These modifications represent a natural progression of both technical and operational knowledge since the NRC SRP 3.6.3 was first established.

The baseline problem achieved its initial objective of being "marginal" because eight participants indicated that it is "not acceptable" for LBB, while six participants indicated that it "is acceptable" for LBB. The principal factors in determining whether the baseline problem met the respective countries' LBB acceptance requirements were as follows: the choice of the material properties used to determine the CCS; the assumed crack type and its associated morphology; and the LRDL used to determine the LCS. A secondary consideration was the type of failure model (i.e. net-section collapse [NSC], failure assessment diagram [FAD] or elastic-plastic fracture mechanics [EPFM]) used in the crack stability analysis. Figure 1 summarises the CCS and LCS values from the LBB evaluations for each participant. The failure model and material properties assumed (i.e. "B"ase metal, "W"eld metal, or "M"ixed) by each participant are also indicated in the figure.

The effects of crack morphology and WRS were systematically evaluated in Tasks 1-4 and the participants were asked to provide the COD, critical bending moment (CBM) and the associated LR for the prescribed crack, geometry and loading. As observed in the baseline problem, differences among the participants' CBM predictions were principally due to the material property choice (i.e. weld, base or mixture), while the type of failure model chosen (i.e. NSC, FAD or EPFM) contributed much less to the differences. Most of the differences

in the LR predictions were directly attributable to differences in the COD models, but a small portion was attributable to the inclusion of crack face pressure (CFP). The small differences in the LR predictions that may be directly attributed to the LR codes implies that the differences in how these specific codes model the relationship between LR and COD might not be significant, or at least for the fixed crack morphology and length that is evaluated here.

Changing the crack morphology from corrosion fatigue (CF) to primary water stress corrosion cracking (PWSCC) decreased the predicted LRs for the specified crack size, with all participants reporting lower LR for the PWSCC morphology. There was much more variability in the LR predictions for the PWSCC morphology compared to those for the CF morphology, and much of the additional variability could be directly correlated with the choice to incorporate CFP; those participants that did not consider CFP typically predicted a greater reduction in LR from the PWSCC crack morphology than those participants that included CFP.

Incorporating the prescribed WRS distribution also had an impact on the predicted COD and LR results. Several participants predicted that WRS resulted in a relatively modest 20% change in LR for the CF morphology, while other participants predicted more significant differences. In general, participants found the smallest LR for PWSCC morphology was when the WRS effect on the COD was included.

The current benchmark identified several additional aspects of a deterministic LBB analysis that are important for when a more realistic LBB evaluation is sought. Several countries allow lower LRDL limits or lower LRDL margins than the values that have been historically used in the United States' LBB applications, which could be justified based on the performance and redundancy of leak detection systems. Realism would also be improved by postulating that cracks be at the most susceptible location within the weld joint, as well as using the appropriate material properties, crack type and associated crack morphology to determine the LCS and CCS at that location. A more accurate consideration of both WRS and CFP is further necessary to improve the accuracy of the LCS estimations. The accuracy of the CCS prediction can only be marginally improved by using EPFM crack stability models. Several countries additionally require a calculation of the time for the LCS to grow to the CCS to ensure that there is sufficient time for operator action.

The variety and potential importance of the issues discussed above to the achievement of a more accurate LBB evaluation also underscore the importance of considering sensitivity analyses as either part of or in support of, the required LBB analyses. Sensitivity analyses can elucidate the important variables associated with the specific piping configuration, materials and loading combination and thus provide a clearer indication of the analysis margins. Guidance on and the use of sensitivity studies could improve the consistency and rigour of a LBB analysis. Finally, a follow-on benchmarking effort will be conducted to further explore LBB evaluations and assess topics that could be addressed in more realistic LBB evaluations. Specifically, the effects of pipe size, weld residual stress, end restraint and piping compliance will be studied, along with an assessment of the possible role of subcritical crack growth within LBB evaluations.

Figure 1. Summary of the CCS and LCS values from LBB evaluations

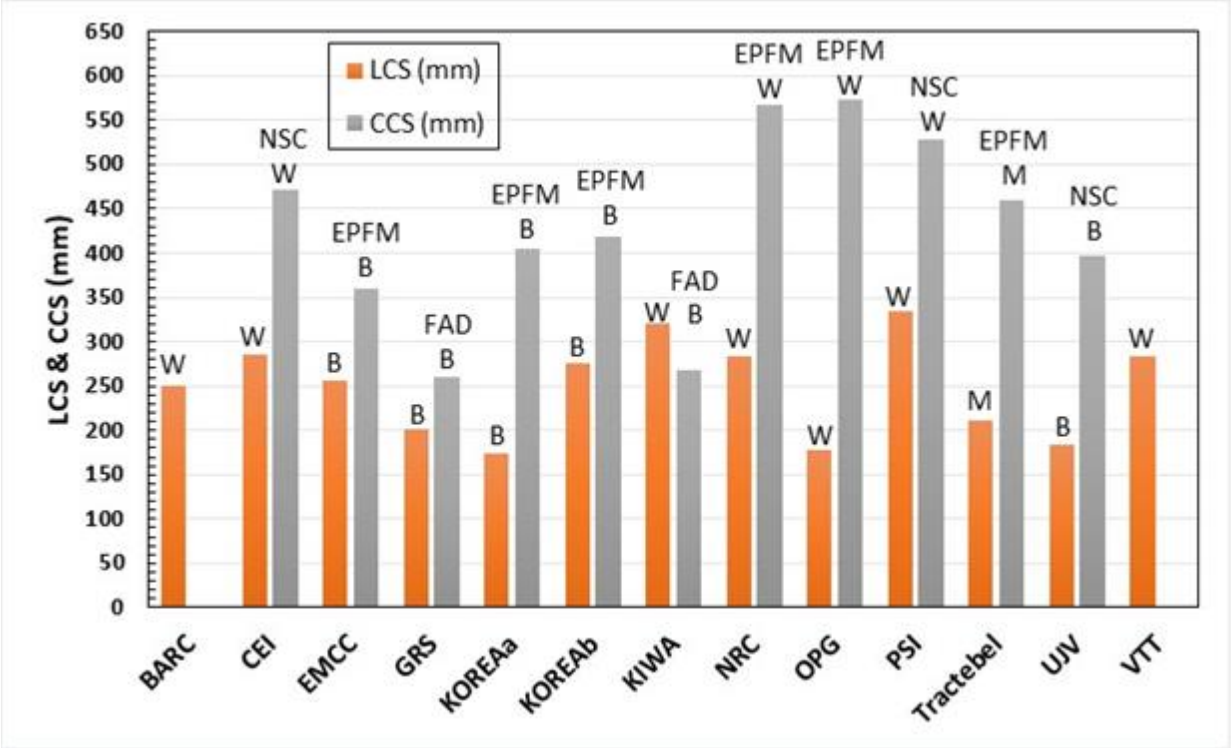

1. Introduction and background

In 2010, the metals subgroup of the NEA Working Group on Integrity and Ageing of Components and Structures (WGIAGE) launched a Committee for the Safety of Nuclear Installations (CSNI) Activity Proposal Sheet (CAPS) activity on leak-before-break (LBB) research. The first phase of this activity entailed conducting a survey on LBB practices in CSNI participating countries. The survey was conducted using a questionnaire with 15 questions. The questions fell into three topic areas associated with LBB: the regulatory framework, research activities and knowledge gaps. The survey also gauged the level of interest in potential collaborative research opportunities. Questions related to collaborative research opportunities asked respondents for their interest in sharing information and conducting collaborative research in both deterministic and probabilistic approaches for evaluating LBB. The results of this survey are published as a WGIAGE working group report [1].

The survey results identified possible topic areas for a follow-on CAPS. These areas were discussed by the WGIAGE members with the aim of more clearly articulating possible follow-on activities. The idea that garnered the most support was conducting a series of benchmark analyses of test cases using the LBB approach utilised in each participant's country. The results of the benchmark analyses would be used to evaluate the differences in the approaches as well as the effects of analysis choices or prominent assumptions about the margins predicted for each test case.

This idea was further refined and a CAPS was developed and co-led by the United States (US Nuclear Regulatory Commission [NRC]) and Sweden (the Swedish Radiation Safety Authority [SSM]). The CAPS was approved by CSNI in 2016. After the CAPS was approved, the co-leads refined the benchmark objectives and developed proposed benchmark problems and approaches. This proposal was presented during the 2017 WGIAGE metals subgroup meeting. The following benchmark objectives were then finalised:

- to compare the results from different LBB analyses among participating countries using common inputs;
- to identify the effects of weld residual stress (WRS) on crack opening displacement (COD) and the effect of crack morphology on leak rate (LR) calculations in LBB analyses.

Following the meeting in 2017, the co-leads created a document describing the LBB benchmark problems and analyses to be conducted, which was circulated among interested participants to review and comment on. The benchmark description was presented and accepted during the 2018 WGIAGE metals subgroup meeting. The benchmark consisted of a baseline problem, which asked participants to perform a LBB evaluation on the piping weld joint using their country's requirements, and four additional problems (Tasks 1-4), which addressed the influence of crack morphology and WRS on LR and crack stability for a fixed crack size.

The NRC developed the initial input parameters needed for a United States LBB evaluation, which was performed following the NRC Nuclear Regulatory Report (NUREG)-0800 Revision 1 Standard Review Plan Section 3.6.3 [2] for the baseline problem, as well as the inputs needed for Tasks 1-4. Participants were asked to identify additional inputs needed to perform a LBB evaluation as per their country's requirements. The NRC then developed the final input parameters to be used for the benchmark problems and identified the outputs

requested from each participant. The NRC also created a spreadsheet template containing the input parameters and requested output information that was provided to each participant in order to unify each participant's reporting.

Calculations were carried out by the participants from November 2018 until August 2019. The benchmark description document was modified a few times during this time to further clarify the problem statement and requested outputs. Ultimately, the following 14 organisations representing 11 countries participated in the benchmark exercise: the Bhabha Atomic Research Centre (BARC), India; Candu Energy Inc. (CEI), Canada; the Engineering Mechanics Corporation of Columbus (EMCC), United States; Gesellschaft für Anlagen- und Reaktorsicherheit (GRS), Germany; Japan Atomic Energy Agency (JAEA), Japan; the Korea Electric Power Corporation Energy and Construction Company (KEPCO E&C), Korea; the Korea Institute of Nuclear Safety (KINS), Korea; Kiwa Inspecta Technology (KIWA), Sweden; US Nuclear Regulatory Commission (NRC), United States; the Ontario Power Generation (OPG), Canada; the Paul Scherrer Institut (PSI), Switzerland; Tractebel, Belgium; ÚJV Řež, a. s. (UJV), Czechia; and the VTT Technical Research Centre of Finland (VTT), Finland.

Section 2 of this report provides the overview and approach used to develop this benchmark. The LBB approach and requirements applicable for each participating country are summarised in Section 3. Section 4 provides more detail on the baseline and Task 1-4 problems that were solved by each participant. The approach used by each participant (Section 5) and the subsequent results (Section 6) for the baseline problem are then discussed. Each participant's approach and the subsequent results for Tasks 1-4 are summarised in Sections 7 and 8, respectively. Finally, conclusions from the benchmark (Section 9) and a summary of important LBB considerations and recommendations for follow-on work (Section 10) are provided.

2. Benchmark overview and approach

The benchmark consisted of a baseline problem and four additional problems to be evaluated in Tasks 1-4 respectively.

2.1. Baseline problem

The baseline problem required each participant to evaluate leak-before-break (LBB) in a surge line pipe containing a circumferential crack located at the weld centreline. Each participant was asked to perform their evaluation according to the methods, requirements and acceptance criteria that are applicable within their country. As indicated previously, participants identified the input parameters needed for their country's analysis method. The US Nuclear Regulatory Commission (NRC) provided a common set of inputs for this calculation, including the weld and pipe geometry, operating temperature, required normal operation (NO) and safe shutdown earthquake (SSE) loads, crack morphology, base metal and weld material properties and leak rate detection limit (LRDL). The NO + SSE loads were assumed to be the bounding transient loads. The NRC developed input parameters so that this baseline problem could meet the acceptance criteria specified in the NRC's Standard Review Plan (SRP) 3.6.3 [2].

Each participant then used these common inputs to determine if this location meets or fails the LBB acceptance criteria under their country's regulations. Each participant was asked to briefly describe their country's LBB procedures and acceptance criteria, report the calculated results and compare these results with the governing acceptance criteria (i.e. the allowable crack size and load margins). More detail on the benchmark problem is provided in Section 4.

2.2. Task 1 – 4 problems

Each participant performed a series of four specific evaluations to identify the effects of crack morphology and the effects of weld residual stress (WRS) on the calculated leak rate (LR) and crack stability. The same surge line and weld joint geometry, weld and base metal properties, operating temperature, and NO loads specified for the baseline problem were used in these tasks. A common through-wall circumferential crack (TWC) at the weld centreline was also specified for all tasks. Participants were asked to calculate the LR and crack stability for Task 1 while assuming there was corrosion fatigue (CF) crack morphology and no WRS. Participants were asked to calculate the LR and crack stability in Task 2 for the CF crack morphology with an axial WRS distribution that was representative of a dissimilar metal surge line weld. Tasks 3 and 4 evaluated the LR for the same crack with a primary water stress corrosion (PWSCC) crack morphology, which was both without WRS (Task 3) and with WRS (Task 4). The morphology and WRS parameters were provided by the NRC. More detail on the Task 1 – 4 problems is provided in Section 4.

3. LBB requirements

This section summarises the leak-before-break (LBB) requirements in each country. A brief description is provided of the approach and evaluation requirements. The required calculations, or results, are also identified, along with the associated acceptance criteria. Further detail can be found in the references provided by each country. More comprehensive summaries of LBB requirements in several countries can also be found in [3, 4 and 5]. The participants that followed these requirements are indicated within parenthesis at each subheading.

3.1. United States (EMCC and NRC)

As indicated previously, the United States typically adheres to the Standard Review Plan (SRP) 3.6.3 for evaluating LBB submittals [2]. A screening review is first conducted to ensure that the piping system being considered for LBB will have a low failure likelihood due to erosion; erosion/ corrosion; erosion/ cavitation; corrosion; creep; creep/ fatigue; water hammer; brittle rupture; stress corrosion cracking; fatigue cracking; and indirect failures during the plant's entire life. The adequacy of the leak detection system is next verified using Regulatory Guide (RG) 1.45, "Reactor Coolant Pressure Boundary Leakage Detection Systems" [6], or by alternatively approved leak detection specifications and capabilities.

A deterministic fracture mechanics and leak rate (LR) evaluation is then performed. The evaluation first determines the size of a through-wall circumferential crack (TWC) (i.e. the leakage crack size) under normal operation (NO) loading that will produce an LR that is 10 times greater than the leak rate detection limit (LRDL) for the assumed crack morphology. Next, the crack size at the onset of instability is determined for NO + safe shutdown earthquake (SSE) loading (i.e. the critical crack size). The crack stability analysis can use a modified limit load approach (for stainless steel piping and stainless steel or nickel-based welds) or a fracture mechanics evaluation as prescribed in NUREG-1061, Vol. 3 [7].

For a piping system to be approved for LBB, the evaluation must demonstrate a margin of at least 2 between the leakage crack size (LCS) and critical crack size (CCS). Additionally, it must be demonstrated that the LCS will not become unstable under NO + SSE loading with an appropriate load margin. A load margin of 1.4 is used if deadweight, thermal expansion, pressure, seismic inertial and seismic anchor motion (SAM) loads are algebraically combined. A load margin of 1.0 is used if deadweight, thermal expansion, pressure, seismic inertial and SAM loads are combined using absolute values.

3.2. Belgium (Tractebel)

The LBB concept has not been used in the design of the seven pressurised water reactors (PWRs) currently operating in Belgium. The design basis of these plants required the consideration of dynamic effects associated with postulated ruptures in the high energy piping. The limited application of LBB to the primary coolant loop in existing plants was approved in the 1990s by the Belgian safety authorities.

The LBB analyses are based on United States' documents and methods, including the requirements of SRP 3.6.3 [2] (see Section 3a). In addition to the SRP 3.6.3 requirements, the Belgian safety authorities impose additional requirements [8 and 9]. Belgium is a low seismic region and therefore earthquake loads are not significant and the steam line break

(SLB), for example, may produce much higher loads than NO + SSE at specific locations within the primary coolant piping. The Belgian safety authorities therefore require that this loading be considered in addition to the loading from a rupture of the main primary-piping auxiliary lines (i.e. the pressuriser surge line, emergency core cooling system [ECCS], line from the accumulators and shutdown cooling line).

The Belgian safety authorities want to ensure that the application of LBB does not reduce the protection against some design basis events that were not analysed in detail because they were enveloped by the postulated double-ended guillotine breaks of the primary loop piping. In particular, the Belgian safety authorities require that the following additional breaks be considered in the design basis of the reactor core and internals, as well as for the steam generator tube bundle:

- rapid rupture (1 ms) of the steam generator manway cover (hot leg or cold leg);
- slow break (3 s) that leads to a break size equivalent to the inner piping diameter, anywhere in the primary coolant piping.

Regarding the adequacy of the leak detection systems, each unit contains several redundant systems that can detect a 1 gallon per minute (GPM) ($\approx$ 0.06 kg/s) leak in under an hour, which fulfils the RG's 1.45 provisions. Some systems are much more sensitive if a longer detection period is allowed such as a period of a few hours or a day. In this case, the LRDL could be as low as 0.2 to 0.3 GPM. Conservatively, a 0.5 GPM ($\approx$ 0.03 kg/s) LRDL was justified and used in the LBB evaluations performed for Belgium plants to determine the LCS under NO loading conditions.

3.3. Canada (CEI and OPG)

The high-level requirements for an LBB assessment for designing a new nuclear power plant in Canada are described in the Canadian Nuclear Safety Commission's (CNSC's) regulatory document REGDOC-2.5.2 [10]:

> *A qualified leak-before-break (LBB) system design will permit the design authority to optimize protective hardware – such as pipe whip restraints and jet impingement barriers – and to redesign pipe-connected components, their supports and their internals.*
>
> *A qualified LBB methodology should include the following:*
>
> - *LBB should be only applied to high-energy, American Society of Mechanical Engineers (ASME) Code Class 1 or 2 piping or the equivalent. Applications to other high-energy piping may be performed based on an evaluation of the proposed design and in-service inspection requirements.*
> - *No uncontrolled active degradation mechanism should exist in the piping system to be qualified for LBB.*
> - *An evaluation of phenomena such as water hammer, creep damage, flow accelerated corrosion and fatigue should be performed to cover the entire life of the high-energy piping systems. To demonstrate that water hammer is not a significant contributor to pipe rupture, reliance on historical frequencies of water hammer events in specific piping systems coupled with reviews of operating procedures and conditions may be used for this evaluation.*
> - *Leak detection methods for the reactor coolant should ensure that adequate detection margins exist for the postulated TWC used in the deterministic*

fracture mechanics evaluation. The margins should cover uncertainties in the determination of leakage from a piping system.

- *Stress analyses of the piping that is considered for LBB should be in accordance with the requirements of Section III of the ASME code or equivalent.*
- *The LBB evaluation should use design basis loads and, after construction, be updated to use the as-built piping configuration, as opposed to the design configuration.*
- *The methodology should take account of potential for degradation by erosion, corrosion, and erosion-cavitation due to unfavourable flow conditions and water chemistry.*
- *The methodology should take account of material susceptibility to corrosion, the potential for high residual stresses, and environmental conditions that could lead to degradation by stress corrosion cracking.*

The detailed LBB evaluations generally follow the SRP 3.6.3 and NUREG-1061 Volume 3 for high-level guidance on LBB assessment and are accepted by CNSC on a case-by-case basis. For a piping system to meet the LBB requirements, the evaluation must demonstrate a margin of at least 2 between the LCS and CCS. It must additionally be demonstrated that the LCS will not become unstable under NO + design basis earthquake (DBE) loading with an appropriate load margin.[1] A load margin of 1.4 is used if deadweight, thermal expansion, pressure, seismic inertial and SAM loads are algebraically combined. A load margin of 1.0 is used if deadweight, thermal expansion, pressure, seismic inertial and SAM loads are combined using absolute values.

The LBB approach presented in REGDOC-2.5.2 has been used during the last decade to support the continued operation of some components that are susceptible to flow accelerated corrosion (FAC) or primary water stress corrosion cracking (PWSCC) [11 and 12] when it could be demonstrated that these degradation mechanisms were effectively controlled by licence ageing management programmes. Deterministic LBB may be supplemented by probabilistic assessments to explicitly address the uncertainties of some key inputs. An LR factor of 5 has been accepted by CNSC for Class 1 feeder piping [13] whose failure has a low impact on core damage frequency.

3.4. Czechia (UJV)

Czechia follows exactly the United States' approach for LBB evaluation as stipulated in the SRP 3.6.3 [2], RG 1.45 [6] and NUREG-1061, Vol. 3 [7]. The LBB requirements were issued by the former Czechoslovak Commission for Atomic Energy in 1991 as part of the general requirements for the preparation and contents of safety reports and their amendments [14]. There is only a slight deviation between Czechia's leak detection requirements [15] and the RG 1.45 in terms of the number of leak detection systems. Czechia requires three independent methods for detecting leaks and at least two of them must be available for use to quantify the leak rate. The third system is used to support leak rate quantification if the other two methods provide conflicting results.

[1] DBE is classified as level C event in Canadian standards. If water hammer is credible, the load will also be considered.

Some other high-level requirements for LBB application in Czechia are presented below:

- Leak-before-break is only typically applied to ASME Code Class 1 and 2 piping or the equivalent. Its application to other high energy piping systems is considered based on an evaluation of the proposed design and in-service inspection requirements compared with the ASME Class 1 and 2 requirements.
- The LBB evaluation uses design basis loads and is based on the as-built configuration as opposed to the design configuration.
- Degradation by erosion, erosion/ corrosion and erosion cavitation due to unfavourable flow conditions and water chemistry is examined. Evaluations must demonstrate that these mechanisms are not a potential source of pipe rupture.
- An assessment of potential indirect sources of pipe ruptures is required to demonstrate that the indirect failure mechanisms defined in the plant final safety analysis report (e.g. heavy component support failure) are remote causes of pipe rupture. Compliance with the snubber surveillance requirements ensures that snubber failure rates are acceptably low.
- It is determined that the piping material is not susceptible to brittle cleavage type failure over the full range of system operating temperatures (meaning the material is in the upper shelf).
- An evaluation is performed to demonstrate that the system does not have a history of fatigue cracking or failure and that fatigue failure is unlikely. This evaluation must address thermal, vibration and mechanically induced fatigue and demonstrate an adequate mixing of high and low temperature fluids.

3.5. Finland (VTT)

The LBB requirements applicable in Finland are contained in the Radiation and Nuclear Safety Authority (STUK) YVL guides. The piping-specific requirements contained in Regulatory Guide YVL E.4 [16] are as follows:

- The LBB analysis shall demonstrate, by fracture and fluid mechanics analysis, the safety margins required in the US Nuclear Regulatory Commission (NRC) Standard Review Plan 3.6.3 (Rev 1, 2007) for the CCS and the LCS.
- No failure mechanisms may be identified for the piping that could present a potential for its complete, instantaneous break.
- The LBB analysis shall be conducted with postulated TWCs in locations where the combination of stresses and the material properties given as input data is the least favourable.
- The CCS shall be determined for service conditions that cause the maximum local stress, considering all specified fast pressure transients and the design basis earthquake.
- For the determination of CCS and crack opening area for LR calculation, applicable elastic-plastic methods shall be used. If the crack is located near a weld which has significantly higher strength values than base material, the weld strength values shall be used to calculate the opening area. However, CCS shall then be based on the base material strength values.
- The LRDL shall be qualified by testing. If the value used in the LBB argumentation is below 3.8 litres per minute, the qualification shall be based on as-built plant

conditions. The method used for calculation of the LR shall have been qualified by applicable test results.

- Fatigue crack growth analysis needs to demonstrate that inner surface cracks in the most susceptible locations will not significantly grow during the service life of the piping.
- The regulatory body will review the analyses that comply with the regulatory guide and approve the methods used in the analyses. When required, the regulator will prescribe how to apply the requirements. The regulator will also assess the quality of the analyses and conducts reference analyses, if needed.

3.6. Germany (GRS)

German regulation addresses LBB within KTA 3206 [17], which provides requirements for the verification of break preclusion. Requirements related to the basic safety and integrity concepts must be initially satisfied prior to performing a fracture-mechanics-based LBB assessment. These requirements include demonstrating that the toughness of ferritic steels is sufficient and that the relevant damage mechanisms have been appropriately mitigated so that they do not significantly affect the structure integrity of the subject component.

The design and construction of the subject component should ensure that corrosive crack-forming damage mechanisms (e.g. stress corrosion cracking [SCC] or strain-induced corrosion [SIC]) are not active and significant vibration loads (e.g. steady-state vibrations and resonant vibrations) do not occur. Furthermore, the design, manufacture and operation of the system that contains the component should ensure that non-specified loading effects (especially short-time dynamic loadings such as water hammer or transient condensation shocks) do not occur. The effectiveness of the measures taken to preclude these issues are to be verified during the manufacturing, commissioning and operational stages.

If new knowledge related to the structural integrity of the component is obtained during operation, the impact of this new knowledge on the break preclusion requirements are to be assessed and additional measures adopted, if necessary, to mitigate the effects of this new knowledge. If this new knowledge pertains to the discovery of service-induced degradation or cracking, the causes of the effective damage mechanisms must be determined and eliminated, and new measures for meeting the break preclusion requirements established. The complete requirements that are to be satisfied before the fracture mechanics analysis are found in KTA 3206 in Chapters 3 and 4 [17].

The subsequent fracture-mechanical analysis is governed by Annex A of KTA 3206 [17]. It consists of the following seven steps:

1. Postulate an initial semi-elliptical crack of a specific size that could be undetected prior to operation.
2. Calculate the growth of the crack depth and crack length during the component's operation.
3. Calculate the critical crack length for a TWC assuming NO loads as well as specific accident conditions.
4. Calculate the critical crack depth for the length of the semi-elliptical crack grown in step 2 assuming NO loads as well as specific accident conditions.
5. Compute the TWC length (i.e. LCS) corresponding to the LR that requires intervention measures to be taken as specified in the plant operation manual. In this

step, the leak opening area must be underestimated, while frictional pressure losses must be overestimated in order to obtain a conservative result.

6. Calculate the acceptable crack length by subtracting the critical crack length (step 3) from the amount of crack growth that could occur during one inspection interval under NO loads. Calculate the acceptable crack depth as the minimum of the critical crack depth (step 4) and 75% of the piping wall thickness. Then, compare both the depth and length of the grown crack at the end of operation (step 2) with the acceptable crack depth and length from this step to ensure that the operational crack depth and length (step 2) are less than the acceptable crack depth and length (step 6).
7. Compare the crack length at the LCS (step 5) with the acceptable crack length (step 6) to ensure that the crack length at the LCS is smaller. If this is not the case, the effect of in-service inspections can be considered for excluding any leak by limiting the possible crack depth.

The safety assessment of the pipe is successful if the acceptance criteria in steps 6 and 7 are met.

3.7. India (BARC)

Three assessment levels must be met to satisfy LBB requirements in India and demonstrate that a sudden double-ended guillotine break within the piping system is not credible. In the first assessment level, it must be demonstrated that there is an adequate design margin against all the potential failures modes, the piping material is sufficiently ductile and tough, and the piping is free from unacceptably sized cracks. Adequacy is demonstrated, in part, by adhering to standard design codes, such as ASME Section III.

The next two assessment levels conduct a LBB evaluation that follows US and international assessment procedure guidance [7 and 18]. In the second assessment level, a credible sized part-through surface flaw is postulated at the inner diameter of the piping system. A flaw within a weld is typically postulated. The postulated surface flaw depth is ¼ of the piping thickness, with a surface length to depth ratio of six to one. This crack size is chosen to represent the largest flaw that may be reasonably expected to escape detection during pre-service inspection. Then, fatigue crack growth resulting from NO service loads is assessed over the entire reactor lifetime to ensure that this crack will not grow to a size where breakage could occur before a leak is detected. It has been determined from primary heavy-water reactor operating experience that fatigue is the only degradation mechanism that cannot be ruled out within the primary heat transport piping system.

Finally, the third assessment level, postulates, as a worst-case assumption, a TWC length (i.e. the LCS) so that leakage can be detected under NO loads. The TWC is evaluated at the locations where the worst combination of NO + SSE stresses and fracture toughness is expected. The LR for determining the LCS is ten times greater than the LRDL, as required in SRP 3.6.3. This LCS is postulated at all the potential locations and a rigorous fracture assessment is performed. Leak-before-break is demonstrated if a sufficient safety margin against failure exists under the postulated design basis and NO + SSE loads. As in SRP 3.6.3, a margin of two between the CCS and LCS is required.

3.8. Japan (JAEA)

The LBB evaluation procedure is prescribed in the current edition of the Japan Society of Mechanical Engineers (JSME) code [19]. The procedure can only be applied to austenitic stainless, ferritic and low alloy steels pipes in which SCC and erosion-corrosion do not

occur. This procedure calculates two TWCs using independent methods. One TWC size is the LCS, which is determined analogously to the methods and provisions in SRP 3.6.3. The LR used to determine the LCS is five times greater than the LRDL. The LRDL is typically approximately 0.06 kg/s (i.e. 1 GPM) so the LR at the LCS is approximately 0.30 kg/s (i.e. 5 GPM).

The second TWC size (operational crack size) is based on operational considerations. An initial semi-elliptical, surface-breaking crack is postulated, and this crack is grown under operational fatigue loading. Transient and seismic loads that do not cause a plant shutdown are considered in the fatigue crack growth analysis. The analysis proceeds until the crack depth penetrates the piping wall thickness, and the length of the semi-elliptical crack at this point is used as the TWC size.

The instability stress is then determined for the larger operational crack size and LCS. A net-section collapse crack stability evaluation method is used for an austenitic stainless steel material and an elastic-plastic fracture evaluation method is used for ferritic and low alloy steels materials. The instability stress is then compared to the applied stress due to combined NO and earthquake loads. A leak-before-break is demonstrated if the applied stress is lower than the calculated instability stress.

3.9. Korea (KEPCO E&C and KINS)

A deterministic LBB evaluation that demonstrates sufficient margin against failure can be used to satisfy the extremely low probability of pipe rupture criterion required in Korean regulations [20]. Korean Safety Review Guide (KSRG) Section 3.6.3 “Leak-before break evaluation” [21] provides the detailed review and inspection guidance, along with the acceptance criteria and review procedures for reviewing the deterministic LBB analysis. KSRG Section 3.6.3 is nearly consistent with the SRP 3.6.3. A high-level summary of an acceptable LBB evaluation procedure in KSRG Section 3.6.3 is as follows:

3.9.1. Screening criteria

It should be demonstrated that the water hammer, creep, erosion, corrosion, fatigue and environmental conditions are not potential sources of pipe rupture.

3.9.2. Leak detection system and leakage size crack

The specifications for plant-specific leakage detection systems inside the containment should be equivalent to those in the RG 1.45 [6]. The application of LBB to piping systems outside containment would require the applicant to demonstrate that leakage detection systems are available that provide equivalent reliability, redundancy and sensitivity to those inside the containment. A margin of ten on the predicted LR is required for determining the leakage size crack, unless a detailed justification accounting for the effects of uncertainties in the leakage measurement can be presented.

3.9.3. Material properties

The material tensile/ fracture tests should preferably be performed using archival material for the piping being evaluated. Plant-specific or industry-wide generic material data bases can be assembled if archival material is not available and used to define the required material tensile and fracture properties. The materials for base metals, weldments and safe ends should be determined at temperatures near the upper range of normal at operation. These effects should be considered in the material properties if the material can have reductions in tensile/ fracture properties due to the dynamic strain ageing. Dynamic fracture

tests should be performed for the carbon steel to consider the effects of dynamic strain ageing.

3.9.4. Load consideration

The NO loads are used to determine the leakage size crack and should be combined based on the algebraic sum of individual values. NO + SSE loads are considered for the crack stability analysis.

3.9.5. Crack stability evaluation

The validity of the evaluation method for the crack stability analysis and LR should be verified either using other acceptable computational procedures or with pipe experimental data. The type, magnitude, sources and the method of combination of loads should be specified and the location that has the least favourable combination of stress and material properties for base metal, weldments, nozzles and safe ends should be evaluated. Analytical methods such as the limit load method, the Z-factor method, the General Electric/Electric Power Research Institute (GE/EPRI) method etc., or numerical methods can be used if the validity of the methods is verified. Additional LBB evaluation procedures are described in the NUREG-1061 Vol.3 [7].

3.9.6. Margins in crack stability evaluation

It should be demonstrated that there is a margin of 2 between the LCS and CCS. It should also be demonstrated that the leakage size crack will not experience unstable crack growth if 1.4 times the normal plus SSE loads are applied. The 1.4 margin should be reduced to 1.0 if the deadweight, thermal expansion, pressure, SSE (inertial) and SAM loads are combined based on individual absolute values.

3.10. Sweden (KIWA)

The Swedish LBB evaluation must first satisfy the following general requirements [22]:

- LBB should be applied to an entire piping segment (within class 1 or 2). Locations with both high and low stresses should be included in the analysis.
- No active damage mechanism (or water hammer loading events) should be present in the piping segment.
- A leakage detection system should be present that, among other requirements, fulfils the RG 1.45 [6].
- The piping segment should have been inspected using a qualified non-destructive examination (NDE) procedure. A qualified NDE procedure would preferably also be used in all future inspections.

Analysis is next performed to determine the leakage and CCS. The through-wall LCS is determined at each chosen assessment location so that the LR is ten times larger than the LRDL. The LR should be calculated using NO loads, including weld residual stresses, if a weld is present at the chosen assessment location. The LCS should be determined at both high and low stress locations along the chosen piping segment. Analyses should also consider the contribution by the flexibility of the piping system, crack morphology on the leakage flow and crack opening displacement (COD) dependence.

The CCS is next determined for the NO loads in combination with the worst loading case/ transient according to the design specification. The margin between the calculated CCS

and the postulated LCS should be at least 2 at each assessment location. In addition, the leakage crack should remain stable when using a load that is 1.4 times larger than the load used to calculate the CCS.

3.11. Switzerland (PSI)

LBB evaluation in Switzerland should be performed based on a state-of-the-art methodology [23], but there are no definitive requirements [24 and 25]. The SRP 3.6.3 and German break preclusion concept have been used in past LBB evaluations. A LBB evaluation is not currently allowed if the piping system is susceptible to SCC.

In a manner consistent with the approach followed in most other countries, the LCS is determined so that the LR is at least ten times the LRDL for a LBB evaluation consistent with the SRP 3.6.3. Different nuclear power plants in Switzerland have justified different LRDLs. Some plants have used a 10 kg/hr (≈ 0.045 GPM) LRDL with a 200 kg/hr (≈ 0.9 GPM) LR (i.e. a factor of 20) to calculate the LCS, while others have used a 0.061 kg/s (≈ 1 GPM) LR with a 0.61 kg/s (≈ 10 GPM) LR (i.e. a factor of 10) to determine the LCS.

The through-wall CCS is next determined for NO + SSE loading. The allowable TWC size is half that of the CCS. This allowable crack size must be greater than the LCS and the crack tip stress intensity factor (K) under NO + SSE loading must be less than 0.707*KIc – where KIc is the linear elastic fracture toughness of the piping material. A fatigue crack growth evaluation must also be performed to demonstrate that the subcritical crack growth through the end-of-life is acceptably low. The starter crack size for the fatigue evaluation is based on the NDE detection limit applicable for the piping system. The fatigue analysis must demonstrate that the starter crack does not grow to the allowable TWC size during the plant's operation lifetime and that existing inspection intervals are conservative.

If LBB is demonstrated to exist in a piping system, a demonstration may be required that the effects of loads due to the instantaneous formation of a hole with 10% of the cross section in the piping system are addressed within the design. This requires a calculation of the dynamic loads (e.g. shock waves, jet forces and temperature transient). Dynamic pressure waves amplitudes were approximately 5% of the static pressure and jet forces typically between 730 and 900 kN in past evaluations. These loading magnitudes are covered by conservatisms in the original design assumptions.

3.12. Summary

Table 3.1 below provides a high-level summary of the LBB requirements in each of the participating countries. The requirements in most countries are rooted in the US NRC SRP 3.6.3 method [2].[2] However, virtually every country has modified either the analysis or the acceptance procedure based on additional research and operational knowledge gained since the NRC SRP 3.6.3 method was established. The three most significant differences between the country-specific requirements and NRC SRP 3.6.3 are also noted in Table 3.1. Some of the more common modifications include explicitly allowing for a lower LRDL than the one specified in the NRC SRP 3.6.3, which requires an additional subcritical cracking analysis in order to demonstrate that LBB or inspection intervals are not challenged, and for worst-case strength and toughness properties to be chosen from the base and weld metal properties.

[2] This benchmark weld configuration is not allowed for LBB consideration in most countries due to the potential for PWSCC. However, this provision has been waived by most participants in order to allow for quantitative LBB analysis.

Table 3.1. Summary of LBB requirements and major differences with the NRC SRP 3.6.3

Country	Basic Requirement	NRC SRP 3.6.3 Difference #1	NRC SRP 3.6.3 Difference #2	NRC SRP 3.6.3 Difference #3
Belgium	NRC SRP 3.6.3	Explicitly identify loading scenarios other than SSE to consider in stability calculations.	Allow LRDL < 1 GPM (0.06 kg/s).	
Canada	NRC SPR 3.6.3	Can qualify systems with active degradation if effective ageing management demonstrated.	Has accepted LR margins less than 10 on a case-by-case basis.	May supplement deterministic with probabilistic analysis.
Czechia	National Req. (1998)	Requires three independent LR systems but only two needed to quantify LR.		
Finland	YVL E.4	Requires fatigue crack growth analysis.	Requires weld properties for COD calc. but base properties for CCS calculations.	Requires that LRDL by qualified by testing and allows LRDL < 1 GPM.
Germany	KTA 3206	Prescribes no explicit LR and critical crack size margins; conservatism included in analysis.	Requires fatigue crack growth analysis of assumed semi-elliptical surface flaw.	Requires stability of surface flaw depth and length; instability length must be > LCS.
Japan	JSME S ND1-2002	Determines second TWC size using fatigue analysis of assumed semi-elliptical surface flaw until thickness breached.	Assesses stability using the larger of the LCS TWC and the fatigue TWC.	Required margin of five between LRDL and LCS.
Korea	KSRG Section 3.6.3	Testing of specific material properties preferred.		
Sweden	SSM 2018:18	Requires both high and low stress locations to be analysed.	Consider WRS in LR calculations, as applicable.	Consider piping system compliance effects and applicable crack morph.
Switzerland	None	No definitive, specific requirements: Both SRP 3.6.3 and break preclusion concepts have been used.	Can allow much lower LRDL (0.045 GPM) with increased leak margins (up to 20).	Requires fatigue analysis of assumed semi-elliptical surface-breaking flaw.
United States	NRC SRP 3.6.3	N.A.	N.A.	N.A.

The German KTA requirements [17], while philosophically analogous to the NRC SRP 3.6.3, differ the most from the NRC SRP 3.6.3. No explicit margins on either the LR or the CCS are required. Instead, the margins are included implicitly in the conservative analysis methods that are used to determine the LCS and CCS. The German method is also the only method that requires a stability analysis to determine the critical surface flaw depth and length and then ensure that an initially presumed surface flaw that could be missed by NDE will not grow to this size during the plant's life.

The Swiss approach is also unique because no specific requirements (other than that the assessment shall be state-of-the-art) exist and each LBB application proposes the method and requirements used to execute the analysis. Both the NRC SRP 3.6.3 and German break preclusion concept have been used and accepted in Switzerland. A novel aspect in the Swedish requirements [22] is that a specified weld residual stress (WRS) distribution is applied when determining both the LCS and CCS. The LBB requirements in Canada are unique because they allow probabilistic analysis to supplement the classical deterministic approach. The Canadian requirements also allow systems with active degradation mechanisms to be granted LBB if it can be demonstrated that effective ageing management is in place to mitigate the degradation. While these, and other, country-specific differences exist, the basic tenets and underlying principles of the LBB philosophy are generally consistent among all the countries.

4. Problem description

Section 2 provided an overview of the benchmark activity. More details on the baseline problem description and the descriptions for the four additional problems in Task 1 – 4 are provided in this section. This section also describes the input parameters used as well as the required outputs.

4.1. Baseline problem: description and input parameters

The baseline and all subsequent problems were conducted on a representative surge line piping configuration operating at a temperature of 340°C, an operating pressure of 15.5 MPa, and an atmospheric pressure of 101 kPa. The pipe has an outside diameter of 406.4 mm, a wall thickness of 40.462 mm (16" nominal pipe size [NPS], Schedule 160), and a 50.8 mm weld width. The weld profile is assumed to be square as indicated in Figure 4.1.

The weld is manufactured using the submerged arc weld process using a nickel-based alloy (Alloy 82) that is often used as a dissimilar metal weld between stainless steel and carbon steel components in western-style light water reactors (LWRs). However, for simplicity, a 304 stainless steel base metal is specified on both sides of the weld. Participants were provided with the tensile properties [i.e. yield strength (σ_{ys}), ultimate tensile strength (σ_{ult}), and elastic modulus E] at the operating temperature. These values are summarised for the base and weld metals in Table 4.1.

Figure 4.1. Piping configuration and associated weld

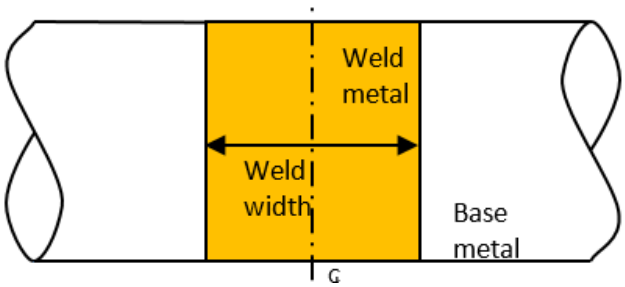

Ramberg-Osgood constitutive parameters were provided for the form of the equation below:

$$\frac{\varepsilon}{\varepsilon_0} = \frac{\sigma}{\sigma_0} + \alpha \left(\frac{\sigma}{\sigma_0}\right)^n \quad (1)$$

where the variables in the equation are summarised for the base and weld materials in Table 4.1.

Finally, the J-R resistance curve (J_{mat}) was described using the following equation:

$$J_{mat} = J_{Ic} + C_1(\Delta a)^{C_2} \quad (2)$$

where the variables in this equation are also summarised in Table 4.1 for both the base and weld materials.

Table 4.1. Base and weld material properties

Tensile properties		
	Weld metal	Base metal
σ_{ys}	316.5 MPa	153.6 MPa
σ_{ult}	542.4 MPa	443.0 MPa
E	196.8 GPa	176.7 GPa
Ramberg-Osgood parameters		
	Weld metal	Base metal
σ_o	332.4 MPa	200.9 MPa
ε_o	0.00169	0.00114
α	0.386	15.64
n	11.39	3.75
J-R curve parameters (Δa in mm)		
	Weld metal	Base metal
J_{Ic}	524.4 kJ/m^2	1182.0 kJ/m^2
C_1	586.3	335.1
C_2	0.661	0.728

Some participants indicated that their country's leak-before-break (LBB) evaluation requires a consideration of subcritical cracking by relevant degradation mechanisms such as fatigue, and, if applicable, SCC. Fatigue and SCC crack growth are assumed to be separable and the crack growth increment for each fatigue loading cycle (*da*/*dN*) is assumed to be governed by the following American Society of Mechanical Engineers (ASME) Boiler and Pressure Vessel Code Section XI, Appendix C relationship [26]:

$$\frac{da}{dN} = C_T S_R S_{ENV} (\Delta K)^p \tag{3}$$

with $$S_R = (1 - 0.82R)^{-2.2} \tag{4}$$

and $$R = \frac{K_{min}}{K_{max}} \tag{5}$$

In these equations, Kmax and Kmin are the maximum and minimum stress intensity factors (SIFs) (in MPa√m) during the prescribed load cycle and $\Delta K = K_{max} - K_{min}$. The remaining parameters in Eq. 3 (i.e. C_T, S_{ENV} and p) for an A82 weld are summarised in Table 4.2.

Similarly, the ASME Section XI, Appendix C formulation [26] is adopted for the SCC crack growth rate (da/dt) using the following equation:

$$\frac{da}{dt} = \Omega (K_I)^m \tag{6}$$

where K_I is the crack tip SIF (in MPa√m) for the constant, or mean, positive tensile load. The remaining parameters in Eq. 6 (i.e. Ω and m) are also defined in Table 4.2.

Table 4.2. Subcritical crack growth parameters

Fatigue crack growth		
from ASME Code – Section XI (Appendix C – 8411) (**da/dN in mm/cycle)**		
	p	4.1
	S_{ENV}	1.0
	C_T	1.02E-10
Stress corrosion cracking		
from ASME Code – Section XI (Appendix C – 8511) (**da/dt in m/s)**		
	m	1.6
	Ω	1.09E-12

The surge line loads used for normal operation (NO) and NO + safe shutdown earthquake (SSE) conditions were initially based on representative deadweight and thermal load values from US plants that have applied for LBB [27]. These values were then adjusted using crack morphology parameters for a corrosion fatigue (CF) crack in order to provide loads that would just meet (i.e. by a margin of 1.0) the Standard Review Plan (SRP) 3.6.3 LBB provisions for a crack that is twice the leakage crack size (LCS) using the weld metal strength and fracture toughness properties. The axial force from the 15.5 MPa operating pressure was also provided in order to ensure consistency and participants were asked to also consider crack face pressure (CFP) loading using a value of one-half of the internal pressure. The load values developed for the baseline problem are summarised in Table 4.3.

Table 4.3. Baseline problem loads

Operational loading						
	Axial force			Moment		
	Deadweight (kN)	Thermal (kN)	Total (kN)	Deadweight (kN-m)	Thermal (kN-m)	Total (kN-m)
NO	17.34	-4.00	**13.34**	21.59	68.00	**89.59**
NO + SSE	52.04	-4.00	**48.04**	310.00	68.00	**378.00**
Axial force from pressure loading = 1 289.6 kN						
Crack face internal pressure loading = 7.75 MPa						

The hypothetical crack for the baseline problem is circumferentially oriented with the crack centreline coincident with the weld centreline (Figure 4.2). The crack mouth at the outer diameter is situated at the location of highest maximum axial tensile stresses due to bending. Crack propagation is assumed to be along the weld centreline so that a failure would occur solely within the weld. An idealised through-wall circumferential crack (TWC) is prescribed so that the crack angle on the inside surface is equivalent to the crack angle on the outside surface (Figure 4.2). The crack is assumed to open with an elliptically shaped profile (Figure 4.2).

Figure 4.2. Crack location and shape

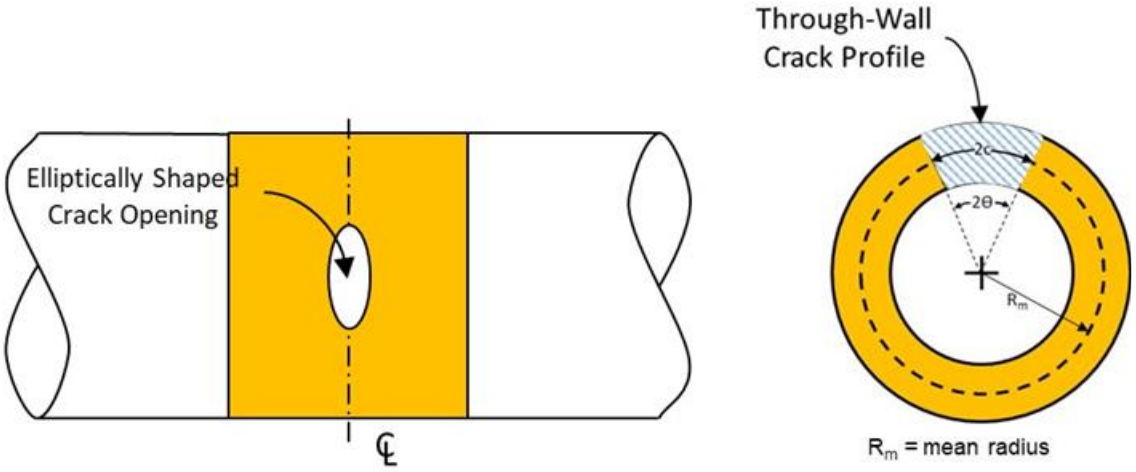

Using the information provided in this section, participants were asked to perform a LBB evaluation of this weld joint using the LBB approach and requirements applicable to their country. As summarised in Section 3, this invariably required the determination of an LCS

under NO loading followed by a comparison of this leakage crack with the critical crack size (CCS) determined under NO + SSE loading. Participants were asked to determine the LCS using a crack morphology that is appropriate for a LBB analysis and meets their country's requirements.

Participants were also provided with a leak rate detection limit (LRDL) of 0.061 kg/s, which is approximately 1 gallon per minute (GPM) for the hypothetical plant. Participants were free to use this value or an alternate LRDL that is more consistent with their country's requirements. As previously mentioned, some countries require a determination of subcritical crack growth between the LCS and CCS. The participants who needed to conduct this evaluation were encouraged to do so using the prescribed material property relationships in Eqs. 3-6 and Table 4.2. However, participants needed to develop their own representative fatigue loading history for the targeted plant life because no fatigue loads were prescribed for the baseline problem.

4.2. Tasks 1-4: description and input parameters

As previously indicated in Section 2.2, the same piping configuration and geometry, weld and base metal properties, operating conditions, NO and NO + SSE loading, crack configuration and assumptions specified for the baseline problem (Section 4.1) were used for these tasks. A common TWC length of 125 mm at the piping mid wall (i.e. mean radius, R_m, in Figure 4.2) was also assumed for all tasks. The use of a common crack length, analysis assumptions and input parameters is intended to decrease variability in the Task 1 – 4 results because different LCS values and other analysis assumptions were anticipated in order to increase the variability in the baseline analysis results.

The only differences among Tasks 1-4 were the crack morphology, which varied between CF and primary water stress corrosion cracking (PWSCC), and the consideration of an applied axial weld residual stress (WRS) profile. The specific attributes of each task are summarised in the table below.

Table 4.4. Task 1-4 problem attributes

Problem	Mid-wall crack length (mm)	Crack morphology	Applied WRS (Y/N)?
Task 1	125	CF	N
Task 2	125	CF	Y
Task 3	125	PWSCC	N
Task 4	125	PWSCC	Y

Different leak rate (LR) codes characterise crack morphology differently. The most prominent LR codes used by the participants (Section 5) were SQUIRT [28] and LEAPOR [29], which both treat crack morphology similarly. The activity leads therefore decided to provide crack morphology parameters that are consistent with the SQUIRT/LEAPOR framework. SQUIRT and LEAPOR define global roughness (μ_G) and local roughness (μ_L) parameters as well as global path deviation (K_G) and local path deviation factors (K_{G+L}) that are defined as illustrated in Figure 4.3.

Figure 4.3. Roughness and path deviation parameters in SQUIRT and LEAPOR

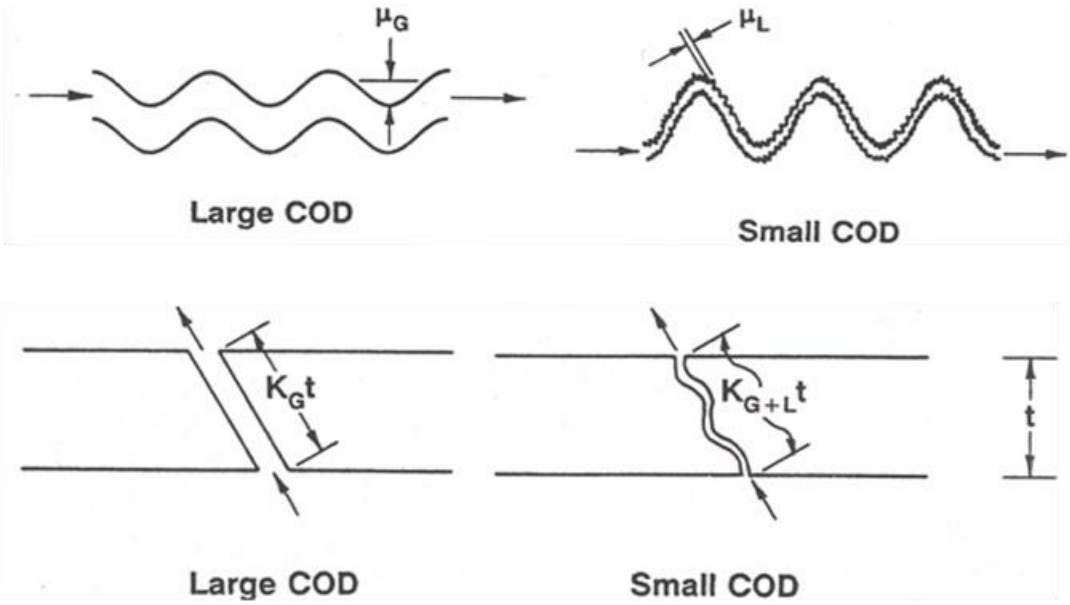

These factors are functions of crack opening displacement (COD) in recent versions of SQUIRT/LEAPOR [28 and 29]. μ_L and K_{G+L} are used for the roughness and path deviation factors for small COD values, while μ_G and K_G are used for large COD values. There is a linear relationship assumed in SQUIRT and LEAPOR for transitioning between small and large COD regimes. The participants decided that the crack morphology parameters should be independent of COD for the benchmark in order to allow for a more straightforward comparison with other LR codes, which treats crack morphology effects using a different framework. μ_L was therefore set equal to μ_G for the benchmark, while K_{G+L} was set as equal to K_G, even though it is recognised that this does not provide a realistic representation of either a CF or PWSCC crack.

The final crack morphology parameter used in SQUIRT/LEAPOR is the number of turns per unit length (η_{tL}) for the crack. This parameter has been binned into categories in order to differentiate between sharp turns of approximately 90 degree turns [$\eta_{tL(90)}$], which result in more head loss, and those that are more gradual [$\eta_{tL(45)}$]. The number of turns is added to a single value in calculations by summing $\eta_{tL(90)}$ with ½ of $\eta_{tL(45)}$. It is assumed that $\eta_{tL(45)} = 0$ and $\eta_{tL} = \eta_{tL(90)}$ in order to have simplicity in the benchmark. The η_{tL} parameter is also a function of COD in both SQUIRT and LEAPOR. There is no way to treat this parameter independently, as was the case with the roughness and path deviation factors. This parameter therefore varies with COD when used in the SQUIRT and LEAPOR code. However, an effective η_{tL} value [$\eta_{t(90)}$] is provided for use in other LR codes, which, based on the estimated COD for the Task 1 – 4 problems, is meant to approximate the $\eta_{tL(90)}$ value used in SQUIRT/LEAPOR.

The entry loss (or discharge) coefficient (C_d) is also provided. The values prescribed for all these parameters for the CF and PWSCC cracks are summarised in Table 4.5. The values for μ_G, K_G and $\eta_{tL} = \eta_{tL(90)}$ are the default values for both SQUIRT [28] and LEAPOR [29] for each crack type. As mentioned, setting $\mu_L = \mu_G$ and $K_{G+L} = K_G$ is simply done in order to make these parameters independent of COD in the SQUIRT/LEAPOR codes. However, it is now recognised that this simplification does not provide a realist representation of either a CF or PWSCC crack.

Table 4.5. Prescribed crack morphology parameters

Parameter	CF	PWSCC	Comments
μ_G	40 µm	114 µm	
μ_L	40 µm	114 µm	
K_G	1.1	1.2	
K_{G+L}	1.1	1.2	
$\eta_{tL(45)}$	0	0	
$\eta_{tL} = \eta_{tL(90)}$	6730 m^{-1}	5940 m^{-1}	COD-dependent equations as in SQUIRT/LEAPOR
$\eta_{t(90)}$	1730 m^{-1}	5020 m^{-1}	COD-independent equations in other LR codes
C_d	0.95	0.95	

The axial WRS profile chosen for this benchmark is intended to be representative of a pressuriser surge line nozzle, nickel-based dissimilar metal weld (DMW). A typical surge line nozzle configuration in a pressurised water reactor joins the carbon steel pressuriser nozzle to a stainless steel safe end with a DMW. The safe end is then welded to stainless steel piping with a conventional stainless steel weld. The WRS profile was taken from the following third-order polynomial fit of finite element analysis (FEA)-based predictions of this configuration [30]:

$$\text{WRS (Axial, in MPa)} = -101.3 - 167.58\left(\frac{x}{t}\right) - 375.76\left(\frac{x}{t}\right)^2 + 1165.75\left(\frac{x}{t}\right)^3 \quad (7)$$

where x is the distance from the inner diameter of the pipe and t is the piping wall thickness. This distribution is illustrated in Figure 4.4 as well. The resultant force from this assumed third-order WRS distribution is not zero as theoretically required for an axisymmetric axial stress distribution. As stated previously, such a WRS would also not result from simply welding two stainless steel piping segments with a nickel-based weld as assumed in the simplified weld joint configuration used in this benchmark (Figure 4.1).

Figure 4.4. Representative surge line nozzle dissimilar metal weld stresses

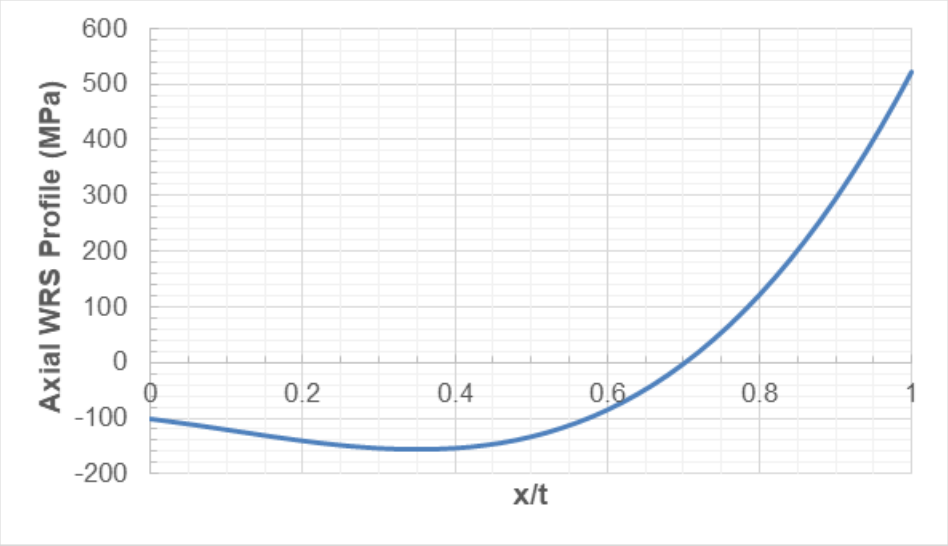

4.3. Baseline problem: requested results

Participants were asked to describe their country's LBB requirements, including the required analysis, results that are reported from the analysis and the associated acceptance criteria. These descriptions are summarised in Section 3. Participants were asked to

determine if their country's LBB requirements are met for the baseline problem. If the requirements are not met, participants were asked to identify and describe those requirements that were not met. The following parameters from the analysis were also requested:

- required LR for evaluation;
- crack length at required LR (i.e. LCS);
- crack size at failure under NO + SSE loading (i.e. CCS).

For the LCS, participants were also asked to provide the axial force at failure and the critical bending moment (CBM) at failure. Participants were initially asked to assume a constant ratio of the NO + SSE axial force to bending moment ratio of 3.54 m^{-1} (i.e. the NO + SSE deadweight and thermal loads, plus the axial force from pressure, divided by the NO + SSE deadweight and plus thermal moments in Table 4.3) to calculate these values. However, this assumption was not clearly communicated to participants. This is not a typical calculation in a LBB analysis in most countries and therefore there was confusion about how it should be performed. Later, after several results were received and this confusion became evident, it was decided to assume a constant axial force of 1 338 kN (i.e. the NO + SSE deadweight and thermal load plus the axial force from pressure in Table 4.3) and then calculate the CBM for the LCS. As seen in the reported results (Table 6.1 in Section 6.1), most participants assumed a constant axial force of 1 338 kN (or close to this value) in order to determine the CBM.

Participants were also requested to provide any supplementary results that were easily available as part of their evaluation. The results were specifically data (i.e. tabulated or graphical) describing the relationship between the LCS, NO bending moment, COD for the required evaluation of LR and data describing the relationship between the CBM and CCS were solicited. Several participants also provided data for the relationship between LR, COD and LCS under the prescribed NO loading conditions. These results are summarised in Section 6.2.

Finally, participants were asked to provide a synopsis of their solution approach, listing of their analysis tools and any applicable comments. All these results are summarised in Section 6. Each participant's detailed responses for the baseline problem are also provided in Annex A.

4.4. Tasks 1-4: requested results

The Task 1 – 4 analyses were intended to be more uniform and consistent than the baseline problem by further refining the problem description (i.e. specifying the crack size and crack morphology) and using input parameters for each task. However, differences in results are still expected based on additional required analysis assumptions that were not specified (e.g. the properties of the mismatched weld joint) and the fact that the participants used different analysis codes, which may have different built-in margins or calculation approaches. The effect of WRS on COD and CCS is not further addressed in most existing regulations and analysis programmes.

Participants were once again asked to summarise their analysis approach, list their analytical tools and provide any applicable comments for each task. For Task 1 (CF crack without WRS) and Task 2 (CF crack with WRS), participants were asked to report the following: the COD values on the inside pipe wall, mid-wall and outside the pipe wall; and the LR and the bending moment at crack instability for an assumed NO + SSE axial force from all loads (i.e. deadweight, thermal and pressure of 1 337.64 kN). For Task 3 (PWSCC

crack without WRS) and Task 4 (PWSCC crack with WRS), participants were only asked to provide the LR because it was assumed that COD and crack instability loads would not be affected by crack morphology. All these results are summarised in Section 8. Each participant's detailed responses for Tasks 1-4 are also provided in Annex A.

5. Baseline problem – approach and individual results

This section provides a summary of the approach that each organisation followed to solve the baseline problem, as well as the computational tools used to evaluate crack opening displacement (COD), leak rate (LR) and crack stability.

5.1. United States (NRC and EMCC)

Separate analyses were performed by the US Nuclear Regulatory Commission (NRC) and EMCC following the United States' approach, albeit with some different assumptions, input parameters and calculation methods. The EMCC performed analyses that were intended to be both conservative and consistent with historical leak-before-break (LBB) evaluations from the 1990s for this baseline problems. They chose conservative material properties and employed models used in these historical analyses. The NRC evaluation was intentionally less conservative and intended to be more representative. The NRC used weld material properties based on the weld centreline crack location and the most current models were used.

5.1.1. NRC

As indicated in Section 3, the NRC analysis followed the provisions of the Standard Review Plan (SRP) 3.6.3 [2]. The screening provisions of the SRP 3.6.3 (for example, water hammer, creep damage, cleavage fracture and active degradation mechanism) were not considered and only the analysis of the proposed welded joint was considered. The LR, load parameters, crack morphology and material properties of the problem statement (Section 4.2) were used for the LBB analysis.

The leakage crack size (LCS) for ten times the leak rate detection limit (LRDL), 0.63 kg/s (i.e. 10 gallons per minute [GPM]), was determined using a General Electric/Electric Power Research Institute (GE/EPRI)-like COD code [31] and the LEAPOR LR code [29]. The inputs into the COD calculation were the pipe diameter and thickness, pressure, normal operation (NO) axial force (i.e. deadweight and thermal expansion loads), NO bending moment and Ramberg-Osgood coefficients for the weld metal. The COD module calculated pressure loads and included an assumed crack face pressure (CFP) contribution equal to 50% of the internal pressure. The effect of weld residual stress on COD was not considered for the baseline calculation. The COD module returned values of COD at the inner diameter (ID), mid-wall (MW) and outer diameter (OD).

LEAPOR (LEAPOR_V1.0) [29] was used to calculate the LR using inputs of pipe ID and thickness, internal pressure, fluid temperature, ID and OD crack lengths, inner diameter CODs (ICODs) and outer diameter CODs (OCODs), and crack roughness parameters. The leakage crack was assumed to have an equal crack angle at the piping ID and OD. Corrosion fatigue (CF) crack roughness parameters were assumed and the calculation used a loss discharge coefficient (LDC) of 0.95. LEAPOR would have internally modified the crack roughness parameters to be dependent on COD if the parameters had not been chosen to be COD independent. Newton's method was used to iterate the crack length for NO load conditions, which produced a COD that resulted in an LR of 0.63 kg/s (≈ 10 GPM).

Crack stability under NO + safe shutdown earthquake (SSE) loading was determined using a J-estimation scheme [32], LBB.ENG2, that had been modified to minimise discontinuities in the ψ-function [33] used to calculate the bending moment vs. critical crack size (CCS) relationship. The NO + SSE loading was based on the algebraic sum of

individual values. The input parameters were the pipe ID and thickness, internal pressure, axial force, Ramberg-Osgood parameters for the weld metal and J-resistance parameters for the weld metal. The effects of CFP and weld residual stress (WRS) were not considered in the crack stability calculation. LBB.ENG2 returned the failure bending moment for the specified conditions, including a fixed axial force value of 1 337.64 kN, which is specified in the baseline problem description.

The fracture mechanics analysis demonstrated that

- twice the LCS did not become unstable under NO+SSE loading;
- the LCS did not become unstable with under 1.4 times NO+SSE loading, including 1.4 times the axial force resulting from internal pressure.

The analysis provisions described in the SRP 3.6.3 were therefore successfully met. Specifically, the LCS and CCS were calculated to be 283.6 mm and 567.8 mm respectively. The values for the relationship between the COD, LR, failure bending moment and the relationship between the COD, LR and failure moment for a crack with an LR of approximately 0.61 kg/s (≈10 GPM) were also provided. Additionally, the NRC calculated a bending moment at instability for the LCS for an assumed axial force of 1 337.7 kN of 1 364 kN-m. The NRC results are summarised in Annex A and further discussed in Section 6.

5.1.2. EMCC

For the baseline problem, the EMCC approached the problem as a vendor would have in their LBB submittal from the 1980s or 1990s, which will hereafter be referred to as a traditional LBB deterministic analysis. A through-wall circumferential crack (TWC) in the weld was therefore assumed. The LRDL was specified as 0.061 kg/s (≈1 GPM) and, as required by the SRP 3.6.3, the target LR of 0.61 kg/s (≈10 GPM) was used to determine the LCS using the SQUIRT4 module of the SQUIRT code [34]. The inputs for the SQUIRT4 module are listed in Table 5.1. The LCS for the baseline case was determined to be 256.84 mm.

The inputs in Table 5.1 are identical to those provided in the input data set for the baseline problem (Section 4.1) with the exception of the crack morphology parameters, which correspond to an air fatigue crack morphology. This morphology was chosen for two reasons. Firstly, traditional LBB deterministic analyses did not typically use the crack morphology parameters, but rather only used a roughness. If crack morphology was included, then the air fatigue parameters were typically used. Secondly, Tasks 1-4 use CF and primary water stress corrosion cracking (PWSCC) crack morphology and therefore the EMCC decided that having a third crack morphology type would provide more insight than using either CF or PWSCC parameters in the baseline analysis. Neither CFP nor WRS were applied in the baseline analysis because these loads were not taken into consideration in traditional LBB deterministic analyses.

Table 5.1. SQUIRT4 input for EMCC baseline analysis

Pipe OD (m)	0.4064
Pipe thickness (m)	0.040462
Total crack length (m)	125
Bending moment (MN-m)	0.08959
Yield stress (MPa)	153.6
Ultimate stress (MPa)	443
Collapse stress (MPa)	298.3
Reference stress (MPa)	200.9
Reference strain	0.00114
Alpha	15.64
Exponent (n)	3.75
Pressure (MPa)	15.5
Temperature (°C)	340
Required LR (kg/s)	0.61
Global roughness (μm)	33.66
Local roughness (μm)	6.53
Number of turns (mm^{-1})	2.01
Global path deviation	1.02
Local path deviation	1.06

Using the LCS calculated by SQUIRT4, the total axial force (1 289.6 kN from operating pressure and 13.34 kN from normal operating loads) was converted into an equivalent pressure. This equivalent pressure was applied in combination with the applied moment in NRCPIPE using the LBB.ENG2 method in order to determine instability [32]. The base metal Ramberg-Osgood material properties and weld metal J-R curve were used for the NRCPIPE analysis.

It is stated in the SRP 3.6.3 [2] that if the algebraic sum method is used to combine deadweight, thermal expansion, pressure, SSE and seismic anchor motion (SAM) loads, then a margin of 1.4 should be applied to the sum of these loads. If the loads are combined using the absolute sum method, then the margin is reduced to 1.0. The EMCC therefore used both load combination methods in order to determine the maximum of these two CCSs.

The associated CCS was determined to be 422.7 mm using the absolute sum method. The associated CCS was determined to be 360.22 mm using the algebraic sum method. Since the LCS was 256.84 mm, the margin of 2.0 was not met for either CCS and therefore the LBB provisions specified in the SRP 3.6.3 were not met. The EMCC also calculated a critical bending moment (CBM) of 732.14 kN-m for the leakage crack with the axial force loading of 1 302.95 kN that was used to calculate the LCS. The EMCC results are summarised in Annex A and further discussed in Section 6.

5.2. Belgium (Tractebel)

Tractebel performed a finite element analysis using Morfeo/Crack [35] in order to determine the relationship between the COD and TWC length. The entire weld joint was modelled with the base and weld metal properties prescribed to the appropriate model zones. The constitutive behaviour at the crack tip is a natural mixture of the base and weld properties using this approach. The Pipe Crack Evaluation Program (PICEP) [36] was used to calculate the LR for each COD and TWC pair. Two LRDL values were considered: ≈ 0.06 kg/s (i.e. 1 GPM), the commonly used value, and 0.03 kg/s (i.e. 0.5 GPM), the LRDL for many Belgium plants as explained in Section 3.2. The LCS is the crack size that produces an LR of ten times the LRDL. Either surface roughness or a friction factor (FF) can be input into the PICEP. The FF is preferred as a way of accounting for possible

degradation mechanisms other than fatigue. A conservative value of 0.15 for the FF and the loss discharge coefficient (LDC) is taken as equal to 0.61 is used in Belgium LBB studies. These values were used in this baseline problem. All other input parameters are as specified in Section 4.1.

Tractebel has developed an in-house computational tool for determining crack stability (JT-crack), which has been historically used in LBB submittals. However, the pipe radius to thickness ratio and material hardening properties for the benchmark are beyond the applicable ranges for a solution with the JT-crack. Morfeo/Crack [35], a commercial computation tool that uses the extended finite element method (xFEM), was therefore employed for evaluating crack stability using an applied J vs. tearing modulus assessment. The weld metal J-R curve toughness was used. As indicated in Section 3.2, the CCS should at least be equal to twice the LCS.

The calculated CCS is 460 mm. If the LRDL is 0.5 GPM, the LCS is calculated to be 211.6 mm, which is less than half of the CCS. If the LRDL is 1 GPM, that leakage crack is not less than half of the CCS. The CCS margin therefore satisfies the factor of two requirement for a 0.5 GPM LRDL, but not for a 1.0 GPM LRDL.

Tractebel also performed several supplemental calculations for the baseline problem. They evaluated and provided tabulated values for the relationship between COD, LR and crack length using PICEP calculations. For a constant axial force of 1 337.7 kN, Tracetebel also calculated a failure bending moment of 985 kN-m for the leak crack using Morfeo/Crack. More details on the Tractebel calculations are provided in Annex B. The Tractebel benchmark results are also summarised in Annex A and further discussed in Section 6.

5.3. Canada (CEI and OPG)

Separate analyses were performed by Candu Energy Inc. (CEI) and the Ontario Power Generation (OPG). While each organisation followed the general principals of a LBB analysis in Canada, there were some differences in the assumed LRDL, analysis approaches and COD models used to calculate the LCS. The analytical methods used for the crack stability analysis were also different. The OPG solely used an elastic-plastic fracture mechanics (EPFM) method, while CEI used both net-section collapse (NSC) and EPFM models to determine the most conservative CCS. These differences are detailed in the subsequent subsections.

5.3.1. CEI

The LBB analysis for the baseline case follows the US NRC SRP 3.6.3 provisions. The flowchart (Figure 5.1) illustrates the LBB analysis approach. The CCS was calculated to be 587 mm when elastic-plastic fracture mechanics (EPFM) was used and 471 mm when the NSC method was used. The CCS calculated from NSC is smaller than that of EPFM and therefore the NSC result was used without a Z-factor for the baseline case. The calculated mid-wall (MW) CCS was 471 and thus the reference crack size (RCS), which is half of the CCS, was 235 mm. The COD for the RCS crack was calculated as 0.2306 mm, and the associated RCS LR was calculated as 0.2462 kg/s (≈4 GPM) under the normal operating conditions and using SQUIRT Version 2.1.3 [37].

The input into SQUIRT is listed in Table 5.2. Since the calculated LR (0.2462 kg/s) is less than ten times the LRDL (i.e. 10×0.061 kg/s or 10 GPM), LBB is not demonstrated for the baseline case. However, if the LRDL (20 kg/h) of a typical CANDU plant is used, LBB is demonstrated with an LR factor of 44, which is much greater than the required factor of 10.

As the evaluation procedure in Figure 5.1 is different than prescribed in the SRP 3.6.3, it is not required to determine the LCS. However, the LCS was also calculated to be 286.32 mm for the purposes of this benchmark. CEI also calculated a bending moment at instability for the LCS for an assumed axial force of 1 337.7 kN of 1 084.43 kN·m.

Table 5.2. Input for LR calculation in SQUIRT

Pipe OD (mm)	406.4
Pipe thickness (mm)	40.462
Total crack length (mm)	471
Absolute pressure (MPa)	15.6
Temperature (°C)	340
Global roughness (μm)	40.5
Local roughness (μm)	8.81
Number of turns (mm^{-1})	6.73
Global path deviation	1.02
Local path deviation	1.06
LDC	0.95

Figure 5.1. CEI LBB analysis procedure

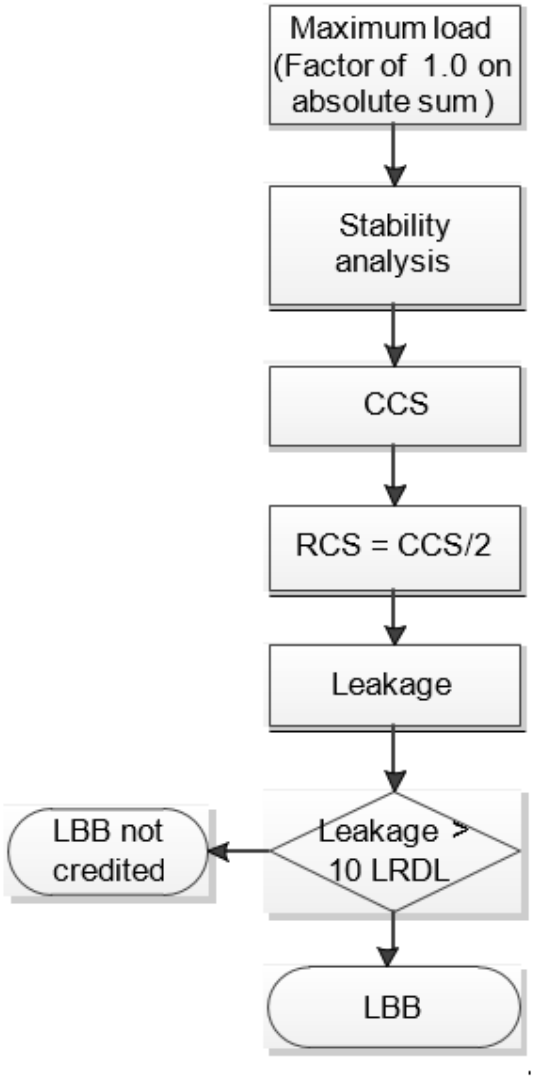

5.3.2. OPG

The OPG typically conducts LBB analyses by initially calculating the CCS, first reducing it by the crack size margin of 2 and then calculating the LR of the reduced crack size in order to determine if it exceeds the LRDL by at least a margin of 10, in which case LBB is demonstrated. However, the OPG initially calculated the LCS by applying a factor of 10 to the LRDL for this benchmark. The LRDL was based on the operating procedures of a CANDU plant that specifies shutdown once a 50 kg/hr leak is detected from the primary heat transport piping. The chosen LRDL was therefore 50 kg/hr or 0.0139 kg/s. After applying the margin of 10 on the LR, the target leak rate for calculating the LCS was 0.139 kg/s.

SQUIRT Windows version 2.0 was used to conduct the leak rate calculations using the default CF morphology parameters. These parameters are similar to those in Table 4.5 and used the following values: μ_G = 40.51 µm, μ_L = 8.814 µm, K_{G+L} = 1.06, K_L = 1.017, $\eta_{t(90)}$ = 6 730 m^{-1} and C_d = 0.95. The fluid thermodynamic state was subcooled liquid at 340 ºC under the prescribed pressure of 15.5 MPa. The crack opening shape was semi-elliptical and the same COD and crack length were assumed at the ID and OD of the pipe diameter.

An in-house crack stability code was used to calculate the elastic-plastic COD – for a given crack length and under the prescribed NO load – based on the EPFM approach [38], using the J-integral equations from [39 and 40]. The weld metal stress-strain properties were used. The COD and crack length were then input into SQUIRT and the values were iterated until the LSC of 177 mm with a mid-wall crack opening displacement (MWCOD) of 0.13923 mm was determined at the target LR of 0.139 kg/s.

The CCS was determined using the same in-house code under the prescribed NO+SSE load (Table 4.3) and including a CFP of 7.75 MPa. WRS was not considered and the weld metal stress-strain properties were again used. The J-resistance code requires the following form in this code:

$$J = C_1(\Delta a)^{C_2} \tag{8}$$

C_1 and C_2 in this equation were determined by fitting this equation to the form of the J-R curve provided in the input data set (Eq. 2). The difference between the CCS and crack size at failure is that the CCS) is the crack size prior to crack growth, while the crack size at failure accounts for ductile tearing preceding instability. The CCS was calculated as 573 mm, while the crack size at failure was 583.9 mm. The Canadian LBB acceptance criteria were satisfied in this analysis because the CCS was more than twice the LCS. The CBM for the LCS was also calculated under an internal pressure of 15.5 MPa, a NO+SSE axial force of 1 337.64 kN (Table 4.3) and CFP of 7.75 MPa using the same in-house crack stability code. The calculated CBM was 1 620.34 kN-m. The OPG results are also summarised in Annex A and further discussed in Section 6.

5.4. Czechia (UJV)

The COD was calculated by the PICEP code [30], while the LRs were calculated by an in-house code (LEAKH) based on thermodynamic laws, steam and a water table. This code treats crack morphology by specifying a global roughness (μ_G) along with an LDC. The LRDL was assumed to be 1 GPM and the LCS was calculated for a 10 GPM LR with the required margin of 10. The in-house code BASLBB was used to calculate the CCS with NSC as per the SRP 3.6.3 [2] in order to govern plastic collapse under NO + SSE loading. The ratio between the CCS and LCS must be greater than or equal to 2 in order to meet LBB requirements and this margin was calculated to be 2.1 for the baseline problem. The

CBM values for the LCS were calculated using German methods [41 and 42], the R6 approach [43] and the NRC LBB approach [44]. The R6 and LBB NRC methods produce similar results, while the German methods are very conservative. Nevertheless, the required LBB margins were met for the baseline problem with all these methods.

5.5. Finland (VTT)

The Finnish requirements dictate that LBB cannot be granted in piping systems with the potential for PWSCC. The required LBB analysis was nevertheless performed despite this limitation. The first step of the analysis was to determine the LCS that results in an LR that is ten times higher (Section 3.5) than the assumed LRDL of 3.8 L/min (≈ 1 GPM). For this purpose, the crack opening areas for different crack lengths were calculated based on the analytical equations developed by Young et. al. [31, 45 and 46]. The LRs corresponding to these crack opening areas were calculated using the LEAPOR code for NO loading and with CF crack morphology parameters, which are provided in the baseline problem description (Section 4.1).

This assessment resulted in an LCS with an included angle of 88.8°. Crack stability was then evaluated using two separate ABAQUS finite element models: one with an 88.8° crack, and one with a 177.6° (i.e. 2*88.8°) crack. The 3D model, which included the weld material and a sufficiently long section of the base material, utilised the Ramberg-Osgood constitutive model for the weld, while the base material was assumed to remain elastic. The crack stability analysis was performed using the NSC method in American Society of Mechanical Engineers (ASME) Section III [47] to determine if failure occurred before the required COD was reached. The possibility of ductile tearing at the required COD was determined using the J-integral method in order to confirm that the amount of ductile tearing was small compared to the initial crack size. The J-integral values were calculated using the ABAQUS contour integral evaluation routine.

The 88.8° crack remains stable under 1.4*NO loading for both the NSC and ductile tearing analysis with thermal loads being treated as primary. However, the NSC analysis predicted that the 177.6° crack was unstable at loads of just under 1.0*(NO+SSE) with thermal loads again being treated as primary. All LBB requirements were thus not satisfied, but the specific crack size at instability was not explicitly calculated. One-half of the CFP was also added to the loads in calculations. The VTT Technical Research Centre of Finland (VTT) results are summarised in Annex A and discussed further in Section 6.

5.6. Germany (GRS)

Two different approaches were used to determine the CCS: plastic collapse and the failure assessment diagram (FAD). The following plastic collapse methods identified in KTA 3206 [17] were employed: plastic limit load (PLL); flow stress concept, MPA (FSC MPA); and flow stress concept, KWU (FSC KWU). The methods are used as implemented in the PROST code (for example, see [48]). The material's fracture toughness must be specified in the FAD approach. The corresponding elastic stress intensity (K_{IJ}) value determined from the stable crack growth initiation value (i.e. J_{Ic}) is used in this assessment. The K_{IJ} value is quite high and therefore crack stability is typically governed by one of the plastic collapse methods. The baseline evaluation used the base metal properties (Table 4.1) to calculate the CCS.

Two different load cases were evaluated. The first case (LOAD) used the NO + SSE moment and axial force loads provided in the input parameter spreadsheet (see Section 4.1). The thermal loads were treated as secondary loads, while all other loads were treated as primary loads. The second load case considered additional effects of WRS (LOAD+WRS)

on crack stability. The SINTAP approach [49] is used to determine the SIF for the WRS distribution (Figure 4.4). The SINTAP solution provides SIF values as a function of thickness and thus the value at the piping MW was used in the assessment. All loads were considered to be primary loads in this load case. The results of the CCS calculations for the two different load cases and the four different crack stability methods are summarised in Table 5.3 below.

Table 5.3. GRS CCS results

	LOAD	LOAD+WRS
Crack stability method	**CCS (mm)**	**CCS (mm)**
FSC MPA	554	730
FSC KWU	426	344
PLL	326	258
FAD	625	260

The LOAD case evaluations produce the largest CCS values for all the crack stability methods, except for the FSC KWU method. The FAD method without WRS loads produces the largest CCS and – because K_{IJ} is so high – failure is governed by plastic collapse. Both the PLL and FAD methods for the LOAD+WRS case produce the smallest CCS values, and these are the results reported in the GRS baseline results (Annex A and Section 6).

The WinLeck 5.0.1 code [48] was used with conservative settings to calculate the LCS. In WinLeck, the COD is computed with the method prescribed in KTA 3206 (see Annex B3.1.2 in [17] for a complete description of the approach and methods), while the FF is determined by bounding the KTA curve. The bounding approach for determining the FF typically leads to very high flow resistance values and subsequently high LCS values. This is the desired result because, as indicated in Section 3.6, no additional margin is added to the LRDL to determine the LCS in the German LBB approach. The flow rate in WinLeck can be determined by any of the following best-estimate methods: ATHLET-CDR [50 and 51], jPana [52], or Henry [53]. The baseline calculations used the ATHLET-CDR approach. The NO loads were used for the LR calculation without a consideration of WRS.

Two different pressure loadings were considered in the baseline evaluation: full pressure (FULLP) and reduced pressure (REDP). The full pressure case used the membrane stress due to pressure as prescribed in the input parameter spreadsheet, although, as has been previously indicated, this value is lower than the value determined by Barlow's formula. The reduced pressure case included a reduced Barlow factor of 0.64 to scale the full pressure. The global roughness value (40 μm) and global path deviation factor (1.1) provided in the input parameter spreadsheet for a corrosion fatigue crack were used to describe the crack morphology. There is no additional margin and therefore the LCS for the baseline problem was calculated for an LR of 0.061 kg/s (≈1 GPM).

The results of these evaluations are summarised in the following table. In this table, the crack opening area (COA) is the crack opening area, ζ is the total flow resistance, $\dot{m}$ is the mass flow rate and G is the flow rate per unit area. While the REDP result evidently reduces the COD compared to the FULLP result for identical crack lengths, a higher LCS is needed to achieve the LRDL under REDP loading. Interestingly, the COD for the calculated LCS values was similar for both the FULLP and REDP.

Table 5.4. GRS baseline LR calculation results

Parameter	Units	FULLP	REDP
LCS	[mm]	177	202
COD	[mm]	0.112	0.106
COA	[mm²]	15.6	16.89
ζ	[-]	470	533
$\dot{m}$	[kg/s]	0.0604	0.061
G	[kg/sm²]	3 876	3 602

A variety of leak rate sensitivity analyses were conducted to evaluate the effect of different LR calculation methods (i.e. WinLeck with Henry, WinLeck with jPANA and LEAPOR) that considered FULLP and REDP loading (WinLeck with jPANA). One set of WinLeck calculations was conducted using a factor of ten margin on the LRDL in order to correspond to the analyses performed by other benchmark participants. The WinLeck with jPANA and LEAPOR results were almost identical and the calculated LCS values using these methods were approximately 10% higher than the values in Table 5.4. The WinLeck with Henry FULLP LCS value was approximately 17% higher than the Table 5.4 FULLP value. The WinLeck calculation for determining the LCS for a flow rate of 0.61 kg/s (≈ 10 GPM) was 290 mm, which falls within the scatter of the other participants' LCS calculations for this flow rate (see Section 6).

5.7. India (BARC)

As discussed in Section 3.7, the level three LBB safety assessment in India consists of postulating a TWC that will ensure a detectable LR. This postulated crack must next be demonstrated to remain stable under the severest loading. The LR and COD is calculated using an in-house code with CF crack morphology parameters that are specified in the problem description (Table 4.5). As prescribed in the problem statement, an LRDL of 0.06 kg/s is assumed so that the LCS corresponds to a 0.61 kg/s LR after incorporating the margin of ten on the LRDL. The calculated LCS is 78.55°.

The crack stability analysis must determine if the minimum required margins on load and critical crack length (Section 3.7) are satisfied for the LCS under NO + SSE loading. The CBM must be shown to be sufficiently higher than the maximum bending moment that can occur during NO + SSE loading, and the critical crack length to be higher than or equal to twice the LCS. The CCS does not have to be directly determined, but merely for a crack that is twice the leakage size crack when the critical load is higher than the NO + SSE load.

The CBM and axial force for both the LCS and twice the LCS were evaluated using an in-house code. The in-house code evaluated crack instability using a J-integral tearing modulus (J-T) approach that is specified in the RCC-MRx A-16 design code [54]. The tensile and fracture toughness properties of the weld region that are provided in the problem description (Section 4.1) were used. The loading was also done as specified for both NO and NO + SSE conditions and neither WRS nor CFP loading were considered in the analysis. The calculated crack stability results are summarised in Table 5.5 for both postulated crack sizes. The results demonstrate that although the margin on loading is satisfied, the margin on the crack size is not satisfied and this problem does not satisfy all of the LBB requirements. The Bhabha Atomic Research Centre (BARC) results are also summarised in Annex A and further discussed in Section 6.

Table 5.5. Results of BARC LBB calculations

Acceptance criterion	Requirement	Margin
Margin on critical NO + SSE loading at LCS	>1.4	1.9
Margin on critical NO + SSE load at twice the LCS	>1.0	0.2

5.8. Japan (JAEA)

The LBB evaluation procedure prescribed in the current edition of JSME code [19] cannot be applied to a nickel-based weld as specified in the baseline problem because it is potentially susceptible to PWSCC. However, the evaluation approach that is used in a LBB evaluation is subsequently described in greater detail than in Section 3.8.

Two analyses were conducted to determine the TWC that is assessed for crack stability. In the first analysis, an initial surface-breaking semi-elliptical crack was postulated and the crack growth due to fatigue is calculated for this crack until it penetrates the piping wall thickness. The crack growth rate was calculated with the Paris law model with coefficients based on Japanese crack growth test data [55, 56 and 57]. Newman and Raju SIF solutions [58] were used until the crack depth (a) penetrated the piping wall thickness (t). Although the applicable range of this SIF solution was $a/t \leq 0.8$, they are conservative when $a/t > 0.8$. Transient and seismic loads that do not cause a plant shutdown were considered in the fatigue crack growth analysis.

The LCS was determined in the second analysis. The LR associated with this crack was determined by the minimum LRDL multiplied by a safety margin. The LRDL was generally approximately 0.06 kg/s (i.e. 1.0 GPM) so that the LR at the LCS was 5.0 GPM (0.30 kg/s) while considering the margin factor of 5 (Section 3.8). The LR was calculated with varying crack lengths under NO loading in order to determine the LCS. In this calculation, the crack opening area (COA) was calculated by the Tada-Paris method [59]. The critical LR was calculated by the Henry model [53] for pressurised water and by the Moody model [60] for saturated water and steam conditions. The crack surface roughness was considered in both LR calculation approaches.

The longer of the two TWC crack sizes determined by these methods was then assessed for crack stability. A net-section collapse crack stability evaluation method was used for an austenitic stainless steel material and an elastic-plastic fracture evaluation method was used for ferritic and low alloy steels materials. The instability stress was then compared to the applied stress due to combined NO and earthquake loads. Leak-before-break was demonstrated if the applied stress was lower than the calculated instability stress. However, as stated previously, this calculation was not performed because the benchmark problem did not pass the initial LBB screening criteria due to the possibility of PWSCC. Notably, the LBB approach in virtually all the participating countries have a similar screening provision (Section 3). However, other participants suspended this consideration so that the calculations could be performed.

5.9. Korea (KOREAa and KOREAb)

Separate analyses were performed by KOREAa and KOREAb following the Korean LBB approach (Section 3.9), albeit with some different assumptions, input parameters and calculation methods.

5.9.1. KOREAa

An in-house code was used to calculate the COD for the baseline problem. The code is based on the elastic-plastic COD solution that is provided in the Electric Power Research Institute (EPRI) ductile handbook [39]. The code used the weld metal constitutive properties for the COD calculations. The LR was calculated using PICEP [36] and selected the air fatigue crack type from the drop-down menu selection. However, the actual crack morphology parameters associated with this crack type could not be provided.

An in-house code was also used to perform the crack stability analysis. The analysis was based on the J-T failure criterion. The applied J was estimated by using the scheme in the EPRI ductile fracture handbook [39]. The axial force due to pressure loading and the other NO + SSE loads specified in the problem description (Section 4.1) were applied along with a CFP that was equal to half of the internal pressure (i.e. 7.75 MPa) as the equivalent load and moment in the equations for predicting the applied J-integral. The tensile properties of the base metal were used in the analysis, while the J-R curve of the weld metal was considered, which is consistent with standard practice in Korean LBB submittals. However, the J-R curve form required for the in-house code takes the form of Eq. 8. C_1 and C_2 in this equation were again determined by fitting this equation to the form of the J-R curve provided in the input data set (Eq. 2).

The specified LRDL of approximately 0.06 kg/s (i.e. 1 GPM) was assumed, which resulted in an LR of 0.61 kg/s (i.e. 10 GPM) for determining the LCS. The LCS was calculated to be 175.44 mm, while the CCS was determined to be 403.7 mm. The margin of two between the CCS and LCS was therefore satisfied and the criterion for establishing LBB met in this analysis. KOREAa also calculated the bending moment at instability for the LCS for an assumed axial force of 1 337.7 kN of 852.7 kN-m. For the loading and other input parameters described in this Section, KOREAa additionally provided tabulated values for the relationship between the COD, LR and failure moment for a crack with an LR of approximately 0.61 kg/s (≈10 GPM). The KOREAa results are summarised in Annex A and further discussed in Section 6.

5.9.2. KOREAb

An in-house code was used to calculate the COD for the baseline problem. The code is based on the elastic-plastic COD solution provided in the EPRI ductile handbook [39]. The code used the weld metal constitutive properties for the COD calculations. The LR was calculated using LEAPOR with air fatigue crack morphology parameters that were previously developed for SQUIRT [61]. The LR was calculated under the assumption that the crack length and COD at the piping ID, OD and MW are identical.

The crack stability was evaluated using the J-T analysis, which was based on the improved LBB.ENG2 J-estimation scheme [33]. The ψ-function was modified in this scheme to minimise discontinuities in the original ψ-function that was used to calculate the bending moment vs. CCS relationship. The tensile properties of base metal were used in the analysis to conservatively bound the weld joint plasticity. The weld metal J-R curve was also used because it is the location of the postulated crack and also lower than the base metal toughness. This approach is consistent with standard practice in Korean LBB submittals. The axial force due to pressure loading and the other NO + SSE loads specified in the problem description (Section 4.1) were applied, but contrary to the KOREAa analysis, the CFP loading was not considered.

The specified LRDL of approximately 0.06 kg/s (i.e. 1 GPM) was assumed, which results in an LR of 0.61 kg/s (i.e. 10 GPM) for determining the LCS. The LCS was calculated to be 275.74 mm, while the CCS was determined to be 419.3 mm. The margin of two between

the CCS and LCS was therefore not satisfied and LBB is not met in this analysis. KOREAb also calculated the bending moment at instability for the LCS for an assumed axial force of 1 337.7 kN of 693.85 kN-m. For the loading and other input parameters described in this section, KOREAb also provided tabulated values for the relationship between COD, LR and failure moment for a crack with an LR of approximately 0.61 kg/s (≈10 GPM). The KOREAb results are summarised in Annex A and further discussed in Section 6.

5.10. Sweden (KIWA)

The baseline problem was analysed using the Swedish LBB procedure along with governing acceptance criteria, as summarised in Section 3.10. This section summarises the KIWA evaluation, while more detail is provided in Annex C. The analysis utilised the input data and assumptions provided for the problem (Section 4). One novel aspect of the Swedish approach is that the effect of WRS is considered in the analysis. Separate evaluations were performed using two different WRS distributions. The "Benchmark" distribution was the one specified in the problem description (Section 4.1), while the "SSM2018:18" distribution is based on Swedish recommendations from the Swedish Regulatory Body (SSM) [22]. A comparison of these two WRS distributions is presented in Figure 5.2.

x/t is the normalised distance from the piping ID to OD in this figure. There are several differences between the distributions. The SSM WRS distribution is positive at the ID, has a compressive peak at $x/t \approx 0.3$, a tensile peak at $x/t \approx 0.8$ and is slightly negative at the OD. Conversely, the benchmark distribution is negative at the ID, has a weak compressive peak at $x/t \approx 0.3$ and then increases monotonically for $0.4 \leq x/t \leq 1.0$ so that the stress is strongly tensile at the OD.

The KIWA limit used the prescribed LRDL of 0.061 kg/s (Section 4.1) and, as required by the Swedish LBB procedure (Section 3.10), the LR used to determine the LCS is ten times this value (i.e. 0.61 kg/s). In-house software was used to calculate the COD values for a range of crack sizes. Both elastic and plastic COD contributions were included and the weld material properties at the operating temperature were used to determine the plastic COD contribution. The COD values were calculated for NO loading conditions, including the additional stresses applied by each WRS distribution (Figure 5.2) in separate analyses. The crack length and COD values determined above were input into the WinSQUIRT Version 1.3 [62] to perform the LR calculations. The PWSCC crack morphology parameters built into WinSQUIRT were selected, instead of the parameters provided for the benchmark problem (Section 4.1). The crack length values resulting in an LR of 0.61 kg/s were chosen as the LCS for both the benchmark and the SSM WRS distributions.

Figure 5.2. Weld distributions used in KIWA analyses

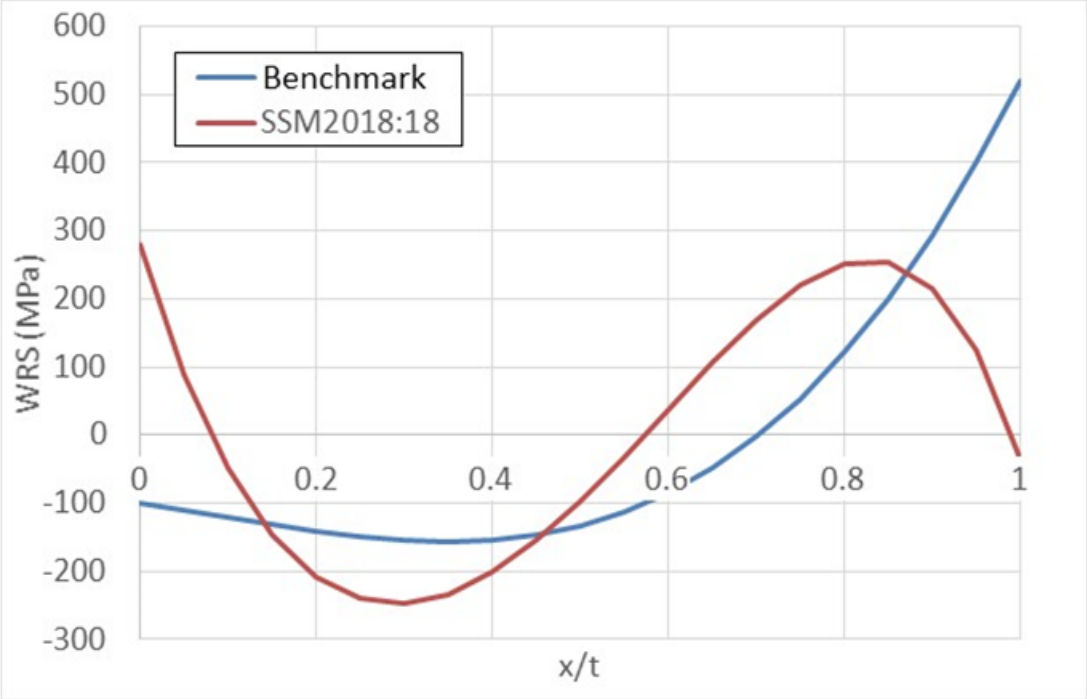

The CCS corresponding to the NO + SSE loading conditions was determined using the ISAAC (Integrity and Safety Assessment of Components) fracture mechanics code [63] that is commonly used in the Swedish nuclear industry. Forces and moments for the NO + SSE loading were transferred into membrane and bending stresses. The softer base metal tensile properties and the more brittle weld metal fracture toughness properties were used in the analysis. The ISAAC code allows for crack stability assessment using several different failure criteria, but a Swedish LBB analysis must use the FAD failure criterion, which is based on an extension of the R6-method that incorporates the addition of WRS in the crack stability calculations [22]. More details on the input stresses and material properties used in this analysis and the crack stability assessment modules provided within ISAAC are provided in Annex C.

The crack initiation values (K_{Ic} and J_{Ic}) are often used to determine the CCS. However, the Swedish approach also allows higher toughness values to be used for very ductile materials, such as austenitic base metals or nickel-based welds, as in the benchmark. This higher toughness value is representative of a maximum of 2 mm of stable crack growth. Although this provision is allowed, the KIWA analysis only considered the crack initiation toughness values (K_{Ic} and J_{Ic}) for conservatism.

The LCS and CCS values calculated for each WRS distribution are summarised in Table 5.6. The baseline results utilise the benchmark WRS distribution, which was consistent with the problem description (Section 4.1). The LCS was 320 mm and therefore the CCS was 268 mm. However, the margin of two between the CCS and LCS was not met for either WRS distribution and LBB was not met by the Swedish requirements. KIWA performed additional sensitivity calculations in order to evaluate the effect of using different strength and fracture toughness values within their LBB analysis, although no permutation led to an acceptable LBB finding. Annex C provides further details. KIWA also provides tabulated values for the relationship between crack length, COD and LR. KIWA also calculated a bending moment at instability for the LCS for an assumed axial

force of 1 337.7 kN of 361.3 kN-m. The KIWA results are summarised in Annex A and further discussed in Section 6.

Table 5.6. CCS and LCS values from KIWA calculation

WRS	MW CCS (mm)		MW LCS (mm)
	NO	NO+SSE	
Benchmark	539.1	267.6	320.4
SSM	538.6	321.7	297.9

5.11. Switzerland (PSI)

The LeakRate_Excel_BetaR1 code was obtained as part of the PARTRIDGE [37] programme and was used to determine the relationship between the LR, crack length and COD in this benchmark. The code employed the Battelle COD model [31, 45, 46 and 64], while the LR was determined using the SQUIRT model, which is described in NUREG/CR-5128 [65]. The code has inputs for the pressure, bending moment, axial force and target leak rate. For the input loads, the code also allows the user to calculate the leak rate for a given crack length. However, in this case, the COD at the inner and outer surfaces also needed to be specified. While the code documentation is not complete, it was believed that the axial force due to pressure could be directly calculated from the input pressure by the code, while the code utilised the half-pressure for the CFP. The LDC was also thought to be fixed as 0.95. The default crack morphology parameters used the parameters provided in NUREG/CR – 6004 [28]. However, the PSI used the code's capability to input user-defined parameters in order to provide the crack morphology parameters that are prescribed by the benchmark.

The LCS was determined for NO loading conditions (Section 4.1) using weld tensile properties to calculate the COD. The PWSCC crack morphology was assumed, also using the prescribed parameters (Section 4.1). For the prescribed LRDL of 0.063 kg/s (i.e. 1 GPM), the LCS calculated at the MW piping thickness was 335.32 mm. As indicated in Section 3.11, an alternative LRDL as low as 0.00556 kg/s (20 kg/hr) has been justified for some Swiss plants. The LCS for this alternative LRDL with the prescribed PWSCC crack morphology parameter was 1 96.85 mm. Detailed sensitivity analyses were also performed to examine the effect of the LRDL and various PWSCC and CF crack morphology parameters on the calculated LCS.

The crack stability calculations were performed with an in-house code that was specifically developed for this benchmark. The code employs the NSC-based failure model. Internal pressure, one-half of the CFP, the bending moment and an additional axial force can be input into this code, together with the failure stress of the material. The PSI performed several different crack stability analyses. The principal method was to use their in-house code with Sf = 429.45 MPa, which is the average of the weld yield and ultimate strengths. In this case, a CCS equal to 528.35 mm (2.888 rad) was obtained. This is the reported value for the PSI benchmark calculations (Annex A).

As a sensitivity analysis, various crack instability sizes were then also determined for the different load combination methods and margins specified in the SRP 3.6.3 (Section 3.1) for the prescribed NO + SSE loading conditions [2]. The NSC model using the SRP 3.6.3 properties for austenitic submerged arc weld were assumed. As required in the SRP 3.6.3, the NO thermal expansion force and moment were combined in order to determine the expansion stress at NO. However, the CFP was not considered in this portion of the analysis. The calculated crack stability sizes (expressed as a crack angle and MW crack length) are summarised in Table 5.7 for each load combination method and required margin (RM).

Table 5.7. NSC instability crack sizes for load combination methods in the SRP 3.6.3

Load combination method	Absolute sum (RM = 1.0)	Algebraic sum (RM = 1.4)	Algebraic sum (RM = 1.0)
Crack angle [rad]	2.253	1.801	2.255
Crack length [mm]	412.2	329.5	412.6

As indicated in Section 3.1, the CCS should be at least twice the size of the LCS for both the absolute and also algebraic summation methods. Additionally, the CCS for the algebraic summation method with a load margin of 1.4 should be greater than the LCS. For the 0.063 kg/s LRDL, none of these criteria were met for any of the CCS values calculated using the principal method (i.e. 5 28.35 mm) or the sensitivity analysis (Table 5.7). However, the required margins are met for all the various CCS values when using the reduced LRDL of 0.00556 kg/s for the assumed PWSCC crack morphology.

The PSI performed several other sensitivity analyses and supplementary calculations in addition to the analyses described in this section. The effect of the CFP internal pressure on the relationship between crack length and the bending moment at failure was assessed. The relationship between the COD, LR and failure moment for a crack with an LR of approximately 0.63 kg/s (≈ 10 GPM) was also calculated. The PSI also calculated a bending moment of 1 017.29 kN-m for the LCS to become unstable under the prescribed axial force of 1 337.7 kN. A simple crack growth assessment was additionally performed to demonstrate that the fatigue crack growth rate is expected to be less than the SCC growth rate. The PSI results are summarised in Annex A and further discussed in Section 6.

5.12. Summary of approaches and tools

A wide range of computational tools, assumptions and approaches were utilised by the benchmark participants. The various computational tools used to calculate COD, LR and assess crack stability are summarised in Table 5.8. In cases where multiple codes are listed and separated by a "/", the code listed first was used in the baseline analysis, while the code listed second was used in at least some part of Tasks 1-4. As seen in the table, a wide variety of tools were employed. Most participants used either commercial codes or codes for calculating the COD that were developed in-house. The common codes used to calculate the LR include PICEP and those that were initially derived from the SQUIRT code, including LEAPOR and the code used by the PSI. There were also a large number of in-house codes for calculating crack stability, even though several participants used various derivatives of the LBB.ENG2 code [32 and 33].

Table 5.8. LBB computational tools

Organisation	COD	LR	Crack stability
BARC	In-house/FEA	In-house	In-house
CEI	In-house	SQUIRT V2.1.3	In-house
EMCC	SQUIRT4/FEA	SQUIRT4/LEAPOR	LBB.ENG2/ NRCPIPE with LBB.ENG2
GRS	WinLeck	WinLeck	PROST
JAEA	FEA	LEAPOR	PASCAL-SP
KOREAa	In-house	PICEP	In-house
KOREAb	In-house	LEAPOR	LBB.ENG2 with psi correction/ in-house
KIWA	In-house	WinSQUIRT V1.3	ISAAC
NRC	xLPR circ_COD DLL	LEAPOR	ENG2 with psi correction
OPG	In-house	SQUIRT V2.0	In-house
PSI	LeakRate_Excel_BetaR1	LeakRate_Excel_BetaR1	In-house
Tractebel	PICEP/Morfeo-Crack	PICEP/LEAPOR	Morfeo-Crack
UJV	PICEP	LeakH	BASLBB
VTT	In-house	LEAPOR	In-house

The LR codes exhibit the least diversity. Unique or in-house LR codes were used by the BARC, GRS and UJV. KOREAa and Tractebel used the PICEP code [36], but it was not clear in either case which one of at least three versions was used. Modifications that have been made to the original PICEP code [36] have not always been clearly documented. The vast majority of the participants used either the SQUIRT or LEAPOR codes. The LEAPOR code was derived from SQUIRT so it could be used as a module in the probabilistic fracture mechanics code, xLPR [29]. A separate standalone executable version of this module was created in advance of this benchmark (LEAPOR-SA) and distributed to interested participants. Most participants used the LEAPOR-SA code and therefore it might be expected a priori that there will be less variability in the LR calculations.

All LBB approaches are fundamentally tailored to ensure that an acceptable margin exists between the LCS for a prescribed LR (and possibly other subcritical crack sizes) and the CCS. Table 5.9 summarises the LR used by each participant to calculate the LCS and provides a high-level summary of the crack morphology that was assumed in the baseline calculations. Annex A provides detailed crack morphology parameters that are consistent with the characterisation used by SQUIRT and LEAPOR (as discussed in Section 4.2; see, for example Figure 4.3 and Table 4.4) for each participant. For many of these LR codes, it was possible to characterise these detailed morphology parameters as being representative of either air fatigue (AF), CF or PWSCC crack morphologies (Table 5.9).

Table 5.9. Principal considerations for LCS calculation

Organisation	LR for LCS (kg/s)	Crack morphology type	Strength properties (B/M/W)	CFP (MPa)	WRS considered
BARC	0.61	CF	W	0	N
CEI	0.61	CF	W	7.75	N
EMCC	0.61	AF	B	0	N
GRS	0.061	CF	B	0	Y
JAEA[1]					
KOREAa	0.61	AF	W	0	N
KOREAb	0.61	AF	W	0	N
KIWA	0.61	PWSCC	W	0	Y
NRC	0.63	CF	W	7.75	N
OPG	0.14	CF	W	7.75	N
PSI	0.63	PWSCC	W	7.75	N
Tractebel	0.30	FF with LDC	M	0	N
UJV	0.61	AF	B	0	NR[2]
VTT	0.63	CF	W	7.75	N

Note:
[1] No quantitative calculations were performed because LBB is not allowed in a system with an active degradation mechanism.
[2] NR = not reported.

However, this characterisation is not consistent with how PICEP treats crack morphology. PICEP uses a more global consideration of the FF and the LDC to characterise different crack types. The FF is proportional to the ratio of the hydraulic diameter against the average roughness [36]. The FF and LDC values are fixed for a given crack type. However, it is not straightforward to relate these parameters to the crack morphology parameters used in SQUIRT/LEAPOR or their high-level crack type descriptions (e.g. air fatigue and corrosion fatigue). Notably, participants used different crack types for the crack morphology in their baseline calculations. It is presumed that the selection of crack type is at the discretion of the applicant as long as it can be appropriately justified within the calculation. Table 5.9 also documents whether each organisation used (W)eld, (B)asemetal or (M)ixture properties for calculating COD and summarises the CFP used in the LCS calculation and if WRS was considered. Different selections were again made in these areas

by the participants in a manner that was consistent with their requirements, past practice, or to model the problem more realistically.

Table 5.10 provides a similar summary of important considerations for the determination of the CCS. While most organisations used EPFM to calculate the CCS, several also employed the NSC method. Several organisations, including GRS, KIWA and UJV, employed a FAD approach to calculate the CCS that used either the R6 [43] or the SINTAP [49] approaches. The CEI and VTT performed both NSC and EPFM analyses (denoted by "All" in Table 5.10) and selected the NSC results because they provided the lowest CCS value, which is in accordance with the LBB requirements in their countries. As in Table 5.9, either (B)asemetal, (M)ixture or (W)eld properties are used to characterise the material's strength and fracture toughness. Some organisations (such as KOREAa and KOREAb) used base metal strength properties with weld fracture toughness for conservatism. The choices for the CFP and WRS for the CCS calculation (Table 5.10) were generally the same as for the LCS calculation (Table 5.9) with the exception of KOREAa, which used the CFP in the LSC calculation, but not the CCS calculation.

Table 5.10. Principal considerations for CCS calculation

Organisation	CCS method (EPFM/NSC)	Strength properties (B/M/W)	Fracture toughness properties (B/M/W)	CFP (MPa)	WRS considered
BARC	EPFM	W	W	0	N
CEI	ALL	W	W	7.75	N
EMCC	EPFM	B	W	0	N
GRS	FAD	B	B	0	Y
JAEA[1]					
KOREAa	EPFM	B	W	7.75	N
KOREAb	EPFM	B	W	0	N
KIWA	FAD	B	W	0	Y
NRC	EPFM	W	W	0	N
OPG	EPFM	W	W	7.75	N
PSI	NSC	W	NA[2]	7.75	N
Tractebel	EPFM	M	W	0	N
UJV	NSC	B	W	0	NR[3]
VTT	ALL	W	W	7.75	N

Note:
[1] No calculations were performed because LBB is not allowed in a system with an active degradation mechanism.
[2] NA = not applicable.
[3] NR = not reported.

6. Baseline problem – collective results and discussion

The previous section summarised the input assumptions, approaches and computational tools used to evaluate the baseline problem. Each participant was requested to determine whether the stated baseline problem meets the leak-before-break (LBB) requirements in their country while employing their chosen evaluation method. Each participant was also asked to provide the leakage crack size (LCS) and critical crack size (CCS) values calculated in this determination, as well as the critical bending moment (CBM) for the LCS. These requested results are summarised in the following section (Section 6.1). Section 6.2 summarises the supplementary results, which were optional or voluntarily supplied as part of the baseline results. Only the common results submitted by several organisations are discussed in Section 6.1, although it is recognised that many of the participants performed interesting sensitivity analyses. A few of these sensitivity analyses are summarised in Annexes B and C.

6.1. Requested results

Table 6.1 summarises the principal quantitative results for the baseline problem. The columns for crack morphology and strength properties in this table have been replicated from Table 5.9 and 5.10 respectively for convenience. Where two different letters are indicated in the strength column, the first letter represents the crack opening displacement (COD) properties used to determine the LCS, and the second letter represents the properties used to determine the CCS. As will be shown, these variables are helpful in generating a better understanding of the results. The LCS and CCS values are the only results that were generally requested, which most organisations provided. Some organisations did not calculate both the LCS and CCS because these values are not explicitly required for a LBB analysis.

Table 6.1. Principal baseline calculations

Organisation	Crack morphology	Strength properties (B/M/W)	Fracture toughness properties (B/M/W)	LCS (mm)	CCS (mm)	F_a (kN)	CBM (kN-m)
BARC	CF	W	W	251	<502	1 381	718
CEI	CF	W	NA	286	471	1 338	1 084
EMCC	AF	B	W	257	360	1 303	732
GRS	CF	B	B	202	260	1 338	553
KOREAa	AF	W/B	W	175	404	1 338	853
KOREAb	AF	W/B	W	276	419	1 338	694
KIWA	PWSCC	W/B	W	320	268	1 338	361
NRC	CF	W	W	284	568	1 338	1 364
OPG	CF	W	W		573		
PSI	PWSCC	W	NA	335	528	1 338	1 017
Tractebel	FF with LDC	M	W	212	460	1 338	985
UJV	AF	B	W	184	397	1 338	770
VTT	CF	W	W	284	<567	1 303	1 098

For example, both the Bhabha Atomic Research Centre (BARC) and the VTT Technical Research Centre of Finland (VTT) calculated the LCS value for their targeted leak rate (LR) and then assessed whether a crack twice the size of the LCS was stable. This crack was not stable in both cases. Consequently, it could be demonstrated that LBB was not met and additional calculations were not needed and thus performed. Similarly, Ontario Power Generation (OPG) initially calculated the CCS value and then determined the LR for a

crack that was half the size of the CCS. OPG was able to demonstrate that this crack had an LR that was greater than the leak rate detection limit (LRDL) by the required margin so that LBB was demonstrated for the baseline problem. Consequently, OPG never calculated the LCS corresponding to their target LR of 0.139 kg/s.

As indicated previously, the JAEA reported no results because the qualitative screening disallowed a consideration of LBB due to the possibility of primary water stress corrosion cracking (PWSCC), which is an active degradation mechanism, in the baseline problem. No further calculations were needed as per the relevant country's requirements. Almost all of the other countries have similar requirements that would technically preclude LBB in the baseline problem, but chose to not invoke them when performing the requested calculations.

Participants were also requested (Section 4.3) to calculate the CBM for the LCS while assuming that the normal operation (NO) + safe shutdown earthquake (SSE) axial force (F_a) was a constant 1 337.64 kN, as prescribed in the baseline problem description. However, as indicated in Section 4.3, this guidance evolved over the course of the project and was not reflected in every participant's calculations. The last two columns in Table 6.1 summarise the results of the CBM calculation. The CBM is indicated in the last column, while the F_a corresponding to this force is identified in the column immediately to the left.

The LCS is plotted against the high-level, crack-morphology type chosen by each participant in Figure 6.1. Notably, the Tractebel results are not included in Figure 6.1 because it is not straightforward to determine how their reported friction factor (FF) and the loss discharge coefficient (LDC) correspond to a specific crack-morphology type. Even without these results, there is, unsurprisingly, considerable scatter in the LCS values. This scatter can be attributed to the target LR used by each participant, the variance in both the implicit and explicit margins applied in the codes used to calculate COD and LR (Table 5.8) and the input parameters and assumptions used to run these codes. For example, the smallest corrosion fatigue (CF) LCS result is from GRS, which used an order of magnitude smaller targeted LR in their calculations than the other participants. However, the GRS LR code (WinLeck), as applied within the KTA methodology, is intentionally conservative [66], which makes considering an additional safety margin on the targeted LR unnecessary.

Another interesting comparison is the KOREAa and KOREAb results because the only substantive difference is that KOREAa used the Pipe Crack Evaluation Program (PICEP) for their LR calculations, while KOREAb used LEAPOR. Each organisation used identical COD input parameters and assumed an air fatigue (AF) crack morphology. However, the two codes characterise crack morphology differently and the impact of these differences appear to lead to significantly different (≈ 60%) LCS values for the baseline problem.

Most of the organisations represented in Figure 6.1 predominantly had a similar target LR for their LCS calculation and used either the SQUIRT or the LEAPOR codes. As previously discussed, the LEAPOR code was based on and evolved from SQUIRT and therefore it is perhaps not surprising that there is less scatter in those remaining LCS results. However, surprisingly the scatter in these remaining results is relatively low. This point is illustrated in Table 6.2. The mean LCS value in this table (LCS_{Avg}) is summarised for each crack type along with the standard deviation (LCS_{SD}), which is reported as a percentage of the mean. Notably, the LCS_{SD} is less than 6% of the mean for each crack type, which is much less than anticipated given that each data point represents calculations from a single organisation using different codes to calculate COD with presumed different input parameters for the parameters that were unspecified in the baseline problem.

Table 6.2. Influence of crack type on SQUIRT/LEAPOR results

Crack type	LCS_{Avg} (mm)	LCS_{SD} (% of LCS_{Avg})	% Increase in AF LCS_{Avg}
AF	266	5	
CF	276	6	3.6
PWSCC	328	3	23

Figure 6.1. Influence of crack morphology on the LCS

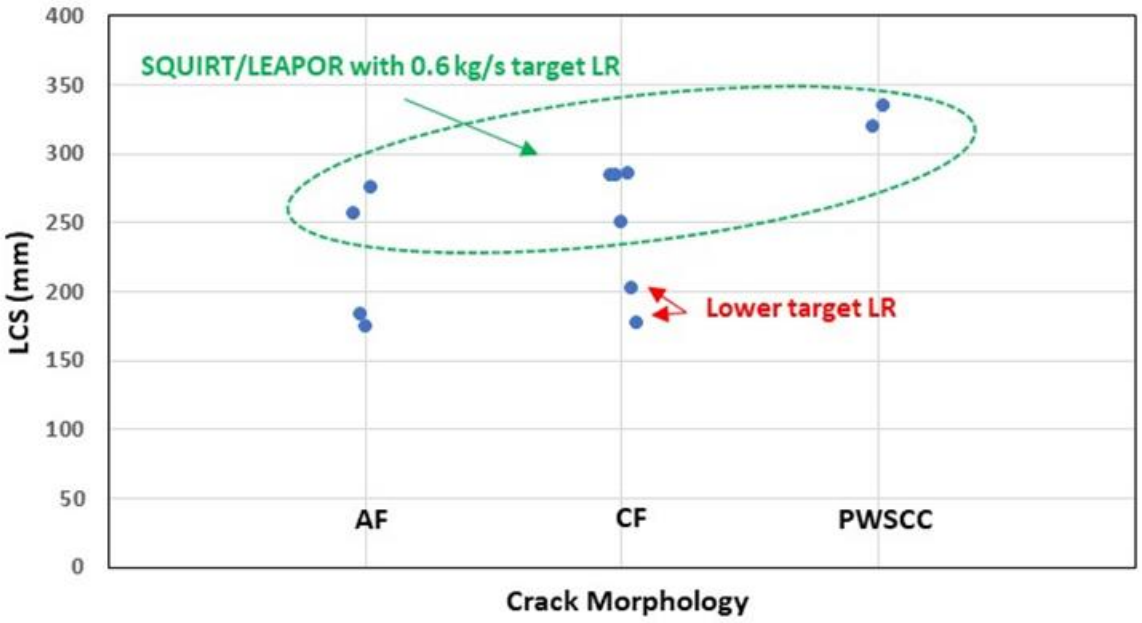

Another interesting result is that the effect of the crack type on the LCS among those remaining results (i.e. those organisations with similar target LRs that predominantly used SQUIRT or LEAPOR) is not as strong as expected. The last column of Table 6.2 provides the percentage increase in either the CF or PWSCC LCS_{Avg} compared to the AF LCS_{Avg}. The CF LCS_{Avg} is less than 4% higher, while the PWSCC LCS_{Avg} is only 23% higher than the AF LCS_{Avg}. These limited results imply (at least for the benchmark problem and similar configurations) that the chosen crack morphology did not significantly affect the SQUIRT/LEAPOR LCS results unless a more tortuous PWSCC morphology was chosen. However, the target LR and choice of the leak rate code appear to be more important reasons for the differences among the participants' baseline problem results.

The LCS and CCS compendium of results (Table 6.1) is illustrated in Figure 6.2. The LCS (orange bars) and CCS (grey bars) values are paired for each organisation. The label above the LCS depicts the strength properties that were used in the COD determination (i.e. B, M or W). The labels above the CCS bars indicate the method (i.e. elastic-plastic fracture mechanics [EPFM], net-section collapse [NSC], or failure assessment diagram [FAD]) used to calculate the CCS on the first line, while the second line summarises the strength properties used in the calculation. All participants used the weld metal fracture toughness in the CCS calculations. Although Candu Energy Inc. (CEI) performed both EPFM and NSC, their reported result was obtained using NSC, which is indicated in Figure 6.2.

Trends apparent in the LCS calculations have been previously discussed, but these values are provided in Figure 6.2 both for completeness and to provide a sense of the ratio between

the LCS and CCS. The average CCS/LCS ratio among participants that calculated both values is 1.8. Since most countries require that CCS/LCS > 2 in order to meet LBB requirements, this average illustrates that the baseline problem would not typically be acceptable. As the LCS increases and/or CCS decreases, the likelihood that LBB can be demonstrated evidently decreases. The reasons for increases in the LCS have been previously discussed, but it is worth noting that LBB was not demonstrated by those participants that assumed a PWSCC crack morphology for the baseline problem.

Figure 6.2. Summary of the LCS and CCS results

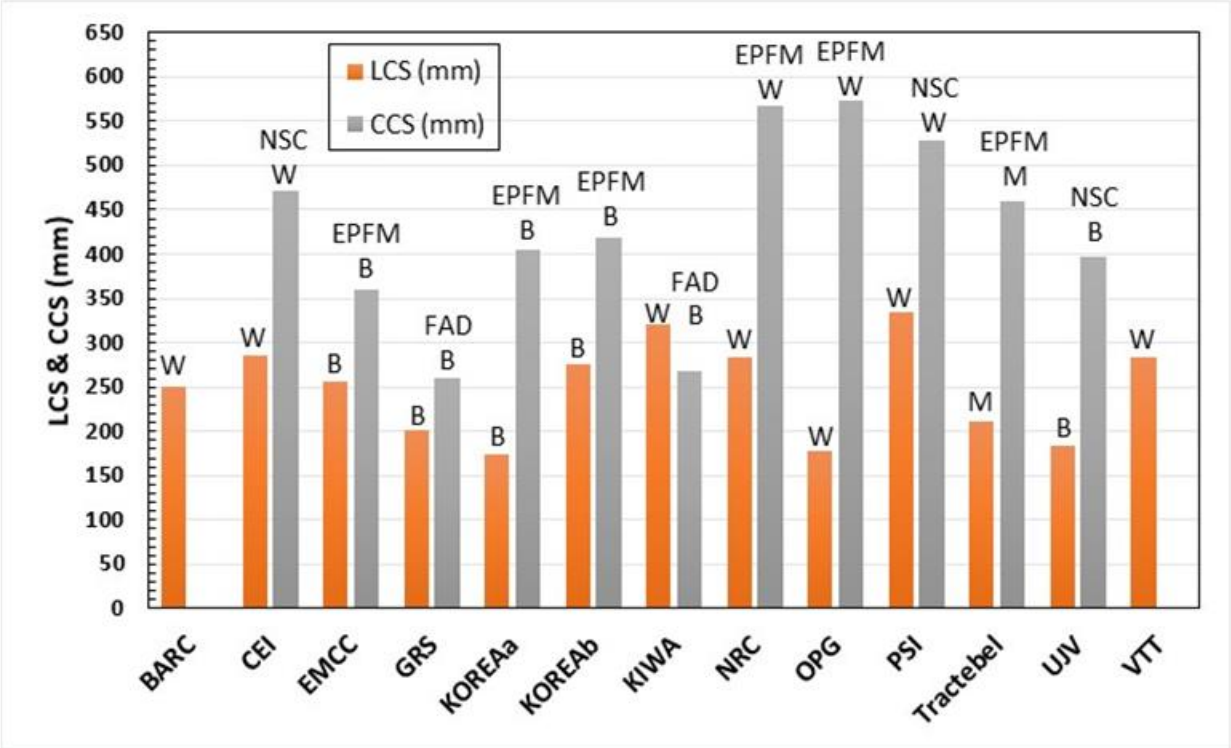

The main purpose of Figure 6.2 is to illustrate trends in the CCS calculation and identify aspects that may cause the CCS to decrease and result in a decreased likelihood of LBB being demonstrated. It is first apparent that using weld properties for both the strength and toughness properties results in a larger CCS than if either base metal or mixture properties are used. This result is unsurprising because the base and weld metals in the baseline problem are ductile. The strength properties thus tend to dictate the calculated CCS values and it is expected that using base metal strength properties, which is a conservative assumption, will result in the smallest CCS.

The CCS values calculated using mixture properties are expected to fall in between the base and weld metal values if all other analysis considerations are equivalent. The CCS trends generally exhibited in Figure 6.2 are that the average EPFM values calculated using weld metal properties are ≈45% greater than the average values calculated using base metal properties. Similarly, the average CCS NSC values calculated using weld metal properties are ≈50% greater than the average NSC and FAD values calculated using base metal properties. This is the biggest single consideration affecting variability in the calculated CCS values.

Some of the differences among participants in their choice of material properties for calculating LBB may exist because several countries require cracks to be considered in the

base metal, weld metal and heat affected zone for a weld configuration, and use the more conservative result. Alternatively, lower bound strength and fracture toughness properties for the weld joint can be used in a single evaluation to accomplish the same objective as postulating cracks in the three separate locations. Several participants adopted this approach and utilised the base metal strength properties and weld metal fracture toughness properties in their evaluations.

It is also apparent that the EPFM approach typically results in a slightly larger CCS than either the NSC or FAD methods for the baseline problem. Organisations performing both EPFM and NSC methods indicated that the NSC CCS values were smaller, or more conservative, and were therefore the results that they reported. For example, the average EPFM weld-calculated CCS values are ≈15% greater than the average NSC weld- calculated values. While these differences are not as great as those resulting from the choice of material properties, they can make a difference in determining whether a marginal LBB configuration, such as the baseline problem, passes the LBB requirements.

There is quite good consistency in the results among organisations that used similar computational approaches and strength properties. This is most apparent in the KOREAb and KOREAa results, as well as the US Nuclear Regulatory Commission (NRC) and OPG CCS results. The remaining variability is due to either intentionally conservative biases in the analysis (e.g. of GRS) or different assumptions or analysis choices that were made by the analyst.

The CBM results (Table 6.1) exhibit some similar trends as the CCS results. It is important to recall that participants were asked to determine the CBM for their LCS using a constant F_a of 1 138 kN. All participants had different LCS values and therefore trends are more apparent by multiplying the CBM by $LCS^{1/2}$. This product is proportional to an elastic stress intensity factor, or K-value. The product of CBM-$LCS^{1/2}$ is illustrated in Figure 6.3, but only for those organisations that used a constant F_a value within 5% of the target 1 138 kN value. As before, the label above each bar indicates the strength properties used by each organisation in their analysis.

These results generally exhibit less variability than the CCS calculations. For example, the uniformity in the predictions for several of those organisations using base metal strength properties (e.g. the EMCC, KOREAa, KOREAb, and UJV) is remarkably good. The effect of choosing base, mixture or weld metal strength properties is also clearer in Figure 6.3, with the weld properties generally leading to the highest CBM values, while mixture properties are expected to fall in between the base and weld metal predictions if the other aspects in the analysis are consistent.

While the trends in the LCS and CCS values are interesting, the fundamental question for each participant was to determine if the baseline problem meets the LBB requirements for their country. Each participant's finding is summarised in Table 6.3. 6 out of 14 participants indicated that the baseline problem meets LBB, while 8 out of 14 participants indicated that the baseline problem does not meet LBB. Table 6.3 also indicates prominent factors that contributed to determining if the LBB requirements are met.

Figure 6.3. CBM calculations for selected participants

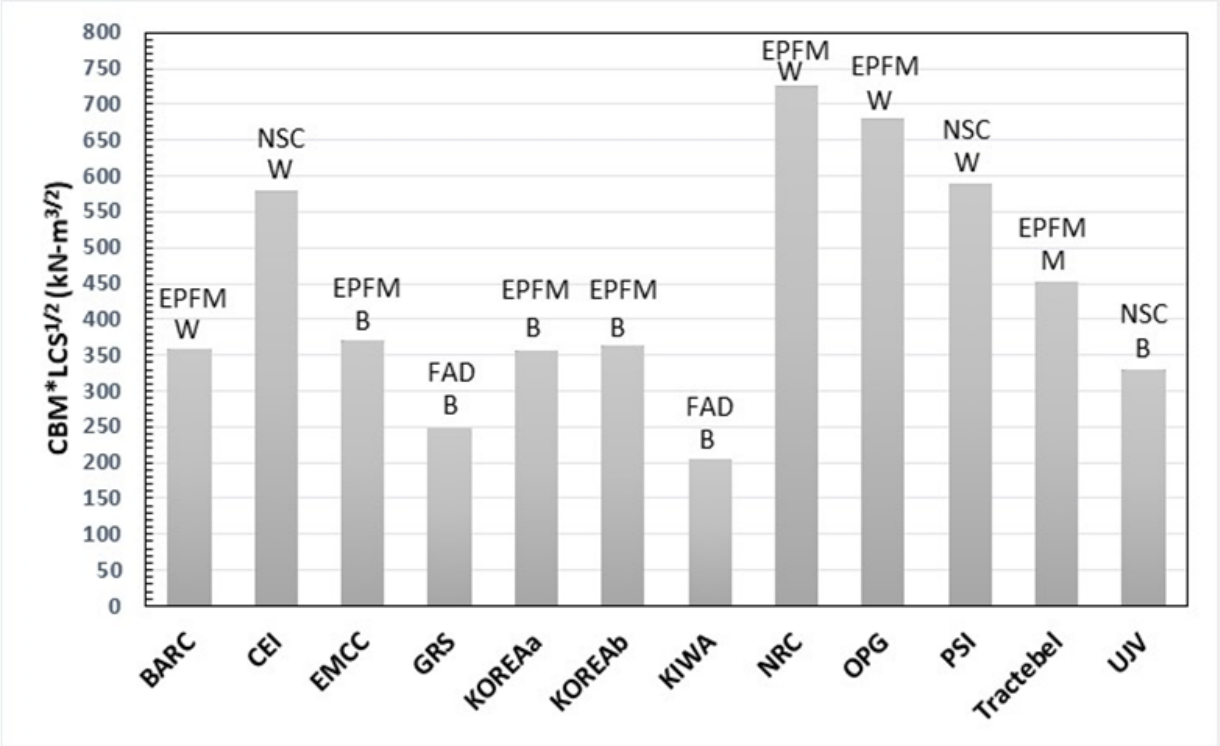

Recall that the NRC designed the baseline problem so that it would just meet the SPR 3.6.3 provisions for the assumptions used in the NRC analysis. The loads were chosen, along with the crack morphology and other analysis considerations so that the CCS/LCS ratio was almost exactly two. The crack was specified in the weld and therefore the NRC chose weld metal properties along with EPFM to calculate the CCS. As seen previously, both these choices lead to increases in the CCS. More conservative choices lead to a lower CCS and this choice is important in determining if LBB is met. In fact, LBB was generally not met for the organisations that used base metal strength properties in their analysis and targeted an LR near 0.61 kg/s for calculating the LCS.

Another important consideration is the selection of the LRDL and associated target LR for calculating the LCS. As described in Section 3, many countries allow either smaller LRDLs or a smaller margin between the LRDL and target LR, with the result that the target LR can be much less than 0.61 kg/s which is used in many initial US LBB applications. Three of the six organisations that indicated that the baseline problem met their LBB requirements (the GRS, OPG and Tractebel) used target LRs that were between two and ten times less than 0.61 kg/s for calculating their LCS value. Two other organisations (the CEI and PSI) indicated that their LBB requirements were not met by the target LR of 0.61 kg/s, but likely would be met if the LRDLs that are allowed in their country (which are about a factor of 10) were evaluated.

Table 6.3. LBB determination for the baseline problem

	LBB met? (Y/N)	Factors contributing to passing or failing LBB analysis	Comment
BARC	No	Relatively small CCS prediction using EPFM with W properties.	
CEI	No	Smaller CCS prediction using NSC with W properties.	Would likely meet LBB requirements if lower Canadian LRDL considered.
EMCC	No	Relatively small CCS prediction using B properties.	Analysis and assumptions performed to be consistent with original United States' LBB submittals.
GRS	Yes	LRDL was a factor of ten less than 1 GPM (0.06 kg/s).	
JAEA	No	LBB is not allowed in system with active degradation mechanism (i.e. PWSCC).	Quantitative analysis not required; system screens out due to PWSCC.
KOREAa	Yes	Chosen air fatigue crack morphology parameters resulted in relatively small LCS.	
KOREAb	No	Smaller CCS prediction using B properties coupled with CF crack morphology.	
KIWA	No	Relatively small CCS prediction using FAD with B properties and consideration of WRS with PWSCC leading to large LCS.	
NRC	Yes	Large CCS prediction using EPFM with W strength properties.	Analysis conditions and input parameters set to just meet LBB in NRC analysis.
OPG	Yes	LRDL was a factor of five less than 1 GPM (0.06 kg/s).	
PSI	No	Increased LCS prediction using PWSCC crack morphology coupled with smaller CCS predictions using M properties.	Would likely meet LBB requirements if lower Swiss LRDL considered.
Tractebel	Yes	LRDL was a factor of two less than 0.06 kg/s.	LBB would not be met using the specified LRDL of 0.06 kg/s.
UJV	Yes	Relatively small LCS prediction, likely influenced by selected morphology parameters.	
VTT	No	Smaller CCS prediction using NSC with W properties.	

A further important consideration in determining if the LBB requirements were met for the baseline problem is the crack morphology evaluated. Crack morphology affects the LCS; a smoother crack morphology leads to a smaller LCS, making it more likely to meet the LBB requirements. The LBB requirements were not met for either of the participants (the KIWA and PSI) that evaluated a PWSCC crack morphology, while the organisations reporting acceptable LBB results (KOREAa and UJV) apparently evaluated relatively smooth air fatigue morphology parameters when determining their LCS.

Another potentially important consideration is weld residual stress (WRS) when determining the LCS. Only KIWA rigorously considered WRS effects when determining the LCS. Their reported results considered the WRS distribution provided (Figure 4.4) but also performed sensitivity analyses using the WRS distribution prescribed in the SSM requirements (Figure 5.2). While it is difficult to generalise findings based on this single evaluation, it is worth noting that the CCS/LCS ratio from the KIWA results was less than one and was the lowest of any participant for both WRS distributions considered. WRS effects are further considered in Section 8.

6.2. Supplementary results

Several participants (the GRS, KIWA, NRC, OPG and Tractebel) provided the relationship among the LR, COD and crack length for the prescribed loading parameters in the baseline

problem. This relationship fundamentally determines the COD and crack length at the target LR, which determines the LCS. The following figures summarise this relationship.

The relationship between crack length and COD for the prescribed loading condition is depicted in Figure 6.4. These results are not sensitive to the crack morphology used in the evaluation and therefore offer a better indication of WRS effects and other differences in the approaches followed by each organisation. It is assumed that the reported COD values are mid-wall crack opening displacement (MWCOD) values. Only the KIWA results are likely to have a significant difference between the inner diameter crack opening area (ICOD), MWCOD and outer diameter crack opening area (OCOD) values due to their consideration of WRS effects. The GRS results are the most conservative (they are intentionally conservative [67]) because longer crack lengths are needed to reach a prescribed COD, while the NRC, OPG and KIWA results are the least conservative. Tractebel's results fall in between. The KIWA results using the benchmark WRS are similar to the NRC results, which do not consider WRS effects. This is likely simply due to compensating aspects between the two different analyses. The SSM WRS is also less conservative than the benchmark WRS that provides a larger COD for a given crack length.

The relationship between the LR and crack opening area (COA) is most useful for examining differences among the LR codes and associated analysis assumptions, such as crack morphology. Notably, KIWA and NRC used SQUIRT/LEAPOR LR codes, while Tractebel used PICEP and GRS used WinLeck (Table 5.8). Furthermore, GRS and the NRC considered a CF-type morphology, while KIWA considered a PWSCC-type morphology (Table 5.9). Tractebel's morphology was based on the friction factor (FF) with LDC, which cannot easily be translated to a high-level morphology type. The COA was provided for the GRS results. For the other results, the COD was assumed to be elliptically distributed along the crack length with the maximum value at the midpoint of the crack having a length of 2c. The crack length and COD were also assumed to be constant through the thickness. Following these assumptions, the COA is simply π(COD/2)c.

Figure 6.4. Through-wall circumferential crack (TWC) length vs. COD for baseline problem

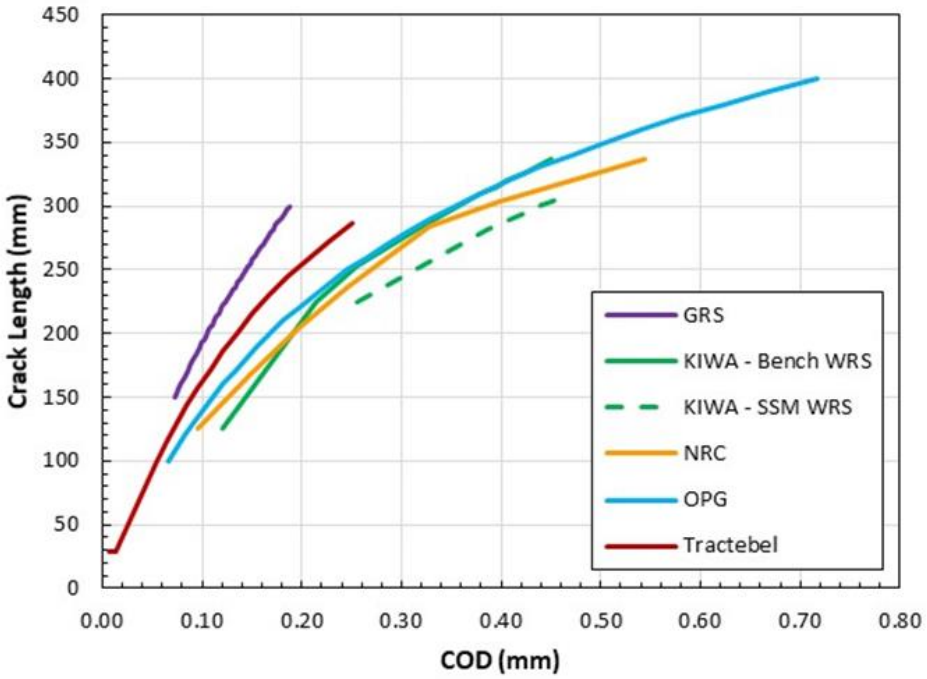

Figure 6.5 illustrates the LR vs. COA relationship. Notably, the following LR codes were used by the respective participants: OPG and KIWA used SQUIRT, the NRC used LEAPOR, GRS used WINLECK and Tractebel used PICEP. The KIWA results are the most conservative (i.e. lower LR for a given COA), which is unsurprising because they utilised the PWSCC morphology that should lead to the lowest leak rate for any of the considered morphologies. As expected, WRS also does not influence the LR vs. COA relationship. The KIWA, OPG and NRC used LR codes with a similar pedigree and therefore the difference between these results naturally can arise from the different crack morphology parameters used by each organisation in the analysis. The ordering of the results supports this contention because the KIWA considered the roughest crack, while the OPG crack was the smoothest of the three participants.

However, crack morphology is expected to cause differences at low values of COD when COD and μ_G have similar orders of magnitude. Once COD >> μ_G, the crack morphology effects on LR should be insignificant. However, this trend is not evident in Figure 6.5 because the differences between the NRC and KIWA results are small for COA < 50 mm^2, while the differences become more significant at higher COA values and the NRC results align more closely with the OPG results. Additionally, the OPG and KIWA LR vs. COA relationships are smooth, whereas the NRC relationship has an inflection point at an LR of approximately 0.5 kg/s. This finding perhaps implies that there are more fundamental differences between the SQUIRT and LEAPOR LR codes used by the KIWA, OPG and NRC respectively.

Figure 6.5. Leak rate vs. crack opening area for the baseline problem

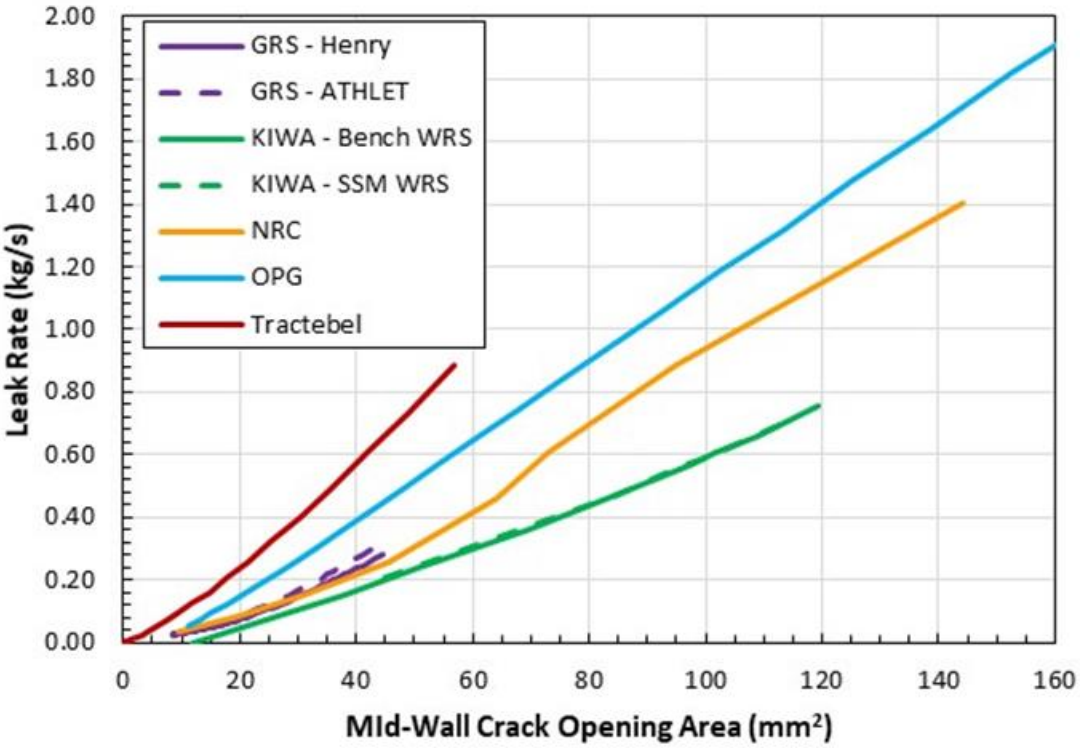

The NRC and GRS LR vs. COA relationships are surprisingly similar, at least out to the final COA that GRS reported. Both organisations assumed a CF crack morphology, so this similarity implies that the WinLeck and LEAPOR codes, at least within the benchmark

problem's flow regime, lead to similar LR predictions. GRS also conducted a sensitivity analysis using the Henry and ATHLET flow-rate models. However, as depicted in this and subsequent figures, there is little difference between the results. The Tractebel LR model provides the highest LR for a given COA but this may be due the crack morphology parameters selected for the baseline problem.

Figure 6.6. then illustrates the LR as a function of the TWC length. The GRS results are the most conservative (i.e. lower LR for a given crack length), but this is expected due to their intentionally conservative COD vs. crack length relationship (Figure 6.4), which compensates for the fact that no additional margin is included in the acceptance criteria. The KIWA results indicate that the benchmark WRS distribution appears to be more conservative than the SSM WRS distribution because the benchmark distribution predicts a lower LR for a given crack size.

It is again interesting to compare the NRC, OPG and KIWA results because they all used LR codes from the SQUIRT/LEAPOR family but considered different crack morphology types. KIWA also incorporated the WRS effects. As expected, the KIWA results are more conservative than the OPG and NRC results because they explicitly considered WRS effects and used a PWSCC morphology. The NRC and KIWA results are analogously quite consistent with the COA results (Figure 6.5) for crack lengths that are less than between 200 and 250 mm. However, when the crack length is greater than 250 mm, the KIWA results start to significantly deviate from the NRC-predicted LR curve, while the NRC curve correlates with the OPG result.

Figure 6.6. LR vs. TWC length for the baseline problem

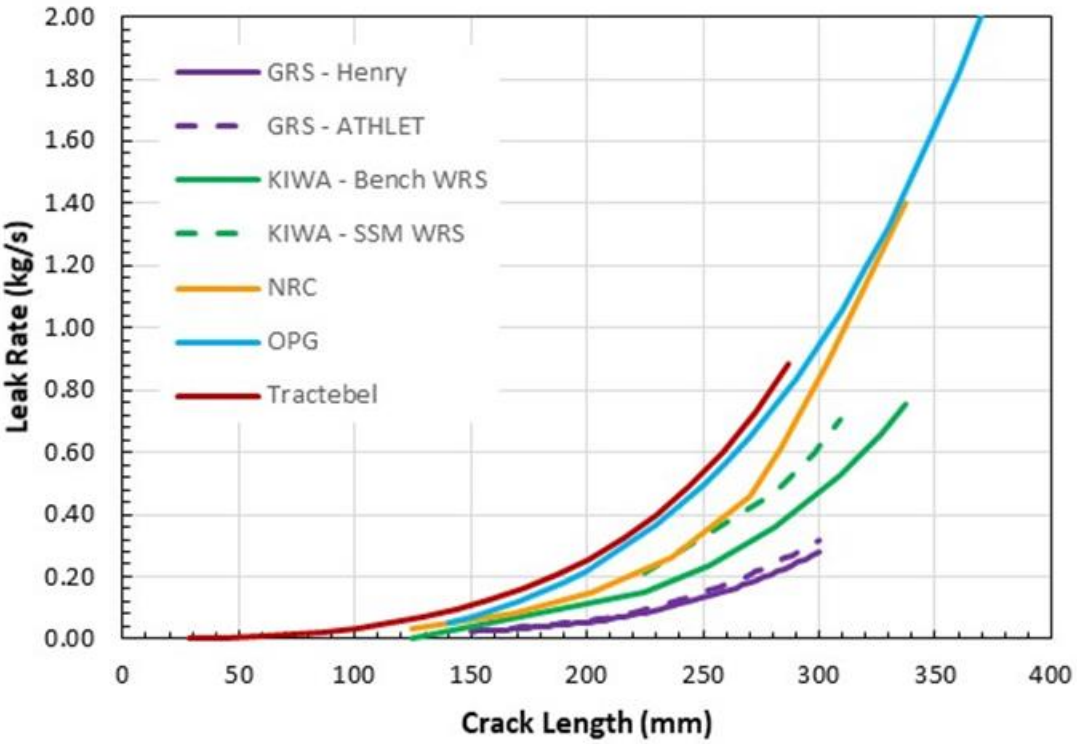

Another supplementary result that was provided by six participants (GRS, KOREAa, KOREAb, the NRC, OPG and PSI) is the CBM as a function of the TWC length (Figure 6.7). This relationship was used by participants to determine the CCS for the NO + SSE

loads. The results fall into one of two groupings based on whether the base or weld metal strength properties were used in the analysis. As mentioned previously, the lower strength base metal properties result in smaller predicted CCS values for a specified CBM. The use of the EPFM also leads to a larger CBM (Figure 6.7) than predicted by a NSC failure model. However, as previously discussed, the effects are less significant than the differences related to the material property selection.

While there is significant variability in the CBM vs. CCS relationship, the variability among results for a selected failure model (i.e. the nominal pipe size [NPS] or EPFM) and selected material type (i.e. B, M or W) appears to be less than the variability that exists among the LR, COD and crack length relationships (Figure 6.4 – Figure 6.6), which are used to determine the LCS. This finding is not surprising because the CCS methodology is more mature, has stronger verification and is simpler than the determination of the LCS, which requires separate COD and LR calculations. For example, the CCS predictions are not significantly affected by localised parameters such as crack morphology, WRS and – to a lesser extent – COD. However, as has already been demonstrated, these localised parameters can significantly affect the LCS calculation.

Figure 6.7. CBM as a function of TWC length for the baseline problem

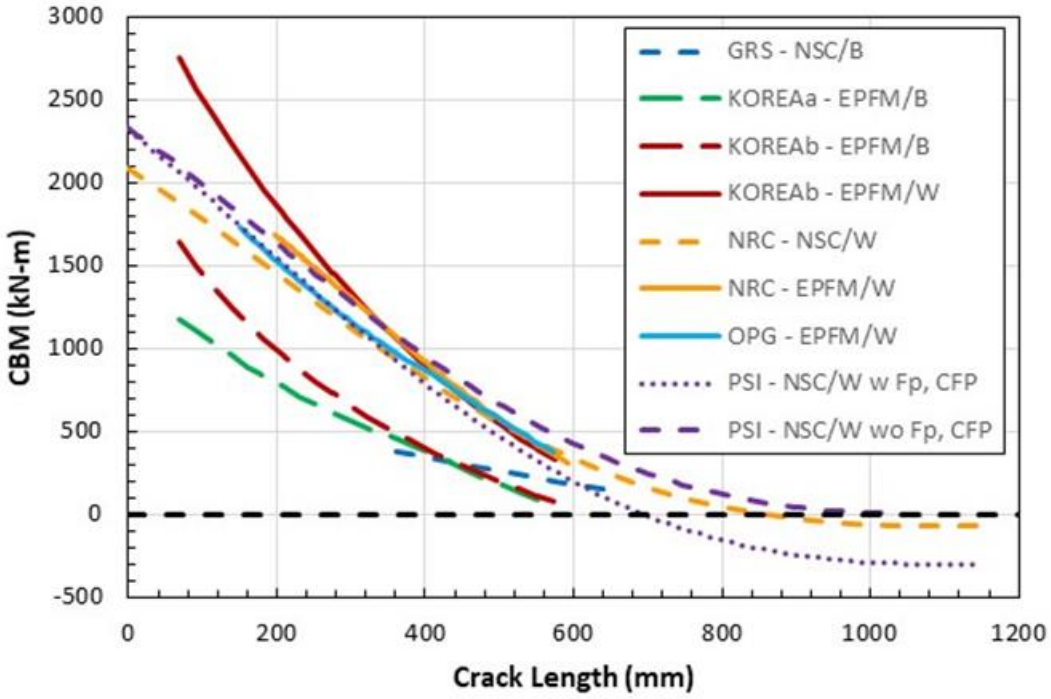

Figure 6.7 also show the results of a sensitivity study performed by the PSI to examine the effects of considering just the deadweight and thermal loading (F_{adt}) in the CBM calculation (the PSI curve wo F_p and crack face pressure (CFP) in Figure 6.7) compared to considering F_{adt} in addition to the axial force due to pressure (F_p) and CFP (the PSI curve w F_p and CFP in Figure 6.7). These effects are more easily evaluated by plotting just the PSI results (Figure 6.8). Including all three loading sources (i.e. F_{adt}, F_p and CFP) obviously results in the lowest CBM for a given crack length. However, the effect of CFP is generally not significant for crack lengths of practical interest (i.e. <<10% effect for crack lengths

< 500 mm). The consideration of Fp becomes significant at much smaller cracks (i.e. ≈10% effect when crack length is 150 mm) and becomes an important consideration for cracks of lengths > 150 mm in CCS calculations associated with this benchmark problem.

Participants were also asked to provide the relationship between the COD, crack length and bending moment for the prescribed target LR of 0.61 kg/s if these results were easily available. Exploring this relationship for a constant LR provides a different context than is commonly reported in LBB evaluations and these results were thought to better illuminate the role of factors that are important in LCS determination. Four participants, KOREAa, KOREAb, the NRC and PSI, provided these results at a target LR of 0.61 kg/s. GRS also provided these results, but because their target LR was 0.061 kg/s, it is difficult to evaluate their results alongside those of the other participants and they are thus not further considered in this section.

Figure 6.8. Effect of loading sources on the CBM

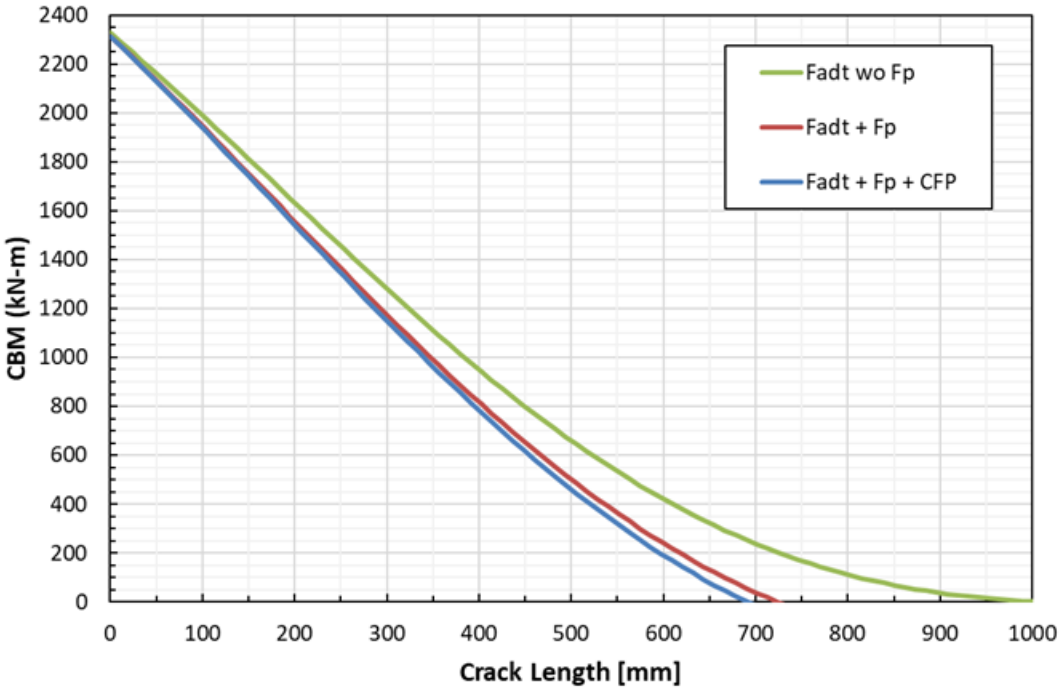

Figure 6.9 illustrates the relationship between the crack length and COD, while Figure 6.10 and Figure 6.11 plot the bending moment vs. the COA and crack length respectively. The COA was determined from the results exactly as for the earlier COA results (Figure 6.5). All four of these participants used the weld metal strength properties for determining COD (Table 5.8 and Table 5.9), although KOREAb also performed sensitivity calculations using base metal strength properties, which are also included in the figures.

The NRC and PSI used similar tools for calculating the COD, while the LR was determined using LEAPOR and SQUIRT respectively. The KOREAa and KOREAb analyses for determining the LCS were very similar. Both used the same in-house code to calculate COD. The principal difference is that KOREAa used PICEP for LR calculation, whereas KOREAb used LEAPOR. The most interesting systematic differences among these relationships are the crack morphology choices: KOREAa and KOREAb used AF (with different morphology parameters), the NRC used CF and PSI used PWSCC crack types for the COD, crack length and bending moment calculations for the 0.61 kg/s target LR.

These figures clearly depict the importance of the crack morphology in predicting the conditions leading to the target LR in the baseline problem. The COD and crack length relationship (KOREAb result shown in Figure 6.9) appears to follow the same relationship – regardless of the strength properties used – but, as expected, the lower strength base material produces the target LR at a shorter crack length. The rougher, more tortuous PWSCC morphology used by the PSI requires a larger combination of crack length and COD in order to achieve the target LR than the other crack types. For example, the PWSCC morphology typically requires more than twice the COD as an AF crack in order to achieve the target LR.

Figure 6.9. COD vs. crack length relationship for the target LR

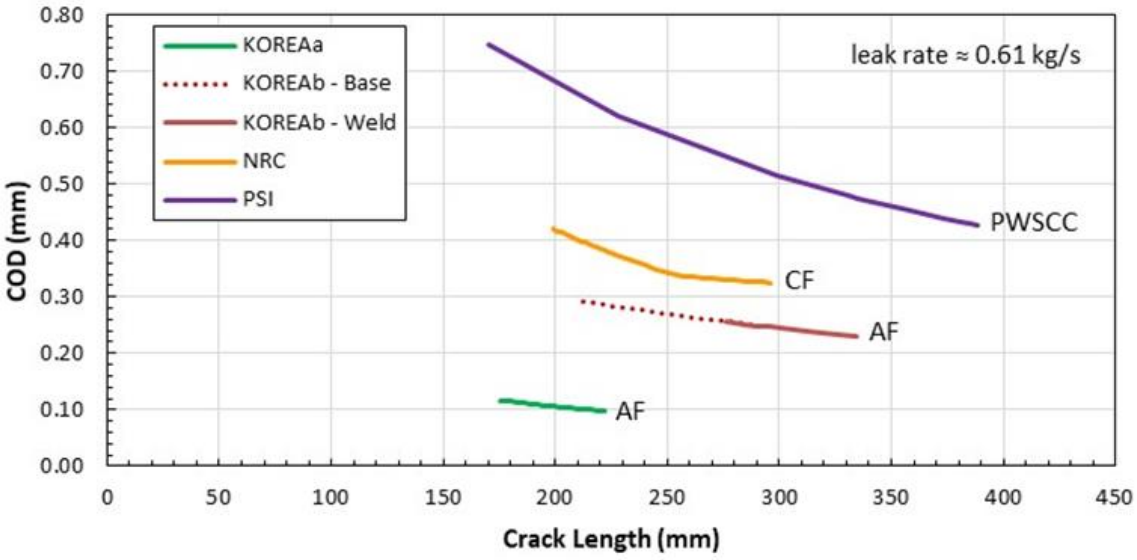

Figure 6.10. Bending moment vs. COA for the target LR

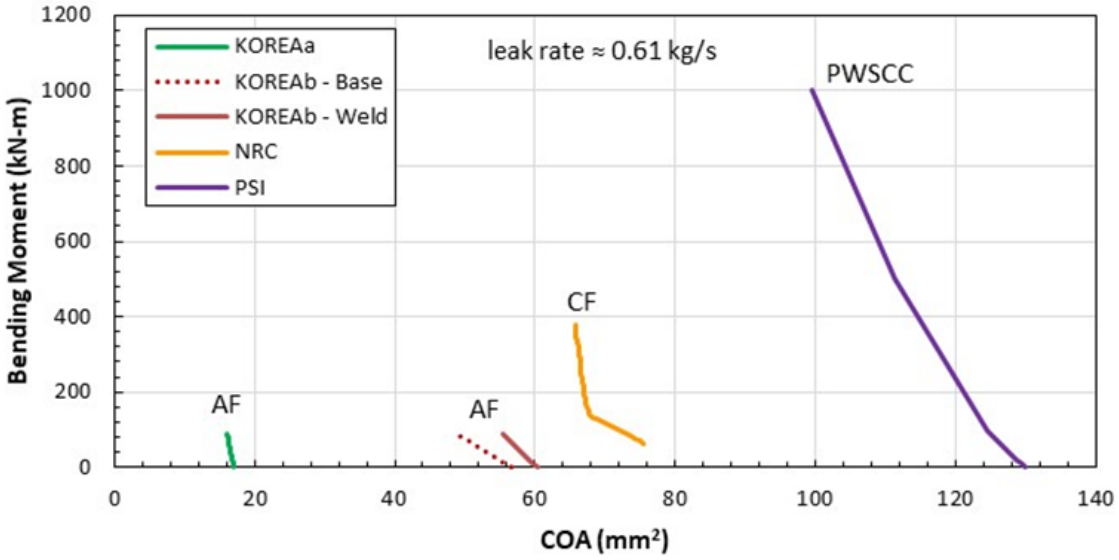

Figure 6.11. Bending moment vs. crack length for the target LR

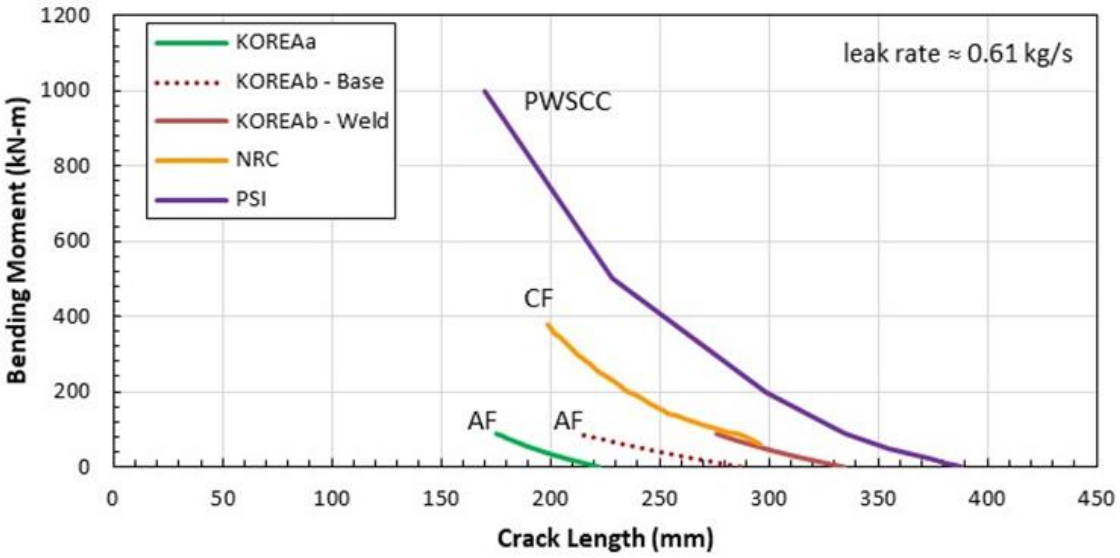

There are also significant differences between the relationships predicted by KOREAa and KOREAb for an AF crack type. However, it is speculated that the AF morphology that KOREAb used in LEAPOR is likely to be rougher than the AF morphology that KOREAa used in PICEP. KOREAa's evaluation of the baseline problem notably met the LBB requirements, while the KOREAb evaluation did not satisfy their LBB requirements. Both organisations calculated similar CCS values, but significantly different LCS values. The differences in the morphology parameters may be a principal underlying reason for the reported LCS differences between the two results.

The significant effect of crack morphology is also exhibited in the bending moment plots (Figure 6.10 and Figure 6.11), although these relationships also illustrate the role of the material strength properties used in the analysis. For a prescribed bending moment (Figure 6.10), rougher cracks required higher COA values in order to achieve the target LR. The effect can be significant because the PWSCC COA value is between two and ten times greater than the AF COA values at a prescribed bending moment. The material strength used in determining the COD also has an effect, although much less of an effect than crack morphology because stronger materials require a higher bending moment in order to achieve the prescribed LR for the required COA. Similarly, for a given crack length (Figure 6.11), the required bending moment to achieve the target LR is significantly increased (i.e. typically > two times) for the PWSCC morphology. The higher strength material also requires a greater bending moment to achieve the target LR at a prescribed crack length, although, similar to before, the effect is not as significant as for the crack morphology.

7. Tasks 1-4 – approach and individual results

This section summarises the approach each organisation used to solve Tasks 1-4. Many of the computational tools employed for the baseline problem are also applicable to these tasks summarised in Table 5.8. Only those tools unique to Tasks 1-4 are highlighted in this section. The consideration of weld residual stress (WRS) effects is the most novel aspect of the Task 1-4 problems because it is not standard practice in most leak-before-break (LBB) analyses. Many organisations therefore performed separate analyses in order to determine the effect of WRS on crack opening displacement (COD) and may have also needed to modify existing computational tools to allow for WRS inputs. The individual results provided by each organisation for these tasks are also provided in this section for completeness. However, a more rigorous comparison and evaluation of these results is contained in Section 8.

7.1. United States (NRC and EMCC)

Separate analyses were performed by the US Nuclear Regulatory Commission (NRC) and Engineering Mechanics Corporation of Columbus (EMCC) and the most significant difference is that the EMCC used a finite element analysis to evaluate COD both with and without WRS, whereas the NRC employed a simplified analytical approach to address the WRS contribution to COD.

7.1.1. NRC

Basic COD calculations were performed using the dynamic link library (DLL) module that was developed for the xLPR probabilistic fracture mechanics piping integrity code [31]. The elastic and plastic contributions to the total COD were determined from the external axial force, bending moment and pressure provided in the input parameter spreadsheet. The COD module internally calculates crack face pressure (CFP) as one-half of the internal pressure and adds the axial force due to internal pressure. The Ramberg-Osgood parameters provided for the weld metal were used to estimate the plastic contribution to COD. This approach was sufficient for determining the COD values in Tasks 1 and 3, but the COD module does not account for the effect of WRS.

The effect of WRS on COD in Tasks 2 and 4 was therefore estimated using an approach developed by Olson [68] that modelled the pipe as an elastic, edge-moment-loaded plate with a fixed boundary condition opposite from the loaded edge (i.e. down the length of the pipe) and simply supported boundary conditions on the other two edges (i.e. the opposing crack tips). The resulting closed-form calculated COD was then modified by a single scaling factor that minimised the differences among the ensemble of outer diameter (OD), mid-wall (MW) and inner diameter (ID) CODs from 48 FEA cases that evaluated a wide range of piping radius to thickness (R/t) values and crack length angles. The COD resulting from the WRS distribution was then simply added to the inner diameter CODs (ICODs) and outer diameter CODs (OCODs) determined using the xLPR COD DLL module, which presumes that the COD remains elastic. While this approach is simple and closed-form (i.e. no FEA is required), ongoing work has shown that this methodology does not accurately calculate the WRS COD effects.

The leak rate (LR) was determined using the LEAPOR [29] code and inputting the ICOD and OCOD values determined above, along with the ID and OD crack lengths, internal and external pressures, temperature, piping wall thickness and crack morphology parameters

that are provided in the input parameter spreadsheet. An elliptical crack mouth shape was assumed for all LR calculations. The critical bending moment (CBM) was determined, as discussed previously in Section 5.1, using the LBB.ENG2 code [32 and 33]. The weld metal properties were used for the strength and fracture toughness properties in both the COD and crack stability calculations.

The COD, LR and CBM results calculated by the NRC from each task are summarised in Table 7.1. Notably, the CBM was not affected by either the crack morphology or WRS selections. The crack morphology also did not impact the COD estimates. The COD values for Tasks 1 and 3 are thus identical, as are the values for Tasks 2 and 4; the LR is the only parameter affected by both crack morphology and WRS.

Table 7.1. NRC results for Tasks 1-4

	Task 1 CF wo WRS	Task 2 CF with WRS	Task 3 PWSCC wo WRS	Task 4 PWSCC with WRS
ICOD (mm)	0.079	0.064	0.079	0.064
MWCOD (mm)	0.096	0.096	0.096	0.096
OCOD (mm)	0.116	0.131	0.116	0.131
LR (kg/s)	0.03343	0.032145	0.028304	0.026563
CBM (kN-m)	1927.94	1927.94	1927.94	1927.94

7.1.2. EMCC

Finite element (FE) analysis was used to determine the through-thickness COD for these tasks. An in-house mesh generator, PipeFracCAE, was used to generate a quarter-symmetry model mesh of the piping configuration and assumed crack, while the FE was conducted using ABAQUS. The prescribed input parameters for normal operation (NO) loading and operating conditions (i.e. 15.5 MPa internal pressure, 340°C temperature, 1.3 MPa axial loading and 7.75 MPa crack face pressure) were employed. The effect of the WRS on the COD (Tasks 2 and 4) was determined using the same FE model. The third-order polynomial prescribed in the input data set was mapped to a temperature distribution. This temperature distribution was then applied to the FE model through the ABAQUS user subroutine UTEMP along with the NO loading and operating conditions in Tasks 1 and 3.

LEAPOR was used to calculate the LR for the given crack size, and the ICOD and OCOD values were calculated using FE and the prescribed crack morphology parameters. Sensitivity analyses were also performed to calculate the LR by using either the default crack morphology parameters in LEAPOR or the mid-wall crack opening displacement (MWCOD) values calculated from the FE analysis.

The bending moment at crack instability was calculated using NRCPIPE [32] by converting the NO + safe shutdown earthquake (SSE) axial force to an equivalent pressure, which was then added to the internal pressure. As specified in the problem description, the equivalent axial force was held constant at 1 337.64 kN and only the bending moment was varied to determine the CBM at instability. Calculations were made with both the algebraic and absolute load summation methods, but there were insignificant differences and this report only provides the algebraic summation results. In both the COD and crack stability calculations, the base metal properties were used for the material strength, while the weld properties were used for the fracture toughness.

A summary of the EMCC results for Tasks 1-4 is provided in Table 7.2. As before, the CBM was not affected by either the crack morphology or WRS and crack morphology did not impact the COD estimates. The sensitivity analyses found that the predicted LR

increases (by less than 20%) when using the default crack morphology parameters in LEAPOR instead of the prescribed parameters. Similarly, the predicted LR decreases (by less than 20%) when the MWCOD values are used instead of the ID and OD values.

Table 7.2. EMCC Task 1 – 4 results

	Task 1 CF without WRS	Task 2 CF with WRS	Task 3 PWSCC without WRS	Task 4 PWSCC with WRS
ICOD (mm)	0.08969	0.05295	0.08969	0.05295
MWCOD (mm)	0.1019	0.09579	0.1019	0.09579
OCOD (mm)	0.12448	0.19449	0.12448	0.19449
LR (kg/s)	0.03998	0.0373	0.03281	0.02963
CBM (kN-m)	1 186.6	1 186.6	1 186.6	1 186.6

7.2. Belgium (Tractebel)

The COD was computed by the Morfeo/Crack code for the 125 mm crack size under NO loading for all tasks. The WRS effects were assessed in Morfeo/Crack by inputting an initial stress profile into the model and then comparing the crack plane stresses after plasticity with the prescribed WRS distribution. The input stress profile was iterated until the crack-plane WRS matched the prescribed WRS distribution. A comparison of the iterated and prescribed WRS distributions is provided in Figure 7.1. It should be noted that the convergence to the prescribed WRS solution is both time consuming and mesh dependent. There currently is no straightforward methodology for efficiently prescribing a complex WRS profile.

The COD value at the MW was then input into LEAPOR for calculating the LR for all tasks using the prescribed crack morphology parameters. Crack stability was assessed with Morfeo/Crack by using a J-integral tearing modulus (J-T) approach with a constant NO + SSE axial force of 1 337 kN to determine the CBM. Base/weld metal mixture properties were used for the fracture toughness in both the COD and crack stability calculations. The CFP contributions were not considered because it was not possible to apply this type of load in Morfeo/Crack elastic-plastic fracture mechanics (EPFM) analyses with the version (version 3.0.2) used for the benchmark calculations. However, the latest Morfeo/Crack version (version 3.2.1) that has been qualified by Tractebel allows for the different CFP profiles to be applied in EPFM analyses as well. The COD, LR and CBM results that were calculated by Tractebel for each task are provided in Table 7.3. Once again, the CBM was not affected by either the crack morphology or WRS and crack morphology did not impact the COD estimates.

Figure 7.1. WRS distribution determined using the iteration of Morfeo/ crack stress input

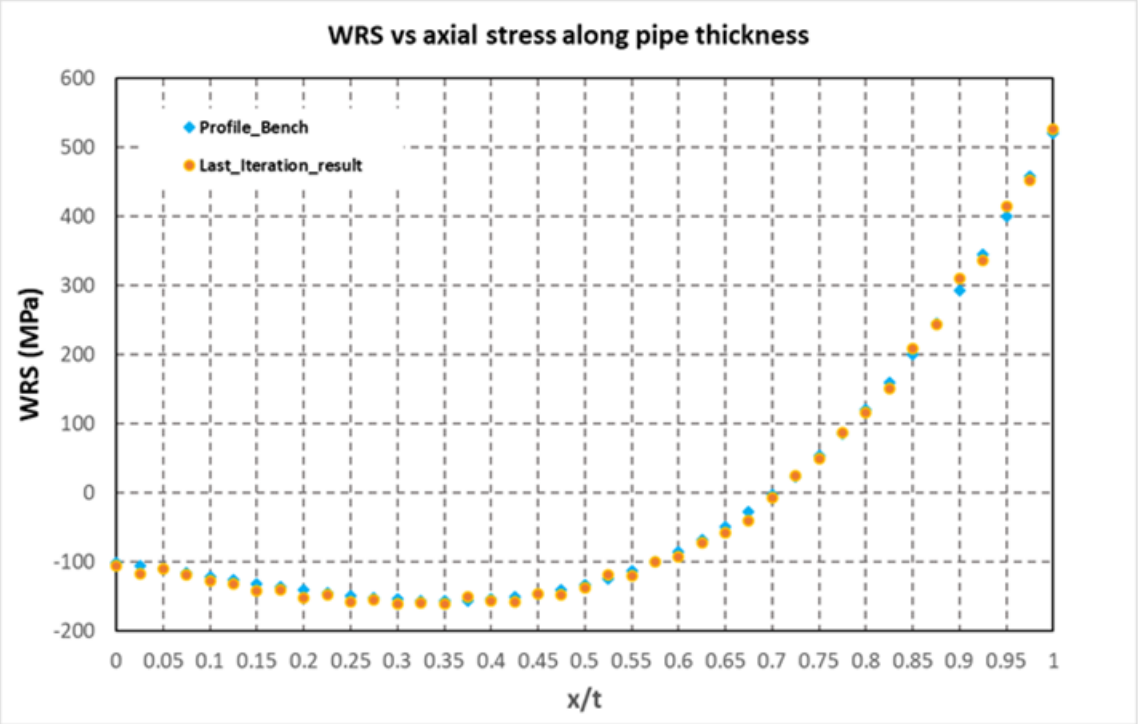

Table 7.3. Tractebel Task 1 – 4 results

	Task 1 CF wo WRS	Task 2 CF with WRS	Task 3 PWSCC wo WRS	Task 4 PWSCC with WRS
ICOD (mm)	0.063	0.055	0.063	0.055
MWCOD (mm)	0.074	0.075	0.074	0.075
OCOD (mm)	0.087	0.120	0.087	0.120
LR (kg/s)	0.0208	0.0211	0.0199	0.0203
CBM (kN-m)	1 300	1 300	1 300	1 300

7.3. Canada (CEI and OPG)

Separate analyses were performed by Candu Energy Inc. (CEI) and Ontario Power Generation (OPG). As described in Section 5.3, they used different tools to calculate the COD and CBM for the prescribed crack size. They also used different methods to incorporate the WRS effects into their COD calculations. These differences are described in greater detail in the subsequent subsections.

7.3.1. CEI

The models and approaches used to determine the COD, crack stability and LR in the baseline case (see Section 5.3) were also used to determine the results for Tasks 1 and 3. As before, the MWCOD values were again input into SQUIRT in order to calculate the LRs. For Tasks 2 and 4, linear elastic FEA was performed using the ANSYS V19.1 code [69] to determine the through-thickness COD values. The prescribed input parameters for NO loading (13.34 kN axial force and 89.59 kNm bending moment), internal pressure (15.5 MPa) and CFP (7.75 MPa) were employed. The prescribed through-wall WRS distribution

was also applied as an additional CFP. The weld metal properties were used for the strength and fracture toughness properties in both the COD and crack stability calculations.

The COD, LR and CBM results calculated by CEI for each task are provided in Table 7.4. The SQUIRT code, used for Tasks 1 and 3, only provides MWCOD values. Additionally, the WRS profile, which is compressive on the ID, results in a negative COD at the ID in combination with the external NO + SSE loads. Consequently, no leakage was judged to be possible for Tasks 2 and 4. However, the LR values reported in Table 7.4 use the MWCOD values. Once again, the CBM was not affected by either the crack morphology or WRS and crack morphology did not impact the COD estimates.

Table 7.4. CEI Task 1 – 4 results

	Task 1 CF without WRS	Task 2 CF with WRS	Task 3 PWSCC without WRS	Task 4 PWSCC with WRS
ICOD (mm)		-0.047386		-0.047386
MWCOD (mm)	0.0888	0.067512	0.0888	0.067512
OCOD (mm)		0.27106		0.27106
LR (kg/s)	0.0276	0.0194	0.0271	0.019
CBM (kN-m)	1 768.09	1 768.09	1 768.09	1 768.09

7.3.2. OPG

The models and approaches used to determine the COD, crack stability and LR in the baseline case (see Section 5.3) were also used to determine the results for Tasks 1 and 3. As before, the MWCOD values were also input into SQUIRT for calculating the LRs. The weld metal properties were used for the strength and fracture toughness properties in both the COD and crack stability calculations.

The effect of WRS on the COD was incorporated in Tasks 2 and 4 by treating WRS as an extra axial force (F_{res}) and bending moment. However, the prescribed WRS is azimuthally constant and therefore symmetry requires that the bending moment be zero. As a result of this calculation, $F_{res} = -445.82$ kN. This force was superimposed on the NO load to determine COD for the LR calculations and on the NO+SSE load to determine the CBM when WRS was considered.

The COD, LR and CBM results calculated by OPG for each task are provided in Table 7.5 The applied axial force decreased the MWCOD by approximately 17%. The WRS was also predicted to suppress the LR by approximately 20%. Once again, the crack morphology did not impact the COD estimates. Finally, contrary to other results, the applied compressive axial force led to a marginal increase in the CBM when incorporating WRS effects on the CBM calculation.

Table 7.5. OPG Task 1 – 4 results

	Task 1 CF without WRS	Task 2 CF with WRS	Task 3 PWSCC without WRS	Task 4 PWSCC with WRS
ICOD (mm)	0.082	0.068	0.082	0.068
MWCOD (mm)	0.0845	0.07	0.0845	0.07
OCOD (mm)	0.087	0.072	0.087	0.072
LR (kg/s)	0.0348	0.0274	0.0299	0.0229
CBM (kN-m)	1 841.8	1 862.9	1 841.8	1 862.9

7.4. Czechia (UJV)

UJV was not able to perform Tasks 1-4 because separate FEA would have needed to determine the WRS effects on COD. However, staff changes resulted in the unavailability of resources for performing such analysis during the benchmark.

7.5. Finland (VTT)

The COD values and crack stability evaluations were calculated using ABAQUS FE analyses. The FE model constructed for the baseline problem was employed. The WRS distribution was introduced through a fictitious temperature distribution in order to produce the prescribed axial WRSs via anisotropic thermal expansion. The following iterative process was used to match the prescribed WRS distribution. The fictitious temperature distribution was determined through iteration by using the analytical stress solution for a cylinder with a radial temperature distribution and finding the temperature polynomial, which induced the prescribed WRS distribution [64]. Although the analytical stress solution provided a perfect match with the prescribed WRS distribution, the distribution exceeded the yield stress at the outer surface of the pipe, which caused stress redistribution. The redistribution of the stresses, which was determined by the FE simulation, mainly occurred on the outside surface of the pipe. The redistribution was assessed to be small enough for the temperature distribution providing the prescribed WRS distribution to be used in the analysis. The selected temperature distribution was defined in the first calculation step in the analyses so the stresses could stabilise before the other loads were applied.

The CODs were then extracted from the FE results and the LRs were calculated – as in the baseline problem – using LEAPOR. The MWCOD value was used as the LEAPOR input, unless the inner COD was negative. In this case, the LR was presumed to be zero. The prescribed corrosion fatigue (CF) and primary water stress corrosion cracking (PWSCC) crack morphology parameters were employed as required for each task. The crack instability was calculated in the FE analysis by increasing the bending moment while keeping the axial force constant (1 337.64 kN). The net-section collapse (NSC) method, which is specified in American Society of Mechanical Engineers (ASME) III NB-3212.25, was used to determine failure. However, it was also validated that the amount of ductile tearing at the instability moment is small enough for the failure to be expected to be governed by the pipe's plastic collapse. All NO + SSE loads were treated as primary in this calculation. The weld metal properties were used for the strength and fracture toughness properties in both the COD and crack stability calculations.

The COD, LR, and CBM results calculated by the VTT Technical Research Centre of Finland (VTT) for each task are provided in Table 7.6. The initially compressive WRS profile was strong enough to close the crack mouth (i.e. negative COD) at the inner surface of the pipe, even after the application of the external loads. No leakage was thus judged to be possible for Tasks 2 and 4. However, if the MWCOD values are used to calculate the LR, the values for Task 2 and 4 are 0.0358 kg/s and 0.0325 kg/s respectively. Once again, the CBM was not affected by either the crack morphology or WRS and crack morphology did not impact the COD estimates.

Table 7.6. VTT Task 1 – 4 results

	Task 1 CF without WRS	Task 2 CF with WRS	Task 3 PWSCC without WRS	Task 4 PWSCC with WRS
ICOD (mm)	0.0697	-0.0272	0.0697	-0.0272
MWCOD (mm)	0.0844	0.0989	0.0844	0.0989
OCOD (mm)	0.1014	0.315	0.1014	0.315
LR (kg/s)	0.0278	0	0.02652	0
CBM (kN-m)	1 701	1 701	1 701	1 701

7.6. Germany (GRS)

As in the baseline task, the CBM was evaluated using the PROST code. The three plastic collapse models (i.e. FSK KWU, FSK MPA and PGL) were once again considered. Five separate SINTAP failure assessment diagram (FAD) analyses were considered, which had various combinations of the analysis level (i.e. Levels 0 – 3) and used either base metal, or weld metal or mixture properties as the failure criteria (as appropriate) for the particular SINTAP level. The effect of WRS on the CBM is only considered for the SINTAP FAD analyses and not for the plastic collapse models.

The results for the SINTAP Level 3 analysis using the weld metal fracture toughness and base/weld metal mixture properties for the material constitutive law was chosen as the best-estimate solution. The calculated CBM was 700 kN-m for Task 1 (without WRS) and 553 kN-m for Task 2 (with WRS) for the prescribed axial force of 1 337.64 kN. The effect of WRS is therefore predicted to be relatively large when using this FAD method. However, the effect of the failure model (i.e. SINTAP FAD level or plastic collapse model) and material properties used in the analysis is even more significant. The CBM varies by a factor of three for the prescribed 125 mm crack length between the lowest and highest failure models.

The COD and LR calculations for Tasks 1-4 were performed using the WinLeck code, as in the baseline analysis. The WinLeck code incorporates various COD models. For the best-estimate calculations, the LBB.ENG2 [32 and 33] model was utilised with the base metal strength properties. For the prescribed NO loading and crack length (i.e. 125 mm), the predicted MWCOD is 71 µm for Tasks 1 and 3 (without WRS). This value compares well with a predicted value of 66 µm using conservative KTA 3206 equations [17]. Notably, all these analytical models only provided a MWCOD value and not ICOD or OCOD values. The ICOD and OCOD are therefore assumed to be equal to the MWCOD in subsequent reporting and analysis. None of these methods are equipped to consider WRS effects and thus the WRS effects on COD could not be evaluated as requested in Tasks 2 and 4.

The LR was also determined using WinLeck. The crack morphology relation provided in the input parameter spreadsheet was used for the best-estimate computation of the crack face resistance with the COD-dependent number of 90° turns. The total flow resistance, ζ, for the prescribed 125 mm crack length was accordingly 1 236 for the CF crack morphology in Tasks 1 and 2. The ATHLET-CDR model was used to calculate the flow rate within WinLeck for this COD and the flow resistance and a value of 0.0153 kg/s was obtained. This value is approximately 50% less than the LR predicted using LEAPOR for the CF morphology, but is more than an order of magnitude higher than the LR predicted by the Henry model. However, the large flow resistance did not lead to choked flow, which is an underlying assumption of the Henry model.

Additional sensitivity analyses were conducted to provide an upper bound LR calculation by ignoring the number of 90° crack face turns. This change increases the calculated flow

rate by approximately 20% for the CF morphology. It is also recognised that the prescribed crack morphology parameters were artificially chosen in order to eliminate the COD dependency on flow resistance. This simplifying assumption is not physically realistic because it implies that the local and global roughness are identical. Using literature values [71] of 40.51 μm for the global roughness and 8.814 μm for the local roughness, the best-estimate LR is 0.027 kg/s for the CF crack, which is approximately 1.8 times greater than the LR for the prescribed morphology parameters.

For the PWSCC crack morphology (i.e. Tasks 3 and 4), the prescribed crack morphology parameters (i.e. roughness = 114 μm, density of 90° turns = 5 940 1/m, and path deviation factor = 1.2) were initially considered as in Tasks 1 and 2 described above in order to determine a best-estimate LR. However, the ratio of the hydraulic diameter to surface roughness for these parameters was less than one for the 125 mm crack, which invalidated the friction factor (FF) formulation for either a best-estimate (i.e. ATHLET-CDR) or conservative (i.e. KTA code) leak rate prediction. An LR determination is thus not possible for the prescribed crack length and crack morphology parameters. The best-estimate model even predicts a lower flow rate for very tight, shorter cracks than the conservative model, whereas the reverse is true for more open, longer cracks. This is because the flow resistance for the crack morphology relations used in this study and in the SQUIRT and LEAPOR codes significantly increases for a tight crack.

Although initial calculations did not include CFP, subsequent evaluation showed that CFP is insignificant for opening the crack further and enabling an LR calculation. For these tight cracks, the fluid model indicates that choking occurs so that the pressure within the crack does not drop from the stagnation value to atmospheric pressure and the CFP input value provided for these tasks may not be appropriate. The subsequent evaluation of the effects of CFP therefore assumed that the pressure dropped to the saturation pressure at the operating temperature.

Although a best-estimate LR prediction is not possible for Tasks 3 and 4, the KTA method can be used to provide an upper-bound estimate of 0.1 kg/s. A best-estimate LR of 0.024 kg/s can additionally be calculated if more representative local surface roughness (16.86 μm) and global surface roughness (113.9 μm) values are used for a PWSCC crack. More information on the LR evaluation and associated sensitivity analyses is provided in Annex C.

The COD, LR and CBM results calculated by GRS for Tasks 1 -4 are summarised in Table 7.7. As described previously, the WinLeck code only calculated a MWCOD value and the ICOD and OCOD results are assumed to be equivalent to this value for Tasks 1 and 3. GRS was not able to account for WRS effects in the COD calculation in Tasks 2 and 4, which led them to report the same COD and LR values as in Tasks 1 and 3 respectively. The Tasks 2 and 4 COD and LR results are therefore summarised in Table 7.7 as not applicable (NA). Best-estimate LR predictions were possible for the prescribed CF crack morphology parameters in Task 1, but no flow was predicted with the prescribed PWSCC crack morphology parameters in Task 3 because of the significant increase in flow resistance predicted for the model. The effects of WRS were not considered for either COD or LR calculations. However, the WRS was applied as an additional load for the CBM calculation, which decreased the crack stability load. The CBM calculated for Tasks 2 and 4 with WRS is therefore lower than the moment calculated for Tasks 1 and 3.

Table 7.7. GRS results for Tasks 1-4

	Task 1 CF without WRS	Task 2 CF with WRS	Task 3 PWSCC without WRS	Task 4 PWSCC with WRS
ICOD (mm)	0.071	NA	0.071	NA
MWCOD (mm)	0.071	NA	0.071	NA
OCOD (mm)	0.071	NA	0.071	NA
LR (kg/s)	0.0153	NA	0	NA
CBM (kN-m)	700	553	700	553

7.7. India (BARC)

The COD distribution through the thickness for the crack and loadings specified in these tasks were evaluated using 3D, elastic-plastic FE analysis that considered the effects of both WRS and CFP. Symmetry conditions were invoked to only model one-fourth of the cracked-piping configuration with 20-noded brick elements. The weld was modelled as a straight and rectangular weld width of 50 mm as specified in the benchmark description. The WRS was imposed by applying temperature gradients in FE analysis. A temperature gradient was chosen to reasonably replicate the input WRS distribution (Figure 4.4).

An in-house code was used to determine the LR using the MWCOD value and assuming a constant COD through the piping thickness. The in-house code assessed the crack morphology effects using the local and global surface roughness parameters provided by the input data. Crack stability was assessed using the J-T approach. Both the J-integral and crack tip opening displacement values were determined using the same FE analysis employed for the COD analysis. For both the COD and crack stability calculations, the weld and base metal constitutive properties were assigned to the appropriate locations within the elastic-plastic FE model so that the strength properties on the crack plane represented a mixture of the individual base and weld metal properties. The weld fracture toughness properties were used because the crack was assumed at the weld centreline.

The COD, LR and CBM results calculated by the Bhabha Atomic Research Centre (BARC) for each task are provided in Table 7.8. There is a small effect of WRS on the CBM, but no effect of crack morphology. Additionally, the crack morphology does not impact the COD estimates and only the calculated LR is unique for each of these tasks. The MWCOD is predicted to increase with WRS and, because MWCOD was used to calculate LR, this increase leads to an increase in the predicted LR that is more significant than the slight differences associated with the crack morphology parameters used in these tasks.

Table 7.8. The BARC results for Tasks 1-4

	Task 1 CF without WRS	Task 2 CF with WRS	Task 3 PWSCC without WRS	Task 4 PWSCC with WRS
ICOD (mm)	0.082	0.0036	0.082	0.0036
MWCOD (mm)	0.105	0.142	0.105	0.142
OCOD (mm)	0.130	0.356	0.130	0.356
LR (kg/s)	0.033	0.045	0.029	0.041
CBM (kN-m)	1 235	1 212	1 235	1 212

7.8. Japan (JAEA)

The COD was analysed using an ABAQUS FE analysis. The analysis model, assumptions and input parameters were based on the benchmark problem description and prescribed

input parameters. A half-symmetry condition was assumed for a through-wall circumferential crack (TWC) centred about the weld centreline. The prescribed weld metal elastic modulus and Ramberg-Osgood parameters were used with a Poisson's ratio of 0.3. The NO axial force of 1 302.94 kN, NO moment of 89.59 kN m and crack face pressure of 7.75 MPa were applied to the FE model. For Tasks 2 and 4, the WRS was applied to the crack surface as a distributed surface load.

The LR was calculated with the LEAPOR code. Although COD was analysed at the ID, MW and OD in the FE analysis, only the MWCOD was used in the LR calculation. The crack morphology parameters were the only other variable input parameters in these tasks. The values for surface roughness, path deviation and 90 degrees turns per metre prescribed in the input parameters for use in LEAPOR/SQUIRT were used.

The crack instability bending moment was analysed with the probabilistic fracture mechanics code PASCAL-SP that has been developed by the JAEA. As prescribed, a fixed axial force of 1 337.64 kN was assumed and the bending moment was varied up to the instability moment. A limit load instability criterion was adopted based on the weld metal's flow stress, which was taken as the average of the weld metal yield strength and tensile strength. The effect of secondary loads on the CBM was not considered in these evaluations.

The COD, LR and CBM results calculated by the JAEA for each task are provided in Table 7.9. Once again, the COD was assumed to be unaffected by the crack morphology and the CBM was unaffected by either the WRS or crack morphology. Notably, WRS caused the COD at the ID to be zero. This practically implies that the LR is zero when considering WRS effects. However, as indicated above, the LR was calculated with the MWCOD value which leads to a predicted increase in the LR with WRS.

Table 7.9. JAEA results for Tasks 1-4

	Task 1 CF without WRS	Task 2 CF with WRS	Task 3 PWSCC without WRS	Task 4 PWSCC with WRS
ICOD (mm)	0.112	0	0.112	0
MWCOD (mm)	0.121	0.27	0.121	0.27
OCOD (mm)	0.135	1.25	0.135	1.25
LR (kg/s)	0.0508	0.17531	0.04202	0.11572
CBM (kN-m)	1 685	1 685	1 685	1 685

7.9. Korea (KOREAa and KOREAb)

Separate analyses were conducted by KOREAa and KOREAb. Their contributions are particularly interesting because many of the same computational tools were used for the COD and crack stability calculations and the assumptions and approaches for these analyses appear similar if not identical. The principal difference is that each organisation used a different LR code.

7.9.1. KOREAa

The elastic-plastic COD solution was extracted from the Electric Power Research Institute (EPRI) ductile handbook [39]. The WRS contribution to ICOD, MWCOD and OCOD was determined as follows:

- COD (ID, w/ WRS) = COD (w/o WRS) + ΔCOD (ID, due to WRS);
- COD (mid-wall, w/ WRS) = COD (w/o WRS) + ΔCOD (mid-wall, due to WRS);
- COD (OD, w/ WRS) = COD (w/o WRS) + ΔCOD (OD, due to WRS).

The ΔCOD values due to WRS were obtained from a linear elastic FE analysis by simulating a temperature distribution that led to the equivalent thermal expansion stress at the weld metal centreline (i.e. the cracking plane). These COD values were then input into the Pipe Crack Evaluation Program (PICEP) in order to calculate the LR. The global parameters for surface roughness and 90 degree turns per length prescribed in the input data were used. The path deviation factor was not used because PICEP does not consider this parameter. The weld metal strength properties were used in the COD calculation.

The crack stability analysis was based on a J-T failure criterion. The applied J was estimated using the J-estimation scheme in the EPRI ductile fracture handbook [39]. The CFP was applied as an equivalent load and moment for predicting CFP contribution to the applied J-integral. The tensile properties of base metal were used to conservatively model the crack tip plastic zone size expansion of the plastic zone, while the J-R curve of the weld metal was used to minimise the material toughness. The required form of the J-R curve (Eq. 8) is different from the prescribed form (Eq. 2). Consequently, as indicated previously, the C_1 and C_2 values in Eq. 8 were fitted to data generated using Eq. 2 in order to approximate the form as closely as possible.

The COD, LR and CBM results calculated by KOREAa for each task are provided in Table 7.10. Once again, COD was assumed to be unaffected by the crack morphology and the CBM was unaffected by either WRS or crack morphology. Notably, the COD values calculated with just the applied loading and without WRS did not distinguish between the ID, MW and OD values and just an average through-thickness value was assumed. The addition of the prescribed WRS distribution decreased the LR. The PWSCC morphology also decreased the LR compared to the CF morphology.

Table 7.10. KOREAa results for Tasks 1-4

	Task 1 CF without WRS	Task 2 CF with WRS	Task 3 PWSCC without WRS	Task 4 PWSCC with WRS
ICOD (mm)	0.0734	0.0172	0.0734	0.0172
MWCOD (mm)	0.0734	0.0738	0.0734	0.0738
OCOD (mm)	0.0734	0.174	0.0734	0.174
LR (kg/s)	0.0208	0.0113	0.0109	0.0077
CBM (kN-m)	1 002.1	1 002.1	1 002.1	1 002.1

7.9.2. KOREAb

The COD was determined using the same approach as for the KOREAa analysis, which is repeated here for completeness. The elastic-plastic COD solution was extracted from the EPRI ductile handbook [39]. The WRS contribution to the ICOD, MWCOD and OCOD was determined as follows:

- COD (ID, w/ WRS) = COD (w/o WRS) + ΔCOD (ID, due to WRS);
- COD (mid-wall, w/ WRS) = COD (w/o WRS) + ΔCOD (mid-wall, due to WRS);
- COD (OD, w/ WRS) = COD (w/o WRS) + ΔCOD (OD, due to WRS).

The ΔCOD values due to WRS were obtained from a linear elastic FE analysis. A temperature distribution was stimulated that led to the equivalent thermal expansion stress at the weld metal centreline (i.e. the cracking plane). The ICOD and OCOD values were then input into LEAPOR in order to calculate the LR. The prescribed crack morphology parameters for surface roughness, path deviation and 90 degree turns per length were used. The weld metal strength properties were used in the COD calculation.

The crack stability analysis used the same approach that was used for the KOREAa analysis, which is repeated below for completeness. The crack stability analysis was based on a J-T failure criterion. The applied J was estimated using the J-estimation scheme in the EPRI ductile fracture handbook [39]. The CFP was applied as an equivalent load and moment for predicting CFP contribution to the applied J-integral. The tensile properties of the base metal were used to conservatively model the crack tip plastic zone size expansion of plastic zone, while the J-R curve of weld metal was used to minimise the material toughness. The required form of the J-R curve (Eq. 8) is different from the prescribed form (Eq. 2). Consequently, as indicated previously, the C_1 and C_2 values in Eq. 8 were fitted to the data generated using Eq. 2 to approximate the form as closely as possible.

The COD, LR and CBM results calculated by KOREAb for each task are provided in Table 7.11. Once again, COD was assumed to be unaffected by the crack morphology and the CBM was unaffected by either WRS or crack morphology. Notably, the COD values calculated with just the applied loading and without WRS did not distinguish between the ID, MW and OD values and just an average through-thickness value was assumed. The addition of the prescribed WRS distribution decreased the LR. The PWSCC morphology also decreased the LR compared to the CF morphology. The COD and CBM KOREAb values are identical to the KOREAa values and the only differences in the results are the PICEP and LEAPOR LR calculations. For these particular problems, LEAPOR predicted a somewhat higher LR for the CF morphology and a significantly lower LR for the PWSCC morphology compared to PICEP.

Table 7.11. KOREAb results for Tasks 1-4

	Task 1 CF without WRS	Task 2 CF with WRS	Task 3 PWSCC without WRS	Task 4 PWSCC with WRS
ICOD (mm)	0.0734	0.0172	0.0734	0.0172
MWCOD (mm)	0.0734	0.0738	0.0734	0.0738
OCOD (mm)	0.0734	0.174	0.0734	0.174
LR (kg/s)	0.0251	0.009	0.0207	0.0082
CBM (kN-m)	1 002.1	1 002.1	1 002.1	1 002.1

7.10. Sweden (KIWA)

The calculation procedure followed for the baseline problem (Section 5.10) was also used for these tasks. The COD values were corrected for plasticity using the weld metal properties. The total COD was calculated for the 125 mm MW crack length both with and without WRS, which was considered to be a secondary stress. KIWA again for these tasks considered the effect of different WRS distributions (Figure 5.2) in the analyses associated with Tasks 1-4. These are labelled Task 2a for the CF morphology with the SSM WRS distribution and Task 4a for the PWSCC morphology with the SSM WRS distribution.

WinSQUIRT v. 1.3 [62] was used for LR calculations. The prescribed crack morphology parameters were entered into the user-defined crack morphology inputs. The CBM was calculated using the ISAAC code. As summarised in Section 5.10, a FAD approach was followed for assessing failure and a fixed, prescribed axial force of 1 337.64 kN was prescribed for these tasks. The crack stability calculations used the base metal material strength properties, while the weld metal fracture toughness properties were used. More details on the approach and results are provided in Annex C.

The KIWA results for these tasks are summarised in Table 7.12. Both the COD and CBM were assumed to be unaffected by the crack morphology, while the CBM was affected by

a consideration of the WRS distribution. The prescribed WRS was predicted to decrease the CBM by approximately 25%. The effect of the SSM WRS on the CBM was not reported, but the SSM WRS is more severe and thus may further decrease the predicted CBM.

For Tasks 2 and 4, which evaluated the prescribed WRS distribution, the ID COD value was zero and the leak flow rate was also assumed to be zero. A possible reason for this result is that the WRS ID compressive stresses have a stronger influence on shorter cracks (e.g. 125 mm) than for longer cracks, which are predicted to have a non-zero ID COD. However, the SSM WRS distribution (Task 4a) did predict a positive LR.

For Tasks 3, 4 and 4a, WinSQUIRT reported a very tight crack due to the prescribed PWSCC morphology and thus no leak flow rate was predicted. A possible option could be employed of using an improved model to determine the effects of crack morphology parameters on COD to generate positive LRs. However, this type of evaluation was not performed because it was outside the benchmark scope.

Table 7.12. KIWA results for Tasks 1-4

	Task 1 CF without WRS	Task 2 CF with WRS	Task 3 PWSCC without WRS	Task 4 PWSCC with WRS	Task 2a CF with the SSM WRS	Task 4a PWSCC with the SSM WRS
ICOD (mm)	0.0651	0	0.0651	0	0.0218	0.0218
MWCOD (mm)						
OCOD (mm)	0.0973	0.2374	0.0973	0.2374	0.1985	0.1985
LR (kg/s)	0.026	0	-0	0	0.037	-0
CBM (kN-m)	732.7	549.8	732.7	549.8	NR	NR

7.11. Switzerland (PSI)

The COD and LR calculations were performed as in the baseline analysis using the LeakRate_Excel_BetaR1 code. However, as indicated previously (Section 5.11), the code only accepts crack size as an input if the COD is also specified. The crack size and COD were therefore determined iteratively in the following manner. An initial LR was guessed and the prescribed NO loads then applied (i.e. internal pressure = 15.5 MPa, axial force =13.34 kN, bending moment = 89.59 kN-m and CFP = 7.75 MPa) in order to calculate the COD and crack size. Subsequent LRs were then specified until the target MW crack size of 125 mm was obtained. There are no capabilities in the current analysis tools to incorporate WRS effects and therefore Tasks 2 and 4 were not performed. The weld metal strength properties were used in the COD calculations.

Crack instability was calculated using the same in-house code that was used for the baseline problem. The code employed the NSC-based failure model and used a weld failure stress of 429.45 MPa, which is the average of the weld yield and ultimate strengths. The specified NO+SSE loads was applied (i.e. internal pressure = 15.5 MPa, axial force = 48.04 kN, bending moment = 378 kN-m, and CFP = 7.75 MPa).

The COD, LR and CBM results calculated by the PSI for each task are provided in Table 7.13. Once again, the COD and CBM were assumed to be unaffected by the crack morphology. As indicated previously, it was not possible to assess the effect of WRS on the COD, LR and CBM as requested for Tasks 2 and 4. However, based on the Task 1 and 3 LR calculations, it seems that the LR associated with the PWSCC crack morphology is approximately 30% less than the LR associated with the CF crack morphology.

Table 7.13. PSI results for Tasks 1-4

	Task 1 CF without WRS	Task 2 CF with WRS	Task 3 PWSCC without WRS	Task 4 PWSCC with WRS
ICOD (mm)	0.0699		0.0699	
MWCOD (mm)	0.0836		0.0836	
OCOD (mm)	0.0991		0.0991	
LR (kg/s)	0.035		0.025	
CBM (kN-m)	1 842.4		1 842.4	

7.12. Summary

The computational tools for Tasks 1-4 are summarised in Table 5.8. In Table 5.8, a single entry in a given cell identifies how the same tool was used in both the baseline and Task 1- 4 problems. If two tools are listed as separated by a "/", the second tool was used in Task 1- 4. Generally, most of the participants used the same COD, LR and crack stability codes in all problems. The exception was the calculation of the WRS contribution to the COD and crack stability as requested for Tasks 2 and 4. The participants assessed this contribution by using either FEA to determine the boundary conditions (i.e. force, pressure, displacement or temperature boundary conditions) to be applied to the FEA model, or by an analytical method (A in Table 7.14), which applied either an effective moment or force to the crack plane in order to represent the WRS effects. A summary of the COD methods used to account for WRS is provided in Table 7.14.

This table also summarises the material used for strength properties (i.e. (B)ase, (M)ixture or (W)eld) and the CFP value used in the COD and LR calculations. The evaluation method used determined the CBM for the fixed axial force of 1 337.64 kN (i.e. the crack stability calculation), as well as the material used for the strength and fracture toughness properties and the CFP value. The participants used the same CBM methods that they chose for the baseline problem. As in the baseline problem, KIWA, KOREAa and KOREAb used different strength properties for the COD and CBM calculations. The NRC, EMCC and JAEA considered CFP in the COD calculations, but not in the CBM calculations. Conversely, KOREAa only considered CFP in the CBM calculations.

Table 7.14. Methods and analysis choices for the COD and CBM calculations

Organisation	WRS evaluation method (A/FEA)	COD strength (B/M/W)	COD CFP (MPa)	CBM method (EPFM/NSC)	CBM strength (B/M/W)	CBM toughness (B/M/W)	CBM CFP (MPa)
BARC	FEA	M	7.75	EPFM	M	W	7.75
CEI	FEA	W	7.75	NSC	W	NA[2]	7.75
EMCC	FEA	B	7.75	EPFM	B	W	0
GRS	A[1] (force)	B	0	FAD	M	W	0
JAEA	FEA	W	7.75	NSC	W	NA	0
KOREAa	FEA	W	0	EPFM	B	W	7.75
KOREAb	FEA	W	0	EPFM	B	W	0
KIWA	A, (force)	W	0	FAD	B	W	0
NRC	A (moment)	W	7.75	EPFM	W	W	0
OPG	A (force)	W	7.75	EPFM	W	W	7.75
PSI	NA	W	7.75	NSC	W	NA	7.75
Tractebel	FEA	M	0	EPFM	M	W	0
VTT	FEA	W	7.75	NSC	W	NA	7.75

Note:
[1] WRS was only evaluated for crack stability calculations.
[2] NA = not applicable.

8. Tasks 1-4 – collective results and discussion

The previous section summarised the computational tools, methods, assumptions, analysis choices and the individual results for Tasks 1-4. The participants provided the crack opening displacements (CODs) values, which were ideally at the ID, mid-wall (MW) and OD, the leak rate (LR) and the critical bending moment (CBM) for the prescribed weld joint configuration, loading conditions, material properties and a fixed through-wall circumferential crack (TWC) of 125 mm. There were the following crack morphology and weld residual stress (WRS) considerations:

- corrosion fatigue (CF) flaw without WRS (Task 1);
- CF flaw with a prescribed WRS (Task 2);
- primary water stress corrosion cracking (PWSCC) flaw without WRS (Task 3);
- PWSCC flaw with the prescribed WRS (Task 4).

8.1. Task 1 results: corrosion fatigue morphology without WRS effects

The reported values for the various COD measures, LR and CBM for those organisations participating in Task 1 are provided in Table 8.1. These are an amalgamation of the results presented for individual participants in Section 7. Eight participants calculated separate inner diameter COD (ICOD), mid-wall crack opening displacement (MWCOD) and outer diameter COD (OCOD) values; four effectively calculated either average or MWCOD values and one participant calculated only the ICOD and OCOD. For those participants that calculated all three values, it is interesting to note that the difference between the MWCOD and the average of the ICOD and OCOD was always less than 5%. Additionally, the difference was less than 2.5% for all but one participant. The implication is that the predicted through-thickness crack profile for this problem is nearly linear.

Table 8.1. Task 1 results

Organisation	ICOD (mm)	MWCOD (mm)	OCOD (mm)	CFP in COD (Y/N)	LR (kg/s)	CBM (kN-m)
BARC	0.082	0.105	0.130	Y	0.033	1 235
CEI	0.089	0.089	0.089	Y	0.028	1 768
EMCC	0.090	0.102	0.124	Y	0.040	1 187
GRS	0.071	0.071	0.071	N	0.015	700
JAEA	0.112	0.121	0.135	Y	0.051	1 685
KOREAa	0.073	0.073	0.073	N	0.021	1 002
KOREAb	0.073	0.073	0.073	N	0.025	1 002
KIWA	0.065		0.097	N	0.026	733
NRC	0.079	0.096	0.116	Y	0.033	1 928
OPG	0.082	0.085	0.087	Y	0.035	1 842
PSI	0.070	0.084	0.099	Y	0.035	1 842
Tractebel	0.063	0.074	0.087	N	0.021	1 300
VTT	0.070	0.084	0.101	Y	0.028	1 701

The average MWCOD among the participants was 0.0889 mm with a standard deviation of 0.015 mm, or approximately 16% of the mean.[3] The average LR was 0.0313 kg/s with a standard deviation of 0.0085 kg/s, or 27% of the mean. While this variation in the LR is not surprising given the different codes used and their inherent differences in the characterisation of crack morphology effects, the variation in the MWCOD values is higher than initially anticipated given that the crack size and loading were prescribed in Task 1. A histogram of the predicted MWCOD and LRs (Figure 8.1) better illustrates the variability in the predictions. The material strength properties used by each participant are also indicated in Figure 8.1. No clear effects of choosing either B, W or M properties can be discerned, but this is unsurprising given that that so few participants used B or M properties.

Further insight into the predictions and differences in the results can be gained by considering the relationship between the MWCOD and LR (Figure 8.2). The black dashed line in the figure is a linear fit to all the data. As expected for a fixed crack size and linear loading conditions, the MWCOD and LR results are fairly well correlated and a linear trend appears reasonable over the range of reported MWCOD values. A similar evaluation of the ICOD and OCOD results demonstrates that neither of these measures are as linearly correlated to the LR as to the MWCOD. The next observation is that the five lowest MWCOD values (i.e. < 0.081 mm) did not incorporate the effects of crack face pressure (CFP), whereas the remaining higher MWCOD predictions did. This explains some, but not all, of the MWCOD variability that is apparent in the participants' results. The variability is more generally explained by the differences in the MWCOD values because these differences contribute approximately 80% of the differences in the LR predictions given the r2 value of 0.81. This highlights the importance of the MWCOD predictions and implies that more accurate and consistent COD predictions would greatly reduce differences in the LR predictions. Furthermore, this insight does not appear to depend strongly on the LR code that was used.

Figure 8.1. MWCOD and LR values for Task 1

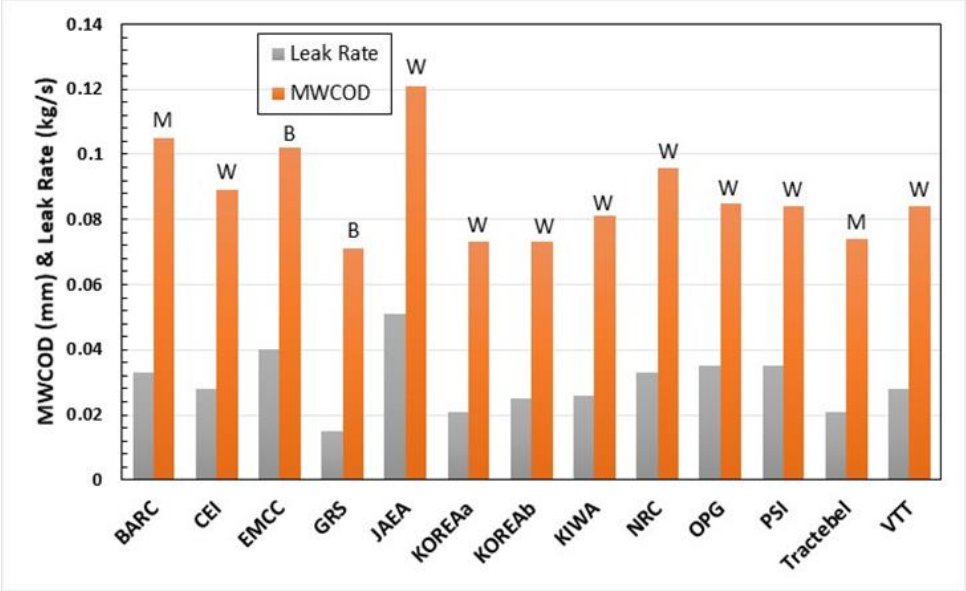

[3] The GRS results were not used to calculate average MWCOD, LR and CBM values for the participants because their leak-before-break (LBB) codes are intentionally conservative since no additional margin is applied on the acceptance criteria.

Figure 8.2. MWCOD and LR Relationship for Task 1

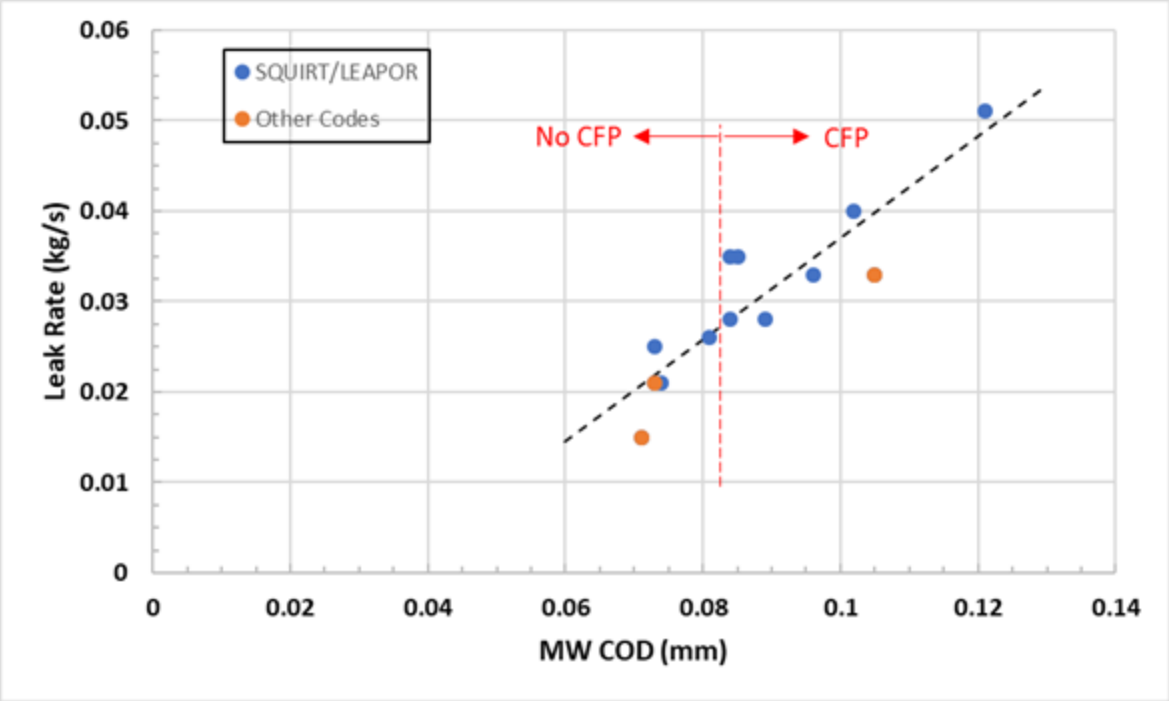

All but three of the participants used a variant of the SQUIRT or LEAPOR codes and therefore these results are identified separately in Figure 8.2. Although the SQUIRT/LEAPOR codes appear to be slight less conservative (i.e. higher LR for a given COD) than the other codes for the prescribed CF morphology, there is not enough data to determine if this trend is statistically significant.[4] Furthermore, the average LR and standard deviation do not significantly change when calculated for all results, or only for the SQUIRT/LEAPOR results. This result provides additional evidence that these apparent leak code differences for this benchmark may largely be a function of the differences among MWCOD results. The CBM results for Task 1 are summarised in Figure 8.3. In this figure, participants have been grouped by the failure model type (i.e. elastic-plastic fracture mechanics [EPFM], net-section collapse [NSC], or failure assessment diagram [FAD]) and the strength properties used within their analysis. This figure again highlights and helps to quantify the trends that are apparent in the baseline results (Figure 6.2). The average CBM value for all results was 1 380 kN-m with a standard deviation that was 32% of the mean.[5] As explained previously, this large standard deviation is primarily due to the choice of material strength. The average CBM for all participants using EPFM with B strength properties for these results is approximately 44% less than the average CBM for those participants using EPFM with W strength properties.

[4] SQUIRT/LEAPOR adjusts the ηtL parameter as a function of the COD, whereas other LR codes may not. The effect of the ηtL adjustment is up to 25% for CF and 10% for PWSCC morphologies respectively.

[5] The GRS results were not used to calculate average MWCOD, LR and CBM values for the participants because their leak-before-break (LBB) codes are intentionally conservative since no additional margin is applied on the acceptance criteria.

Figure 8.3. CBM results for Task 1

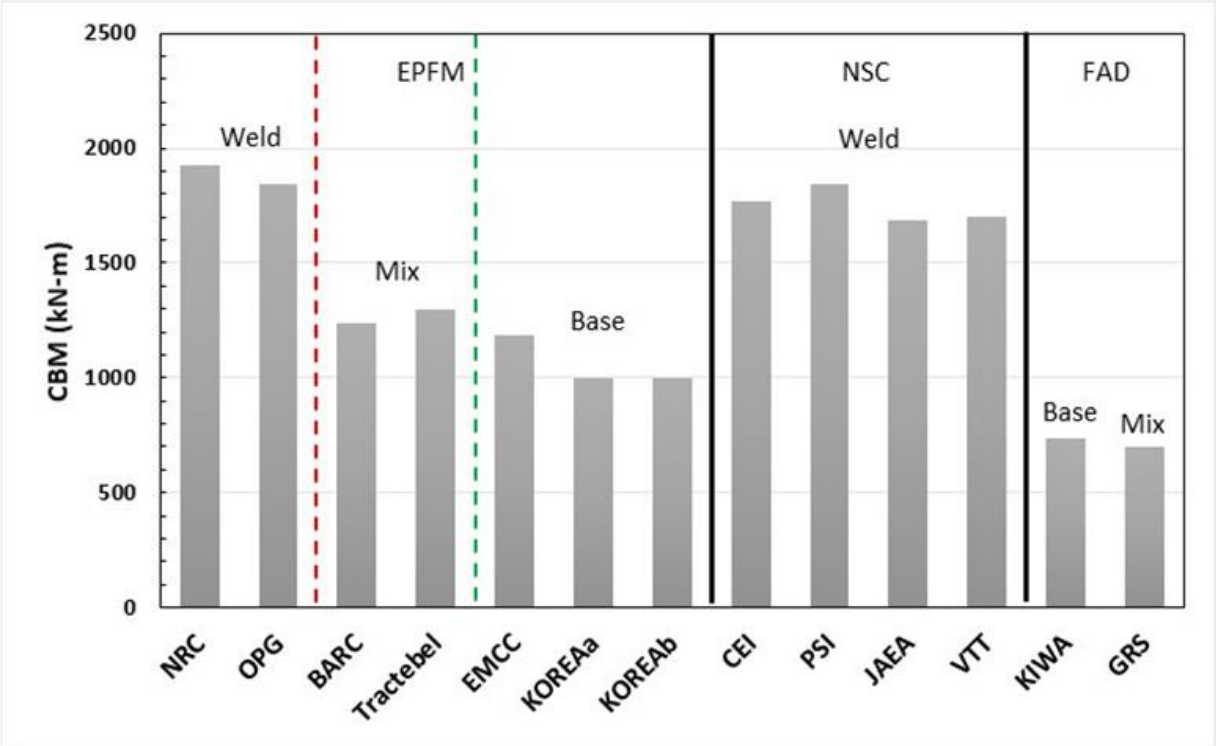

As also previously discussed, a secondary reason for the high variability in the CBM results is the failure model type that was used in the analysis. The average CBM for those participants using NSC with W properties was 7% less than the average CBM for participants using EPFM with W properties. Furthermore, when the results are grouped by the failure model and material property choices (i.e. EPFM/W, EPFM/M, EPFM/B, NSC/W, FAD in Figure 8.3) and separately analysed, the variability among the participants' predictions is substantially reduced. The standard deviation is 5% or less of the average value for all the binned groups, with the exception of the EPFM/B combination where the standard deviation is 10% of the average. These grouped CBM results are significantly more consistent than those considering the global average, which have a standard deviation that is 32% of the mean. The consideration, or lack, of CFP adds some additional variability because it decreased the predicted CBM. However, as shown in Figure 6.8, this effect is expected to be much less significant than the material property or failure model type selections.

8.2. Task 2 results: corrosion fatigue morphology with WRS effects

Task 2 results are summarised in the table below. These results include the COD, LR and CBM values. Also included are columns depicting whether the participant incorporated CFP in their COD predictions and if an (A)nalytical or (F)EA method was used to incorporate WRS into the COD predictions. Most participants used FEA to derive the boundary conditions (for example, temperatures and displacements) to match the prescribed WRS distribution on the uncracked piping configuration and then applied these boundary conditions to the cracked configuration in order to predict COD. The analytical approaches either applied an equivalent moment or force to the crack plane to simulate the WRS distribution, or, in KIWA's case, their in-house software directly incorporated the WRS distribution to determine COD.

Table 8.2. Task 2 results

Organisation	ICOD (mm)	MWCOD (mm)	OCOD (mm)	CFP in COD (Y/N)	WRS Method	LR (kg/s)	CBM (kN-m)
BARC*	0.004	0.142	0.356	Y	F	0.045	1 212
CEI*	-0.047	0.068	0.271	Y	F	0.019	1 768
EMCC	0.053	0.096	0.194	Y	F	0.037	1 187
GRS*				N	NA		553
JAEA*	0	0.270	1.25	Y	F	0.175	1 685
KOREAa	0.017	0.074	0.174	N	F	0.011	1 002
KOREAb	0.017	0.074	0.174	N	F	0.009	1 002
KIWA	0		0.237	N	A	0	550
NRC	0.064	0.096	0.131	Y	A	0.032	1 928
OPG	0.068	0.070	0.072	Y	A	0.027	1 863
Tractebel*	0.055	0.075	0.12	N	F	0.021	1 300
VTT	-0.027	0.099	0.315	Y	F	0	1 701

Note: * LR in the table that has been calculated using MWCOD values

GRS did not incorporate WRS into their COD predictions, but they did incorporate them analytically into the CBM predictions. The CBM predictions for most of the participants are identical to their Task 1 values (Table 8.1), implying that they either assumed that WRS loading, being secondary, would not impact crack stability, or that their crack stability code may not have sufficient capabilities to consider secondary loads. Ontario Power Generation (OPG) and Bhabha Atomic Research Centre (BARC) predicted some impact of WRS because their Task 2 CBM estimates were 1% higher and 2% lower respectively than their Task 1 values. The most significant effects of WRS on CBM were reported by GRS and KIWA. Both participants used the R6 method [43] for crack stability, which explicitly considers WRS to be an additional contribution to the stress intensity factor. Using this approach, GRS and KIWA predicted Task 2 CBM values that were 21% and 25% lower, respectively, than their Task 1 CBM predictions as a result of the prescribed WRS profile.

The through-thickness COD profiles for each participant are presented in Figure 8.4. In this figure, the reported values for the ICOD, MWCOD and OCOD are connected by a smooth line. This is done solely as a visual aid and is not intended to denote the through-wall COD profile for each participant based on their three reported values. These profiles are much more interesting than the nearly linear or constant profiles that were reported for Task 1, for which WRS was not considered. The average of the ICOD and OCOD closely matched the MWCOD for all participants in Task 1. This linearity is only evident in the few results that analytically incorporated WRS effects in Task 2 (i.e. the US Nuclear Regulatory Commission [NRC], OPG and KIWA). The COD profiles for the participants using FEA are all non-linear and the predicted MWCOD is between 17% and 66% less than the average of the ICOD and OCOD in the FEA-based results. This nonlinearity underscores the notion that no single measure can be expected to accurately represent the COD profile when WRS effects are incorporated.

As is also evident in Table 8.2 and Figure 8.4, incorporating WRS creates more variability in the predicted ICOD and OCOD results and thus in the through-thickness profile than in Task 1. The variability (i.e. standard deviation/mean) in the Task 1 ICOD, MWCOD and ODCOD values was between 16% and 21%, while the variation in the Task 2 ICOD and OCOD values was greater than 44%. Several of the participants using FEA predicted that the ICOD would be close to zero or negative.[6] Whereas the ICOD and OCOD values vary tremendously between Tasks 1 and 2, the reported MWCOD values (Table 8.2) are not as

[6] Negative ICOD values are non-realistic but they are retained to reflect the results provided.

significantly different. The average Task-2 MWCOD value is 0.0911 mm (compared to 0.0860 mm for Task 1, for the same participate population) and the standard deviation is 27% of the mean (compared to 13% for Task 1).[7] This result should not be overly surprising because the axial WRS distribution is nearly self-equilibrating over the cracking plane cross section, which mitigates large additional mid-wall displacements compared to the ICOD and OCOD.

A comparison of the LR plotted with respect to the ICOD, MWCOD and OCOD value for this task is provided in Figure 8.5. Linear trend lines are shown for each COD value in this figure simply in order to provide a visual reference. This figure illustrates that no single COD measure is well-correlated with the LR when WRS effects are incorporated. In fact, the OCOD values do not appear to correlate at all. The MWCOD seems to have the best correlation and, for this reason as well as due to consistency, will be used to evaluate the effects of WRS and crack morphology throughout the remainder of this report.

Figure 8.4. Task 2 through-thickness COD profile

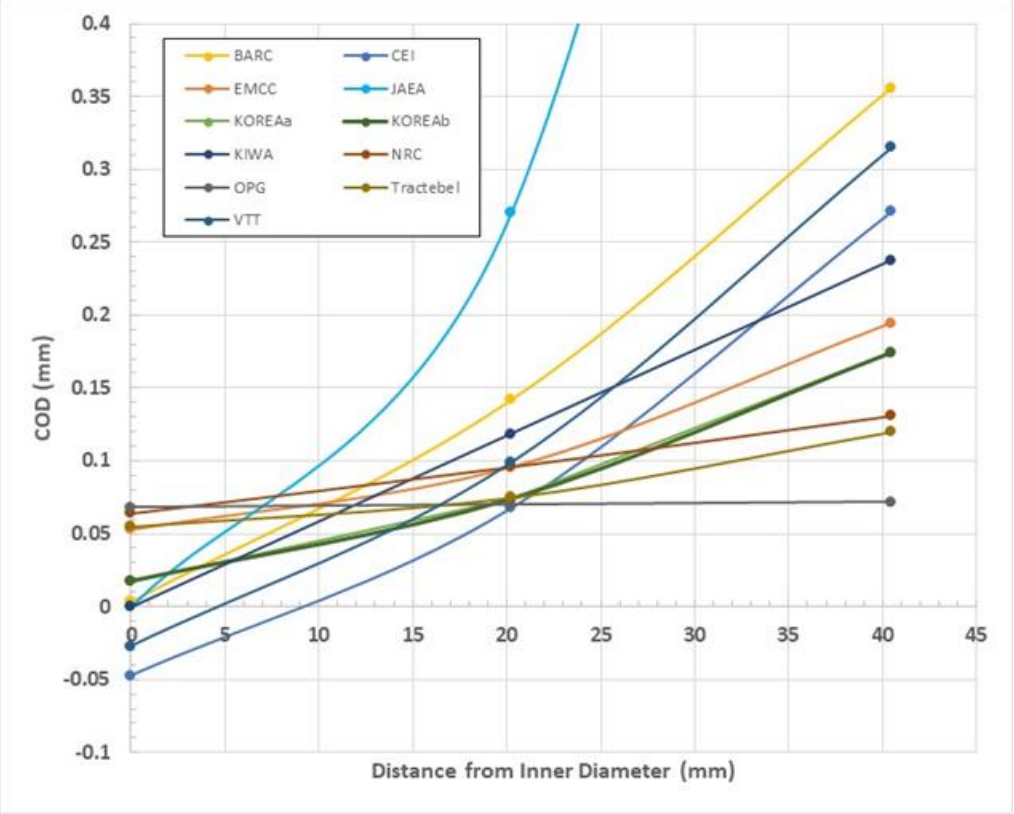

While the ICOD does not appear to be well-correlated with LR (Figure 8.5), it should be recalled that several participants used the MWCOD (for example, the BARC, Candu Energy Inc. [CEI] and JAEA) to perform their LR calculation, even though their ICOD values were small or negative. Other participants with zero or negative ICOD values (for example, KIWA, the VTT Technical Research Centre of Finland [VTT]) simply presumed a zero LR without carrying out further calculations. Adjusting for these differences in Figure 8.5 would improve the efficacy of the ICOD correlation. The fact that the WRS distribution led to negative ICOD values, and consequently a zero LR, for some participants

[7] Average COD values reported are determined without including the GRS or JAEA results.

highlights the importance of considering WRS effects. However, a WRS distribution that led to positive COD values throughout the thickness for all participants may also have been valuable because it would have required all participants to perform LR calculations.

The Task 2 absolute MWCOD and LR values are illustrated in Figure 8.6. It should again be emphasised that all organisations reporting negative or zero ICOD values (i.e. the CEI, JAEA, KIWA and VTT) would predict the LR to be zero. However, the CEI and JAEA also calculated an LR using the MWCOD and this is the result reported in Table 8.2 and Figure 8.6. While Figure 8.6 is meant to be directly compared with Figure 8.2 in order to assess the differences in Task 1 and 2 values, the additional variability in the Task 2 results makes such an assessment challenging. A direct assessment of the differences is nevertheless provided in Figure 8.7. This figure reinforces the point that the predicted MWCOD values were reasonably consistent between Tasks 1 and 2. In fact, most of the values differed by less than 25%.

Figure 8.5. Leak rate vs. COD measures for Task 2

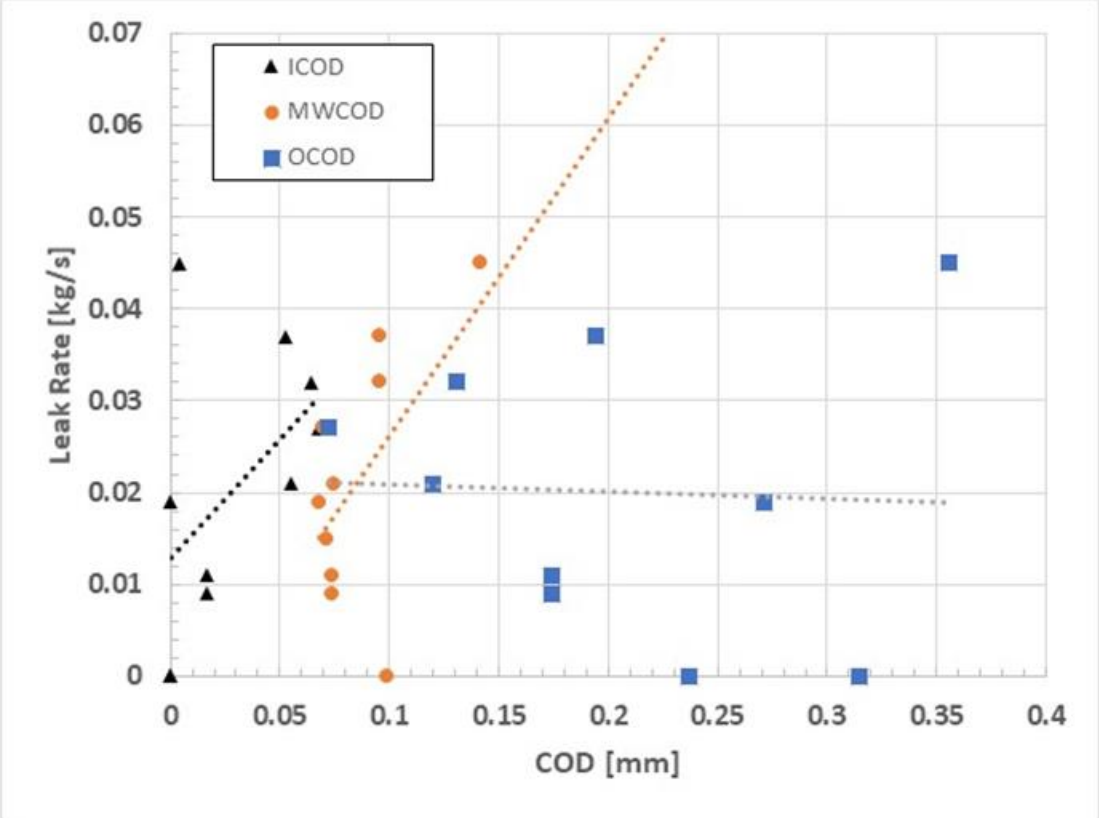

The LR results, however, are much more variable. While several participants (the EMCC, NRC, OPG and Tractebel) predicted Task 2 LR values within 20% of their Task 1 values, the remaining participants predicted more significant differences. It is also illuminating to compare the absolute LR differences predicted in Tasks 1 and 2 (Figure 8.8). Most participants expected smaller LRs due to the WRS effects, especially those predicting zero (or negative) ICOD values (e.g. the KIWA and VTT). However, two of the participants predicted higher LRs due to the prescribed WRS distribution when using the MWCOD as the input into their LR codes. This likely occurs because they predicted that the WRS increases the MWCOD (Figure 8.7). The increased variability in the LR predictions was driven by the increased differences among the participants' predicted COD profile induced

by WRS and the input COD parameters chosen by the participants for the LR calculation, the inclusion of CFP (see below). Moreover, the variability was also driven by possible differences in how the LR codes manipulated the input COD parameters (e.g. by averaging them to obtain a single measure) in order to ultimately determine the predicted LR.

Figure 8.6. Task 2 MWCOD and LR values

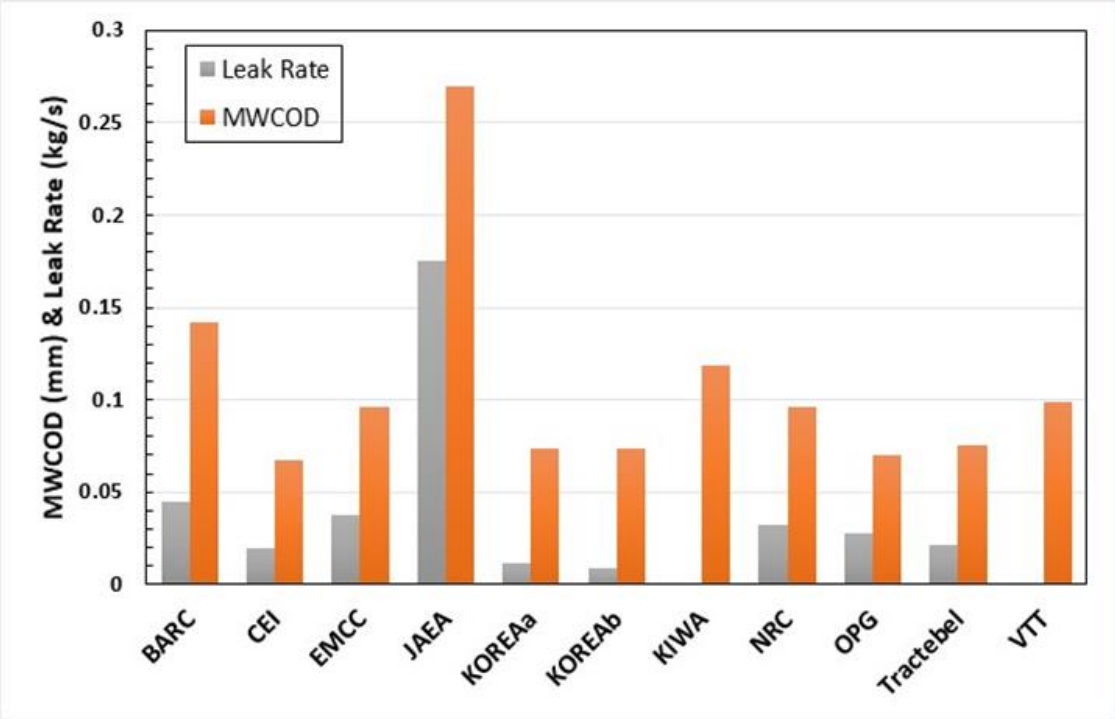

Figure 8.7. Effect of WRS on MWCOD and LR for CF morphology

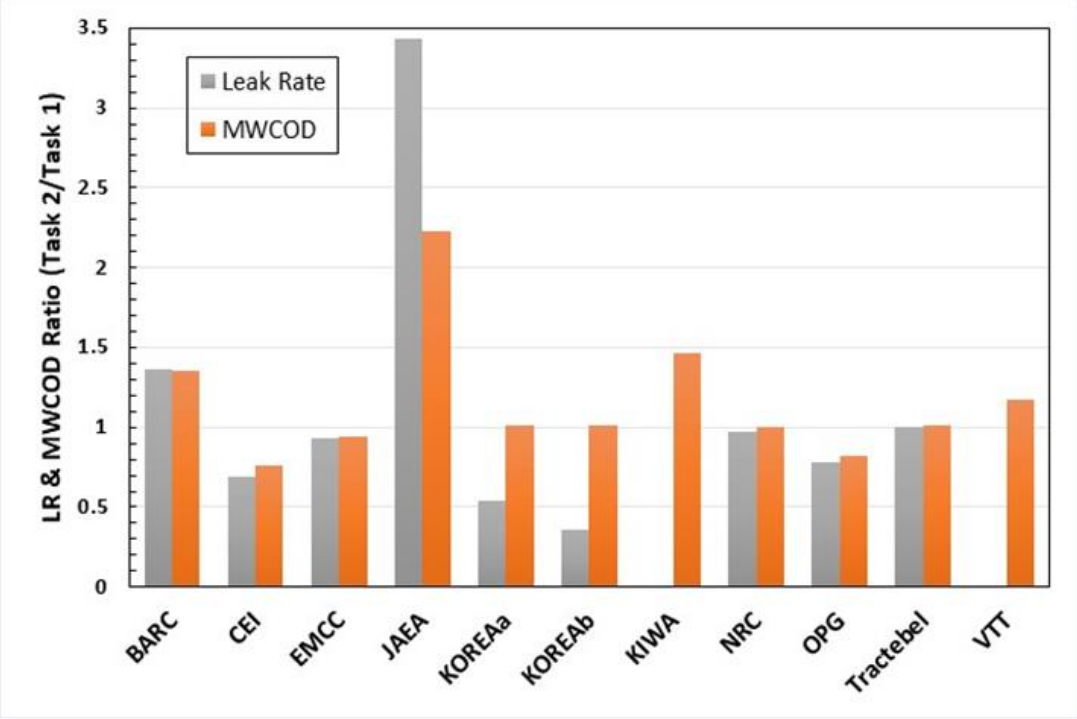

Figure 8.8. Absolute effect of WRS for CF morphology predictions

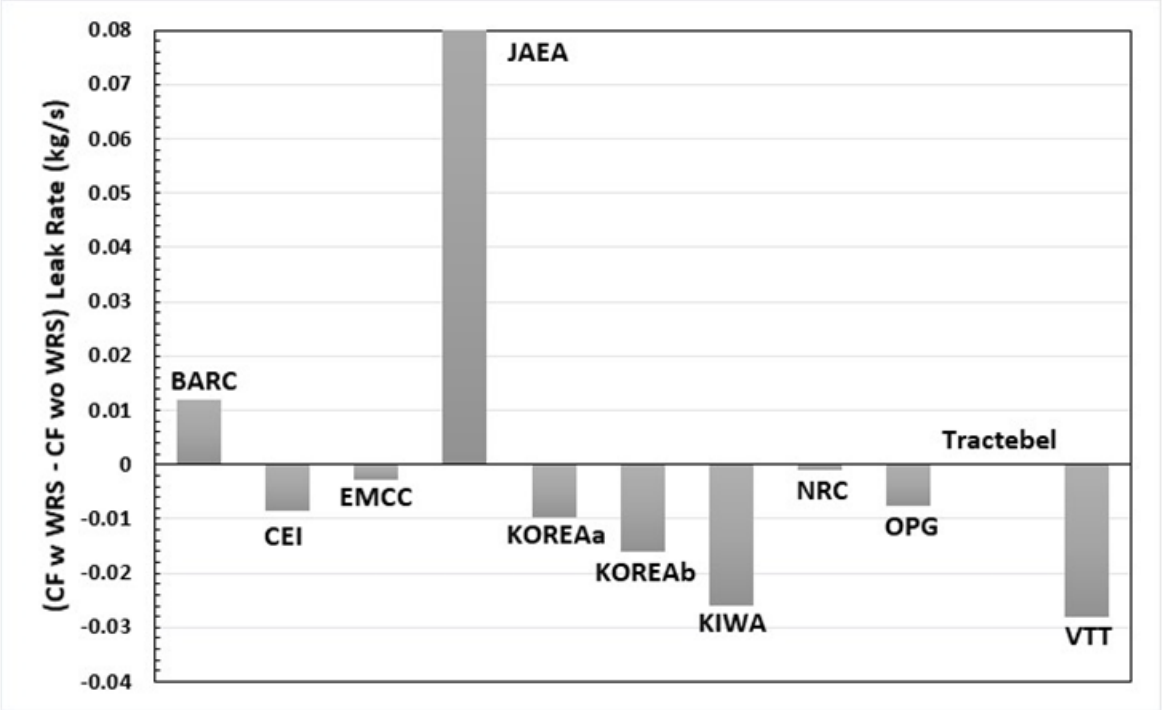

The relationship between the MWCOD and LR for Task 2 is plotted in Figure 8.9, but it excludes the highest predicted LR, and all zero LR values. The results that did not consider CFP are indicated by a square box around the data point. As with Task 1 (Figure 8.2), those results without CFP had among the lowest MWCOD values and predicted LRs. The LR codes used are also indicated in the figure. As in Figure 8.2, the SQUIRT/LEAPOR codes often gave higher LR values for a given MWCOD, but it is difficult to determine if this difference is statistically significant due to the small sample size and the inherent variability in the MWCOD prediction.

A linear fit of the plotted data has a lower slope than without WRS effects (Figure 8.2), which is expected because WRS tended to decrease the predicted LR values. Additionally, the r^2 value for the linear fit is only 0.68 (0.80 in Figure 8.2), which is indicative of the greater variability in the LR predictions. The worse fit is also a reflection of the inability of the MWCOD to accurately represent those aspects of the COD profile that are important in governing fluid flow. For example, either a measure of the complete COD profile (such as an integrated average) or the minimum COD at any through-thickness location may better correlate with the predicted flow rate.

Figure 8.9. Relationship between the MWCOD and LR for Task 2

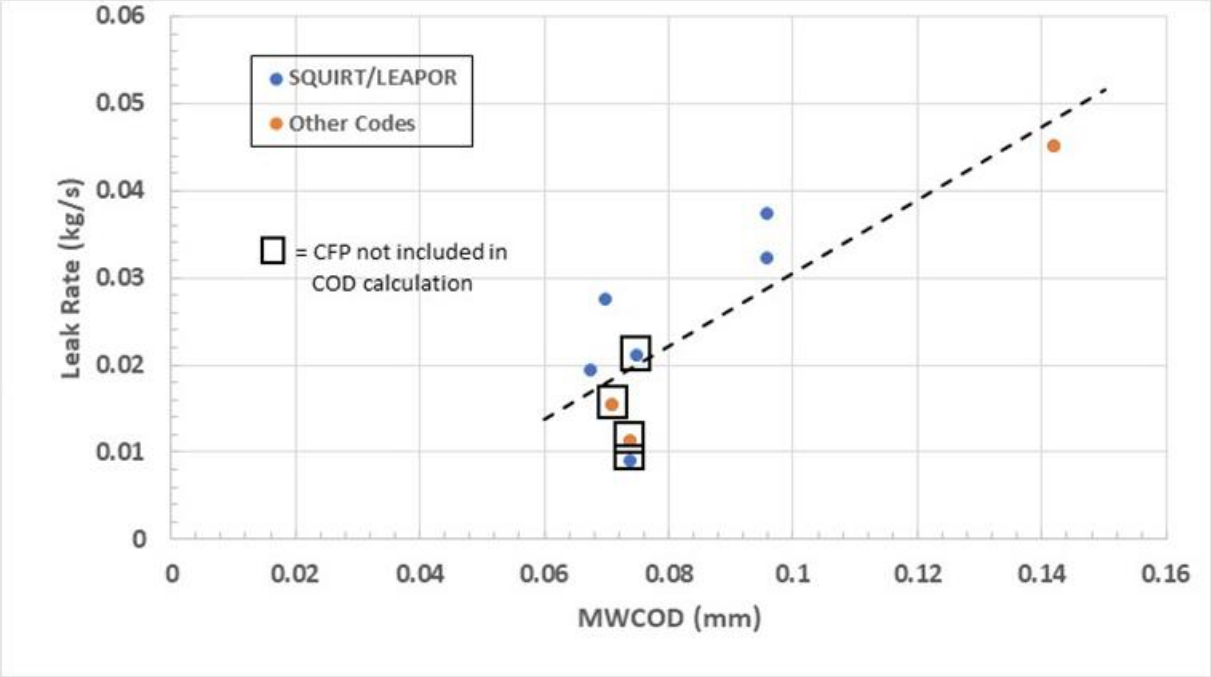

8.3. Task 3 results: PWSCC morphology without WRS effects

The Task 3 results are summarised in Table 8.3. The only difference between the Task 1 and 3 problems are that Task 1 evaluated a CF crack morphology, while a PWSCC crack morphology was prescribed for Task 3. The COD and CBM results for Task 3 are therefore identical to those reported for Task 1 (Table 8.1). Only the LR predictions are distinct. However, the various COD results and treatment of CFP from Task 1 (Table 8.1) are also provided in Table 8.3 for convenience. Notably, the KIWA results are reported as N/A because they indicated that the crack was too tight to get valid results. However, it is assumed in future treatment of the KIWA Task 3 data that their reported LR is 0 kg/s. GRS similarly reported a zero leak rate due to the tortuosity of the PWSCC crack morphology provided for the benchmark problem.

Figure 8.10 summarises the difference between the Task 3 and Task 1 LRs reported by each participant. As seen in this figure, all participants reported lower LRs for the PWSCC crack, which was anticipated for the COD values associated with the prescribed conditions. The average reported LR is 0.0244 kg/s for the PWSCC crack morphology compared to an average LR of 0.0313 kg/s for the CF morphology.[8] This represents an average difference of 0.0069 kg/s, or a decrease of approximately 22%. There is also more variability in the PWSCC morphology LR predictions because the standard deviation is about 44% of the mean compared to only 27% for the CF morphology LR predictions in Task 1.

[8] Average Task 3 values are determined without the GRS results for consistency with Task 1 calculation.

Table 8.3. Task 3 results

Organisation	ICOD (mm)	MWCOD (mm)	OCOD (mm)	CFP in COD (Y/N)	LR (kg/s)
BARC	0.082	0.105	0.130	Y	0.029
CEI	0.089	0.089	0.089	Y	0.027
EMCC	0.090	0.102	0.124	Y	0.033
GRS	0.071	0.071	0.071	N	0
JAEA	0.112	0.121	0.135	Y	0.042
KOREAa	0.073	0.073	0.073	N	0.011
KOREAb	0.073	0.073	0.073	N	0.021
KIWA	0.065		0.097	N	N/A
NRC	0.079	0.096	0.116	Y	0.028
OPG	0.082	0.085	0.087	Y	0.030
PSI	0.070	0.084	0.099	Y	0.025
Tractebel	0.063	0.074	0.087	N	0.020
VTT	0.070	0.084	0.101	Y	0.026

Figure 8.10. Absolute effect of crack morphology on LR without WRS

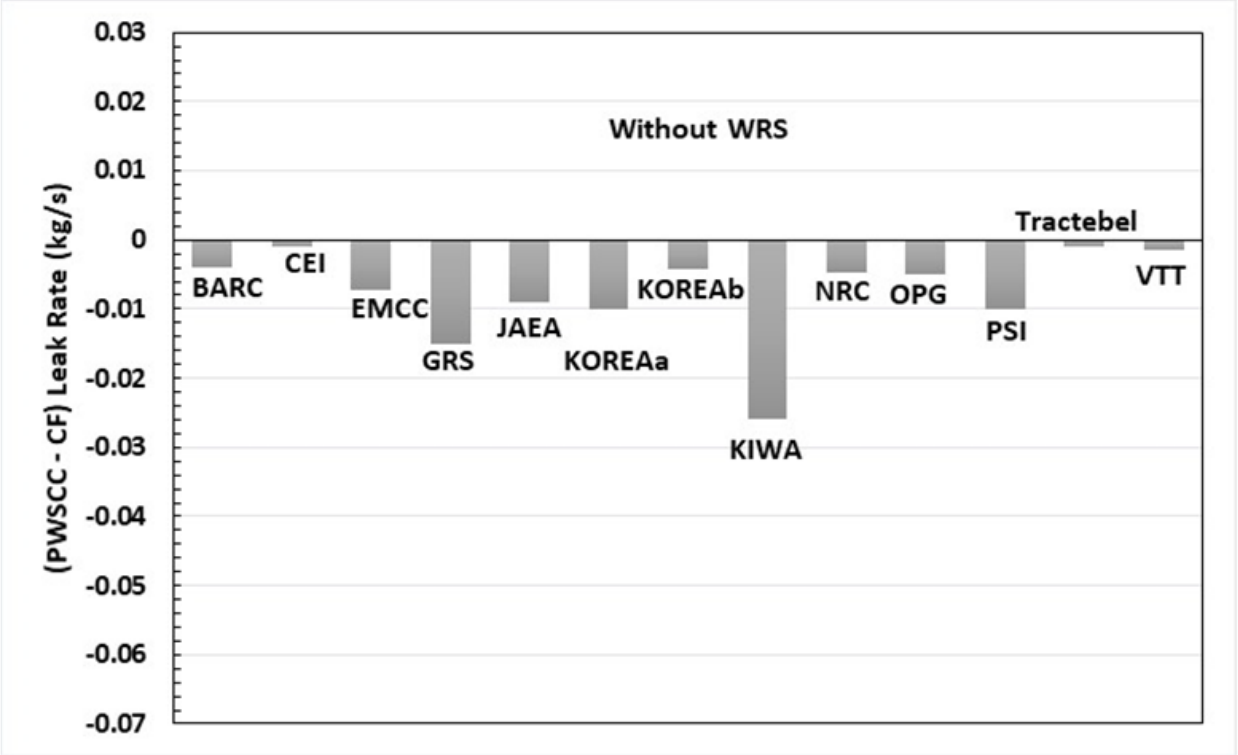

Figure 8.11 illustrates the pairwise LR values from Tasks 1 and 3 for each participant. A true linear relationship would imply that the differences among participants PWSCC LR predictions can be entirely explained by the initial differences in the CF predictions. The fact that there is not true linearity demonstrates that there is additional variability introduced in the LR predictions due to the PWSCC morphology. However, this additional variability primarily stems from the participants that predicted a zero leak rate for the PWSCC crack. For remaining participants, the reasonable linear relationship implies that a significant portion of the differences among their PWSCC LR predictions is due to the initial variability in the CF predictions.

Furthermore, it is also interesting to note that there are not significant differences in the pairwise relationship of the Task 1 and 3 LR values calculated using SQUIRT/LEAPOR and the other LR codes in Figure 8.11. The implication of this observation is that the ratio of the Task 1 to Task 3 LRs is reasonably consistent for the various LR codes used in these tasks. The variability in the CF LR predictions appears to account for the PWSCC LR prediction differences and therefore it seems that the differences among the COD predictions account for a significant portion of the differences in the LR predictions among participants for both Tasks 1 and 3, as was implied in Section 8a.

Figure 8.11. Leak rate comparison without WRS

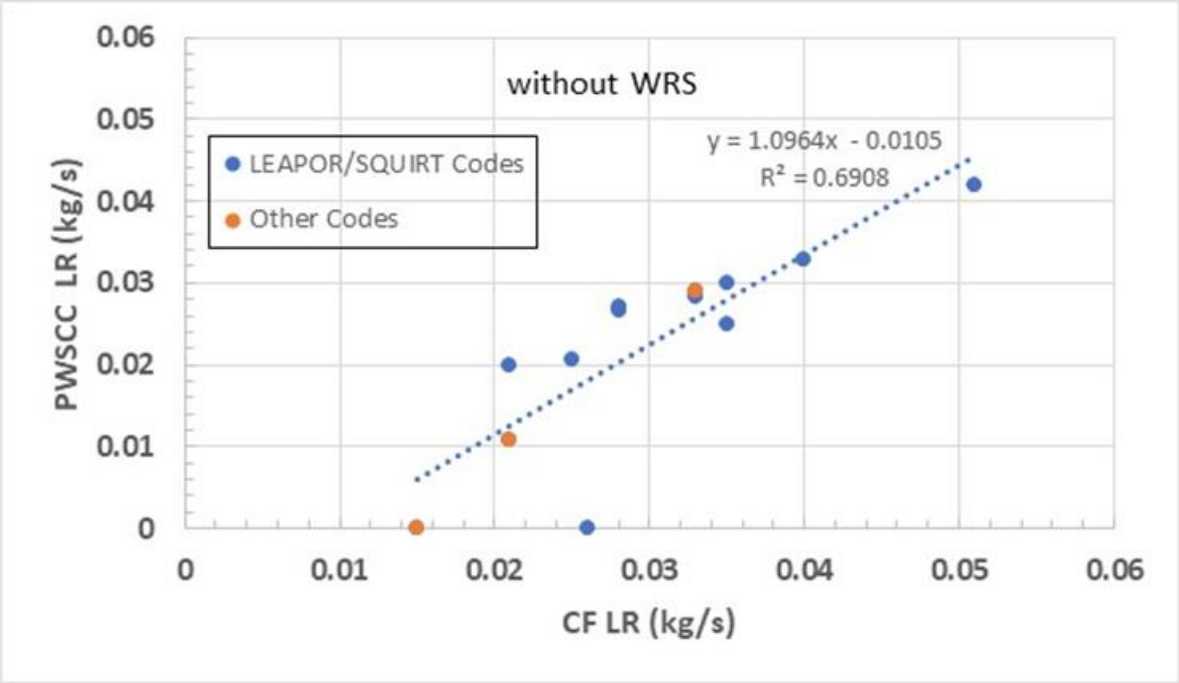

The relationship between the MWCOD and LR is provided in Figure 8.12. The data and the trend curve for the CF results (Figure 8.1) are included for comparison. It is interesting to note that the participants that did not consider CFP generally predicted the lowest LRs and the greatest decrease in the LR was due to the PWSCC morphology. If the average LR for only the participants that considered CFP is calculated, the average PWSCC and CF LRs are 0.0301 kg/s and 0.0354 kg/s, which is approximately 13% and 23% respectively higher than the values with all the data (i.e. 0.0244 kg/s and 0.0313 kg/s for PWSCC and CF respectively, as reported above).

More importantly, the variability among the PWSCC and CF CFP results are 18% and 21% of the mean value, which is similar. However, the standard deviation for the PWSCC morphology is 44% of the mean compared with 27% of the mean for the CF morphology when the results of all participants are considered. Consequently, much of this additional variability in the LR predictions for the PWSCC morphology is directly correlated with the choice to incorporate CFP.

Figure 8.12. MWCOD vs. LR without WRS

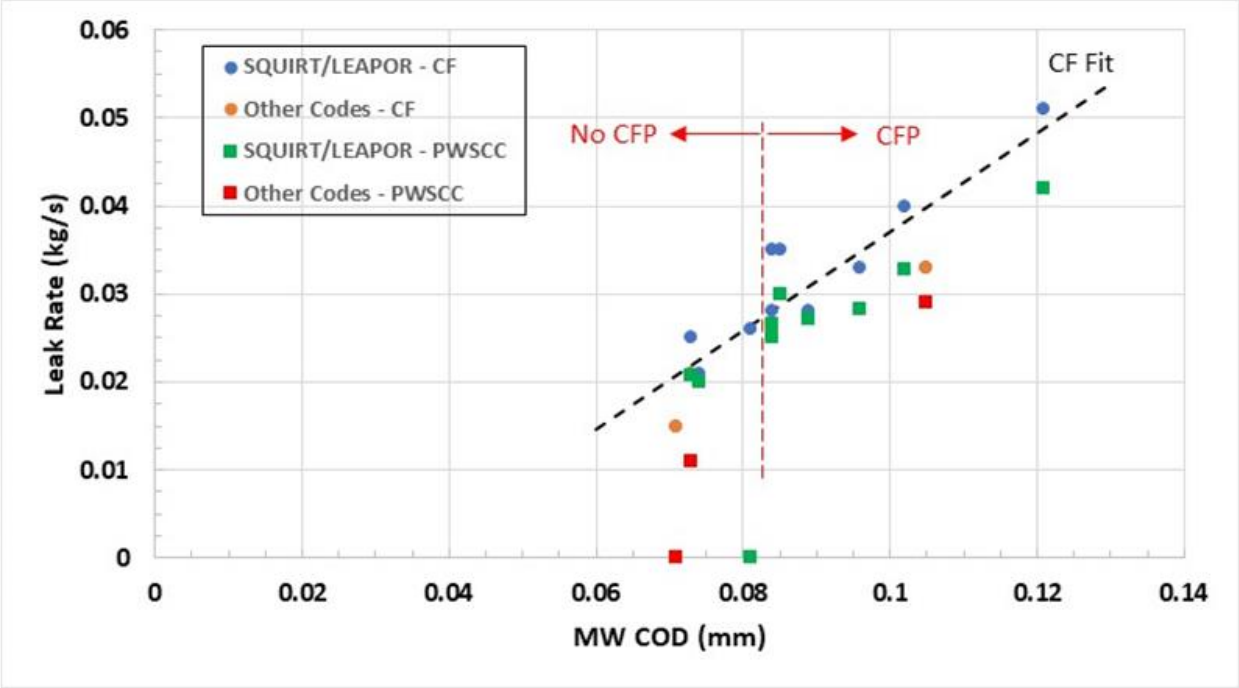

8.4. Task 4 results: PWSCC morphology with WRS effects

The Task 4 results are summarised in Table 8.4, while the LR predictions for Tasks 2 and 4 are illustrated in Figure 8.13. Task 4 considered the PWSCC crack morphology with WRS effects. The only difference between the Task 2 and 4 problems are therefore that Task 2 evaluated a CF crack morphology, whereas a PWSCC crack morphology was prescribed for Task 4. Additionally, the only difference between the Task 3 and 4 problems was the consideration of the prescribed WRS distribution in Task 4. As a result, the various COD and CBM predictions are identical to those reported for Task 2. The only unique result is the LR prediction. However, Table 8.4 includes the COD results from Task 2 and the treatment of CFP in the COD analysis for completeness.

The average predicted LR for cracks with the prescribed PWSCC morphology (Table 8.4) is 0.0264 kg/s.[9] This can be compared with the average LRs from Task 2 (i.e. CF morphology) of 0.0344 kg/s for the same applied WRS profile. The average decrease in LR due to the PWSCC morphology was thus approximately 0.008 kg/s. The scatter in both the Task 2 and 4 LR predictions is significant because the standard deviation was greater than 120% of the mean value in both instances. However, if the highest and lowest (i.e. zero) LR predictions are not considered in the average, the average Task 4 LR was 0.0219 kg/s, compared with an average Task 2 LR using the same participant population of 0.0253 kg/s, a decrease of 0.0034 kg/s (13%). The standard deviation of both the Task 2 and 4 results thus decreased to ≈50% of their respective means.

[9] Average values reported in this section do not include the GRS results as they did not evaluate WRS effects.

Table 8.4. Task 4 results

Organisation	ICOD (mm)	MWCOD (mm)	OCOD (mm)	CFP in COD (Y/N)	LR (kg/s)
BARC*	0.004	0.142	0.356	Y	0.041
CEI*	-0.047	0.068	0.271	Y	0.019
EMCC	0.053	0.096	0.194	Y	0.030
GRS*				N	
JAEA*	0	0.270	1.25	Y	0.116
KOREAa	0.017	0.074	0.174	N	0.008
KOREAb	0.017	0.074	0.174	N	0.008
KIWA	0		0.237	N	0
NRC	0.064	0.096	0.131	Y	0.026
OPG	0.068	0.070	0.072	Y	0.023
Tractebel*	0.055	0.075	0.12	N	0.020
VTT	-0.027	0.099	0.315	Y	0

Note: * LR calculated using MWCOD values.

Figure 8.13 and Figure 8.14 can be used to further explore the differences between the Task 4 (i.e. PWSCC) and Task 2 (i.e. CF) LR predictions, while recognising that both tasks incorporated WRS effects in the COD calculations. All reporting participants expected the LR to decrease for the PWSCC morphology compared to the CF morphology. However, most participants only predicted a modest decrease in LR, which is consistent with the small average LR decrease from Tasks 2 to 4 that is reported above. The JAEA reported the largest absolute decrease in LR from Tasks 2 to 4. However, this is primarily due to the relatively large LR that the JAEA had predicted for the CF morphology based on the larger MWCOD predicted upon incorporating WRS effects (Task 2). A large absolute decrease to the PWSCC LR is therefore unsurprising because the PWSCC morphology is a much greater percentage of the COD.

Another way to examine the differences in the LR due to crack morphology with the addition of WRS effects is to directly compare the LR predictions from Tasks 2 and 4 (Figure 8.15). This figure is analogous to figure 8.11, which directly compared the Task 1 and 3 LRs. Figure 8.15 exhibits an even stronger linear correlation than 8.11, which once again indicates that the differences among the participant's Task 4 results can be attributed to the difference in their Task 2 results and that they more fundamentally reflect the underlying Task 2 calculation methods and inputs.

Figure 8.13. Leak rate predictions with WRS

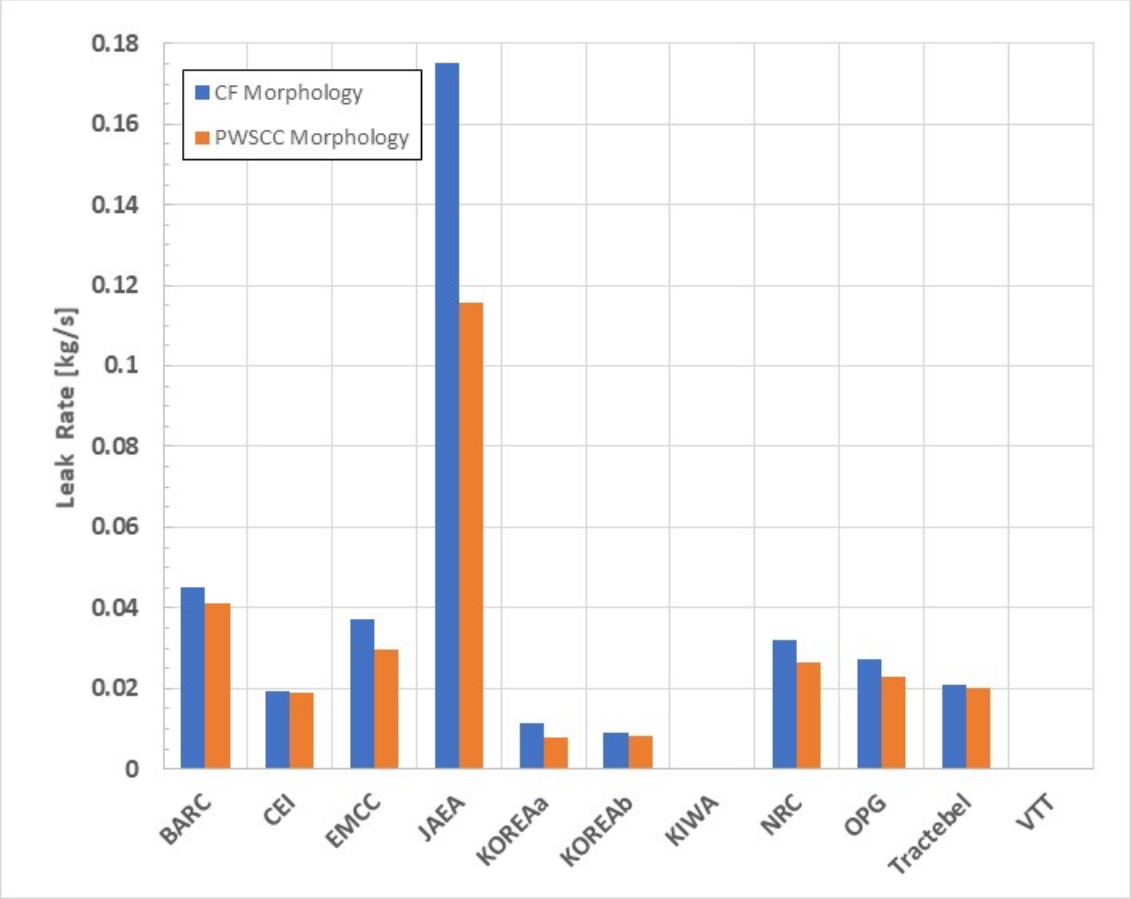

Figure 8.14. The absolute effect of crack morphology on LR with WRS

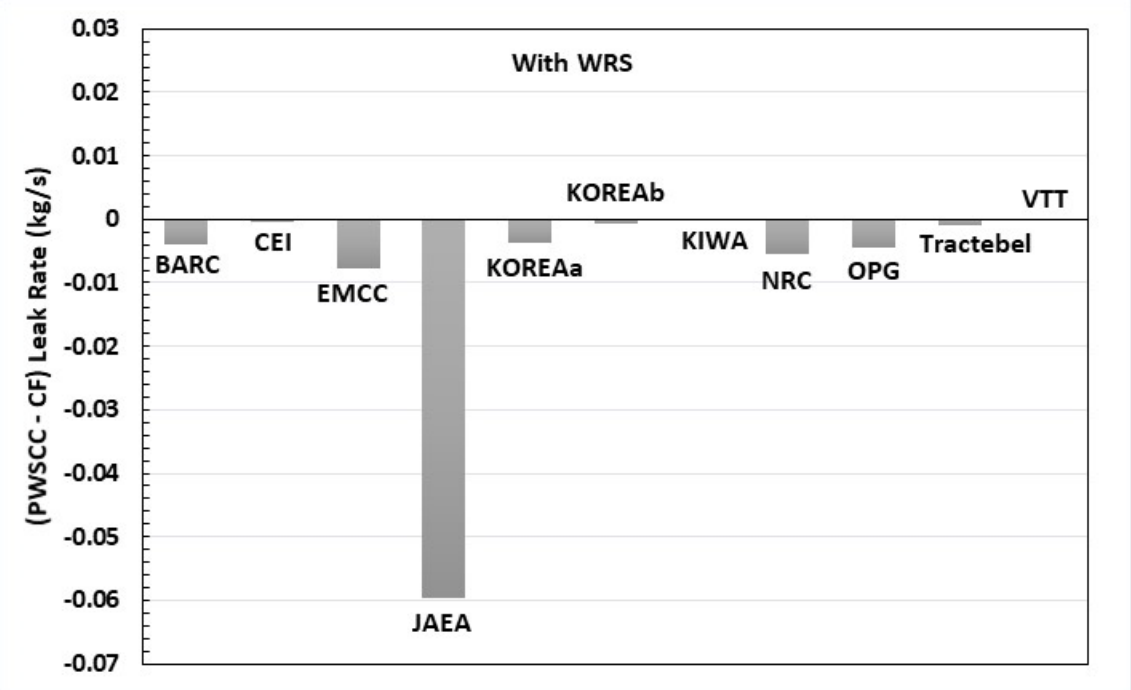

Figure 8.15. Leak rate comparison with WRS

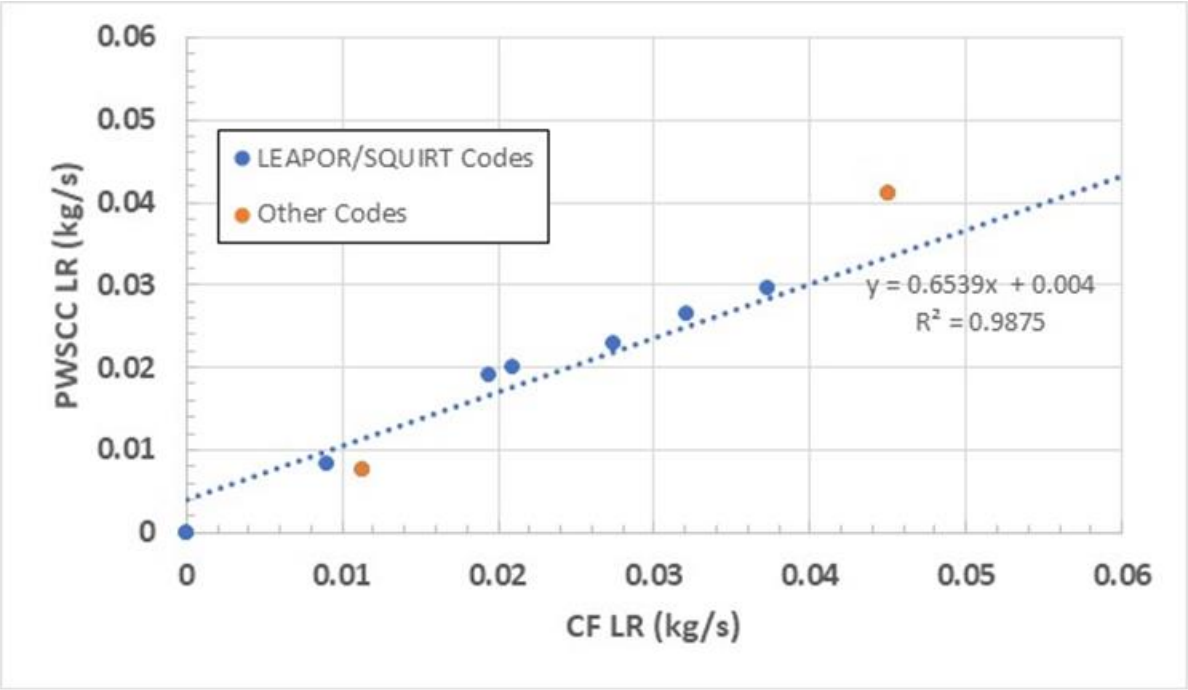

As discussed earlier, the differences in the Task 2 results are a function of the variability induced by incorporating WRS effects, selected COD input parameters for the LR code (e.g. ICOD vs. MWCOD), incorporation of CFP (see below) and the manner in which the LR code processes the input values to calculate the LR. However, as in Figure 8.11, there does not appear to be significant variability associated with the particular LR code used in the benchmark because no additional bias is obvious (Figure 8.15). As stated previously, there is a limited sample of results from codes other than the LEAPOR/SQUIRT family.

The effect of WRS on the decrease in the LR between the CF and PWSCC crack morphologies can be examined by comparing Figure 8.10 with Figure 8.14, or alternatively by directly plotting the percentage decreases (Figure 8.16).[10] The x-axis in Figure 8.16 is the percentage decrease between the CF and PWSCC LR predictions without WRS (i.e. 1- Task1 LR/Task 3 LR), while the y-axis is the percentage decrease with WRS (i.e. 1 – Task 2 LR/Task 4 LR). The 1:1 line in this figure depicts an identical percentage decrease both with and without WRS effects. Most of the participants are either on, or close to, the 1:1 line. The most disparate data points belong to KOREAa, KOREAb and the JAEA. KOREAa and KOREAb both predicted a smaller relative LR decrease due to PWSCC with WRS effects, while the JAEA predicted a greater difference in the LR due to PWSCC if WRS effects are considered.

The absolute WRS effect on the LR for the PWSCC morphology can also be examined by comparing the LR differences between Task 3 (no WRS) and Task 4 (with WRS), as in Figure 8.17. As seen when comparing the Task 1 and 2 LR predictions, the effects of the prescribed WRS distribution are not as consistent. Several participants predicted that the WRS addition would further decrease the LR, while two participants predicted that the LR would increase. However, the trends and results in each participant's prediction in Figure 8.17 are reasonably consistent with their prediction of the effects of WRS on the LR for the

[10] KIWA and VTT results are not shown in Figure 34 as neither calculated a leak rate from MWCOD for Tasks 2 and 4.

CF morphology (Figure 8.8). The average predicted Task 4 LR, after excluding the highest predicted LR and all zero LR predictions, was 0.0219 kg/s. The average Task 3 LR for the same subset was 0.0250 kg/s, which is a difference of only 0.031 kg/s, or approximately 14%. A comparison of the same participant subsets for the Task 1 (0.0299 kg/s) and Task 2 (0.0253 kg/s) LR predictions results in an average reduction WRS of 0.046 kg/s, or approximately 15%.

Figure 8.16. Effect of WRS on the percentage decrease in the LR due to PWSCC

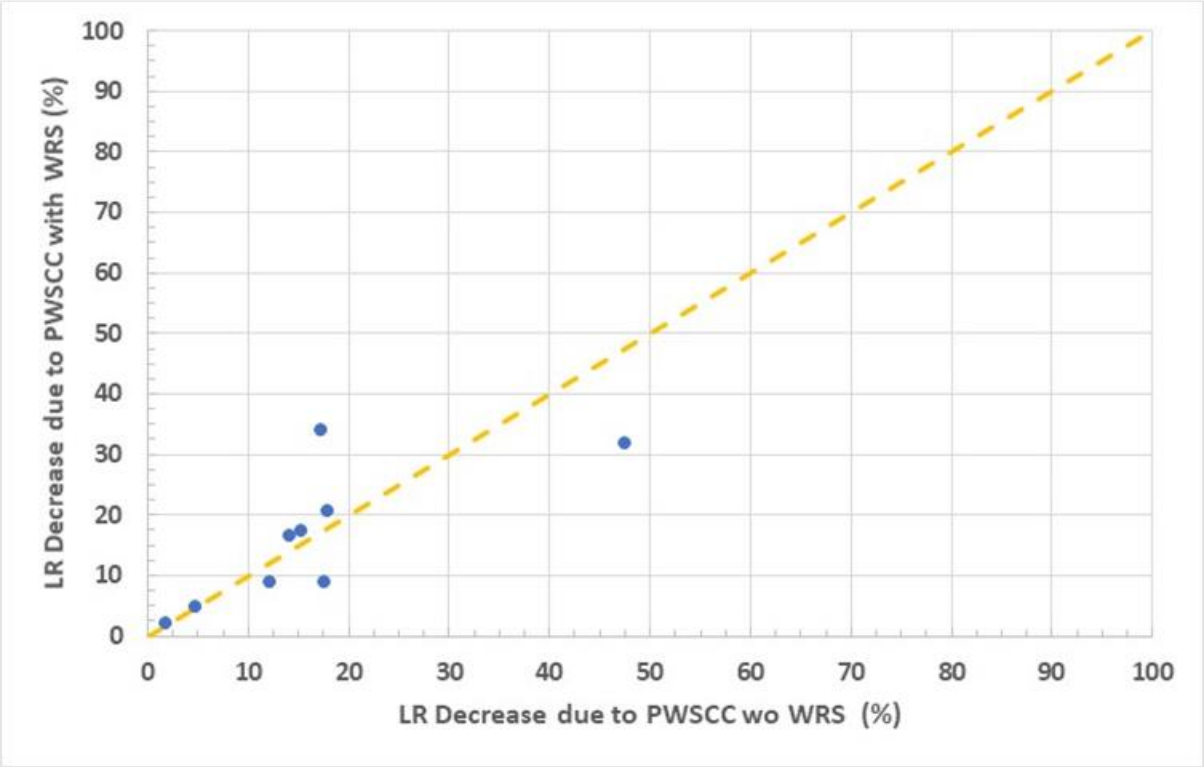

Figure 8.18 depicts the relationship between the MWCOD and LR for Task 4 for the same participants, which is shown for Task 2 in Figure 8.9. The Task 2 data and associated trend line (labelled CF fit) from Figure 8.9 are also included in Figure 8.18 for convenience. The results, while not as clear as in Figure 8.12, highlight the previously discussed importance of CFP in the LR predictions. Those participants that did not consider CFP typically predicted a greater LR decrease for the PWSCC crack morphology than those that included CFP. Including CFP obviously increases the COD, which may decrease the influence of crack morphology on the LR.

As before, if only the participants that included CFP are evaluated, the average decrease in the LR due to PWSCC was approximately 0.004 kg/s. This difference is similar to the LR decrease due to PWSCC without WRS of 0.005 kg/s. Furthermore, the variability in the Task 2 and 4 results for the participants that considered CFP is approximately the same. Consequently, as was the case when WRS was not considered, most of the additional variability in the PWSCC LR predictions directly stems from the decision to incorporate (or not incorporate) CFP into the LR predictions.

Figure 8.17. Absolute effect of WRS on the LR predictions for PWSCC morphology

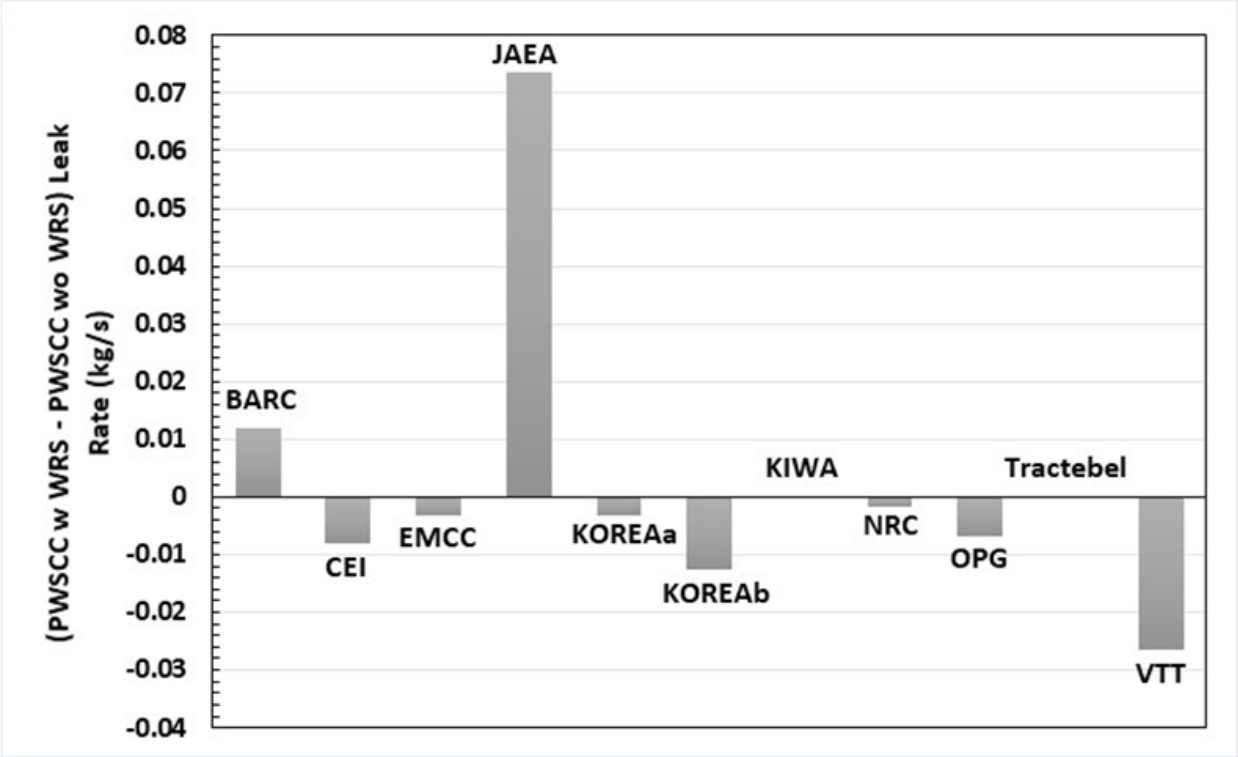

Figure 8.18. MWCOD vs. LR for the CF and PWSCC morphologies with WRS

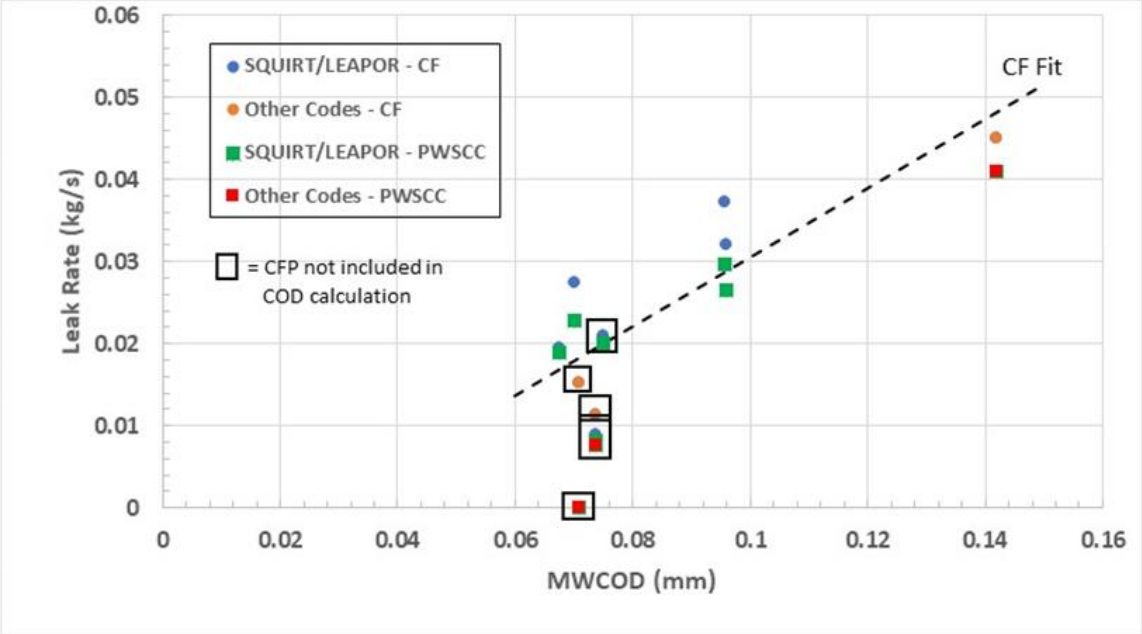

9. Benchmark summary

This leak-before-break (LBB) benchmark was initiated in 2017 with the intention of comparing the results from different LBB analyses among participating countries using common inputs. The intention was also to identify the effects of weld residual stress (WRS) and crack morphology on the crack opening displacement (COD) and leak rate (LR) calculations in LBB analyses. The benchmark consisted of a baseline problem that was developed so that it would marginally pass the US Nuclear Regulatory Commission (NRC) Standard Review Plan (SRP) 3.6.3 acceptance criteria for the piping configuration, assumptions and inputs considered. Participants were asked to evaluate the baseline problem using their country's LBB requirements. Four additional tasks were defined for the same configuration and loading, but with a fixed crack length. Each task then varied either the WRS or crack morphology in order to systematically address these effects. Task 1 evaluated a corrosion fatigue (CF) morphology without WRS; Task 2 considered the same CF morphology with a prescribed WRS distribution; Task 3 evaluated a primary water stress corrosion cracking (PWSCC) morphology without WRS; and Task 4 considered the effects of the same WRS distribution in Task 2 on the PWSCC morphology from Task 3.

Participants from 14 organisations, representing 11 countries, performed the benchmark exercise. Each participant provided a high-level summary of the LBB requirements in their country and documented the computational codes and approaches that they used in their evaluations. The participants were first asked to determine whether the baseline problem would meet their country's LBB acceptance criteria. They were also asked to provide supporting information, which included the leak rate detection limit (LRDL), the LR used to determine the leakage crack size (LCS), the LCS value and the critical crack size (CCS). Several participants provided other supplementary results. For Tasks 1-4, the participants were asked to provide the inner, mid-wall and outer COD values, the associated LR and the critical bending moment (CBM) for the prescribed crack.

The high-level summary of the LBB requirements in each of the participating countries revealed that the basic tenets and underlying principles of the LBB philosophy are generally consistent among the considered countries. Most countries' procedures are rooted in the US NRC SRP 3.6.3 method, but virtually every country has modified either the analysis or acceptance procedure based on additional knowledge that has been gained since the NRC SRP 3.6.3 method was established. Some of the more common modifications include explicitly allowing a lower LRDL than the one specified in the NRC SRP 3.6.3, requiring an additional subcritical cracking analysis in order to demonstrate that LBB or inspection intervals are not challenged, and requiring that worst-case strength and toughness properties are chosen from the base and weld metal properties.

The German KTA requirements are the most unique because no explicit margins are used on either the LR or the CCS. The margins are instead implicitly included in the conservative analysis methods that are used to determine the LCS and CCS. Other unique requirements adopted by individual countries include a consideration of the effects of a prescribed WRS distribution (Sweden), a stability analysis to determine both an acceptable critical surface flaw depth and length (Germany) and the allowance of probabilistic analysis to supplement the classical deterministic approach (Canada). These differences represent a natural progression of both technical and operational knowledge since the NRC SRP 3.6.3 method was first established. Any of these approaches and requirements are worthy of consideration for developing more realistic and less conservative LBB approaches.

The benchmark participants used a wide range of computational tools, assumptions and approaches. Most participants used either commercial codes or codes that were developed in-house for calculating COD. The LR codes exhibit limited diversity, with the majority of the participants using SQUIRT or its derivatives (i.e. LEAPOR and LeakRate_Excel_BetaR1) and only a few using other codes (e.g. the Pipe Crack Evaluation Program [PICEP] and WINLECK). There were a large number of in-house codes for calculating crack stability. Several participants used various derivatives of the LBB.ENG2 code, although net-section collapse (NSC) models, failure assessment diagrams (FADs) and other elastic-plastic fracture mechanics (EPFM) models were also used. A few participants used both the EPFM and NSC and chose the method that resulted in the lowest CCS.

The most unique aspect of the benchmark was the incorporation of the WRS effects into Tasks 2 and 4. Most participants assessed the contribution of the WRS to the COD using finite element analysis (FEA) to determine the applicable boundary conditions (force, pressure, displacement or temperature) to mimic these effects' model. A few participants used an analytical method to apply either an effective moment or force to the crack plane.

The most common differences among the analysis assumptions for the baseline problem were the LR used to determine the LCS, the crack morphology, the material strength properties employed, whether crack face pressure (CFP) was used for the analysis and if WRS was considered in the calculation of the LCS and/or CCS. There were similar differences among the analysts' choice of material strength properties and whether they considered CFP in Tasks 1-4. However, the crack morphology and WRS were explicitly specified in these problems so there was much less variability introduced in Tasks 1-4 by analyst discretion. The CFP was also specified in the Task 1-4 problems, but not every participant could evaluate this effect using their chosen computational tools.

9.1. Baseline problem

The baseline problem achieved its initial objective of being "marginal" because eight participants indicated that it is "not acceptable" for LBB, while six participants indicated that it "is acceptable" for LBB. The principal considerations in determining if the baseline problem was acceptable were the choice of the material properties to determine the CCS coupled with the crack morphology and LRDL limits used to determine the LCS. Using lower strength properties (stainless steel base metal) decreased the LCS and CCS predictions, while using a higher LRDL (and associated margin) and more tortuous crack morphology (PWSCC) increased the LCS prediction. Decreases in the CCS and increases in the LCS, either independently or in combination, make achieving LBB acceptance less likely.

Other secondary considerations also affected LBB acceptance in the baseline problem. The CBM values determined by the NSC and FAD methods were approximately 15% less than the values determined by the EPFM method. The NSC or FAD models therefore predicted a lower CCS value for the benchmark. The treatment of WRS is also a potentially important factor in calculating the LCS and can significantly decrease the CBM (and subsequently the CCS) if it is treated conservatively (as a primary load) within the analysis. However, only one participant explicitly considered WRS effects in the baseline problem and therefore no definitive conclusions can be drawn. Finally, the baseline problem also identified that the way different LR codes model and treat crack morphology effects for a prescribed crack morphology (e.g. air fatigue) can affect the LCS result. Understanding the effects of these differences is outside the scope of this benchmark, but this should be addressed by the companion CSNI Leak Rate Benchmark exercise.

Analysis of supplemental results supporting the baseline analysis provided additional insights and reinforced those that were apparent from the principal results. The CBM predictions, and consequently the resulting CCS, for a consistent set of inputs revealed much smaller differences than the LR and LCS predictions. This result was expected because the crack stability predictions are more mature and less impacted by analyst choices than the LCS predictions. The most important variable that led to differences among the predictions is the material strength and toughness properties used within the analysis. Including CFP was shown to have little impact on the CBM, and consequently CCS, predictions.

The supplemental results also demonstrated that the LCS prediction in the baseline problem can be affected by the chosen crack morphology if significantly different crack types are considered (e.g. air fatigue vs. PWSCC) and if WRS is considered. Crack morphology effects are important because the rougher and more tortuous cracks (e.g. PWSCC morphology) require a greater crack opening area (larger crack length and COD combination) to achieve the target LR. Additionally, there appear to be differences in the COD, crack length and LR relationship between some of the codes used in the benchmark for nominally similar crack morphologies. These differences could result from the way that the codes characterise crack morphology, the material strength properties selected in the analysis, parameters used for a specified crack morphology (e.g. air fatigue or corrosion fatigue), or differences in the fundamental relationship between the morphology and LR for a given COD. A sensitivity study of two different WRS distributions by one of the participants illustrated that the differences between the distributions became more significant as the through-wall circumferential crack (TWC) length decreased. This interesting result requires more study to improve understanding of and characterise WRS effects.

9.2. Tasks 1-4

The effects of crack morphology and WRS were more systematically evaluated in the Task 1-4 problems. The differences between participants' COD and LR predictions for the prescribed CF morphology in Task 1 were higher than initially expected. Differences in COD predictions are expected based on the material properties used in the analysis. However, most of the participants utilised weld properties and there was insufficient evidence to attribute differences among the benchmark COD predictions to material property selection. Some of the COD differences can be attributed to the consideration of CFP. Those participants that included CFP in their COD calculations generally had the highest predicted COD values. However, this consideration does not explain the bulk of the differences among the COD predictions. The COD prediction is fundamental to predicting the LCS and possibly the CCS (depending on the analysis method) and therefore it is important in order to better understand how COD is modelled within the codes used in this benchmark for LBB analyses.

A somewhat surprising result was that most of the differences in the LR predictions were directly attributable to the COD differences. Furthermore, differences among participants' LR predictions that can be directly attributed to the LR codes are not as apparent as they were in the baseline problem. The LR predictions are based on the COD input, model of the relationship between crack morphology and flow resistance and two-phase flow model (i.e. Henry-Fauske). These observations therefore imply either that the participants' LR codes employ relatively consistent crack morphology and two-phase flow models, or that the differences in how these codes model the relationship between the LR and COD may not be significant for the fixed crack morphology and crack length conditions evaluated in Tasks 1-4. Other variables that were not explicitly fixed in the baseline problem (for

example, the input parameter selection, crack morphology parameters and crack length effects) can more significantly contribute to the LR code-related differences exhibited in the baseline problem results.

The CBM predictions provided by the participants for the CF morphology reinforced the trends evident in the baseline problem; the material property choice is the most significant cause of differences, while the crack stability approach employed (NSC, FAD or EPFM) also contributes, albeit far less, to the differences. Some interesting CBM results were provided in Task 2 that accounted for WRS effects on crack stability. Most participants either did not explicitly consider the effect of WRS on the CBM predictions or predicted a difference of less than a 2%. However, two participants independently used the R6 code to incorporate WRS effects and reported that the CBM values were approximately 30% lower than without WRS.

Incorporating the prescribed WRS distribution in Task 2 also has, as expected, a substantial impact on the predicted COD and LR results. Firstly, the predicted through-wall COD profiles are generally non-linear due to WRS, especially for participants that determined WRS contributions using FEA. Furthermore, it was demonstrated that no single COD measure can accurately represent the non-linear COD profile. The mid-wall crack opening displacement (MWCOD) values were on average not significantly affected by the prescribed WRS distribution, whereas the inner diameter COD (ICOD) and outer diameter COD (OCOD) predictions were substantially affected by the incorporation of WRS. Several of the participants that used FEA predicted that the ICOD would be close to zero or negative.

The effect of the prescribed WRS profile on the LR results was even stronger and introduced significant variability among the predictions. The significant impact of the WRS on the LR predictions highlights the importance of considering WRS effects when performing more accurate LBB analyses. Several participants predicted that WRS only resulted in a 20% change in the LR for the CF morphology. However, other participants predicted more significant differences. Some of this variability arose because some participants assumed a zero leak rate if the ICOD due to WRS was predicted to be zero or negative. Other participants used the MWCOD to calculate the LR even if there were substantial differences between the MWCOD and the ICOD or OCOD. Most participants expected smaller LRs due to the prescribed WRS profile, but a few participants predicted an increased LR. As was the case without WRS, those participants that included CFP in determining the COD had higher predicted LRs. Finally, when WRS was incorporated, MWCOD did not correlate well with the predicted LR, as for Task 1. This finding is plausible because, as stated above, no single COD value accurately captures the non-linear COD profile. It may be more accurate to predict the LR for a non-linear COD profile using an average COD, which is obtained by integrating the entire COD profile, or using the minimum COD through the thickness.

Changing the crack morphology from CF to PWSCC in Task 3 had the expected effect of decreasing the predicted LRs for the fixed crack size. All participants reported lower LRs for the PWSCC morphology, with an average decrease of approximately 20%. There was also much more variability in the PWSCC morphology LR predictions compared to those for the CF morphology in Task 1. However, much of the additional variability due to PWSCC directly correlates with the choice to incorporate CFP. Those participants that did not incorporate CFP generally predicted greater LR decreases for the PWSCC morphology. This is likely attributed to the fact that the PWSCC roughness is a much greater percentage of the COD when CFP is not considered.

Combining the WRS profile with the PWSCC morphology in Task 4 generally reinforces previous trends and findings. While most participants predicted the lowest LR for this task,

a few participants predicted that incorporating the WRS effect on COD would increase the LR. However, each participant's predictions of the WRS effects on the LR were consistent for both the CF (Task 2) and PWSCC (Task 4) morphologies. Additionally, the variability among the Task 4 LR predictions was not significantly higher than for Task 2. This reinforces the observation that most of the differences in the LR predictions were due to differences in the prediction of the WRS contribution to the COD through-thickness profile, (i.e. ICOD, MWCOD and OCOD) and how this profile was then used within the various LR codes.

Finally, the effect of considering CFP on the COD for the PWSCC (Task 4) and CF (Task 2) morphologies with WRS was consistent with the effects evident without WRS, as discussed above. Those participants that did not consider CFP typically predicted a greater reduction in the LR from the PWSCC crack morphology than those that included CFP. Furthermore, as was the case when WRS was not considered, most of the additional variability in the PWSCC LR predictions appears to directly result from the decision to incorporate CFP into the LR predictions. These results imply that the differences among LR codes relating to modelling and predicting the morphology effects on the predicted LR for a prescribed crack morphology are not as significant as factors affecting the associated COD, such as CFP, WRS, material properties and other additional conservatisms that may be present in existing codes.

10. Important LBB considerations and recommendations for further work

The governing leak-before-break (LBB) philosophy and associated analysis principles are generally consistent among countries, and many specific procedures are rooted in the US Nuclear Regulatory Commission (NRC) Standard Review Plan (SRP) 3.6.3. However, virtually every country has modified aspects of either the analysis or acceptance procedure. Several of the more common and a few of the more novel modifications are discussed in Section 9. All of these various modifications represent a natural progression of both technical and operational knowledge gained since the NRC SRP 3.6.3 was first established. Any of these approaches and requirements are worthy to consider in developing more realistic and less conservative LBB approaches.

The current benchmark has identified several additional aspects of a deterministic LBB analysis that are important when a more accurate LBB evaluation is sought. General considerations are first discussed, followed by those that affect the leakage crack size (LCS) calculation, and finally by those associated with the calculation of the critical crack size (CCS). The first general consideration is the location of postulated cracks at weld locations and the corresponding choice of the material properties used in the LCS and CCS calculations. Many countries currently require that cracks be postulated in the base, weld and HAZ locations and then the most conservative LBB assessment is used to determine if the weld configuration meets the LBB acceptance criteria. This is one area where reduction in conservatism using both the knowledge of likely areas of degradation and cracking may be warranted.

An important related consideration is the material strength and fracture toughness properties used in the analysis. As seen in the benchmark, this choice can significantly affect the CCS determination. Although this was not apparent in the benchmark results, the calculated crack opening displacement (COD) can also be significantly affected by the chosen strength properties if the plastic COD contribution is significant and the base, weld and/or HAZ strength properties differ significantly (i.e. by more than 10%). The fracture toughness properties for the material at the crack location should be chosen to produce more accurate results. Determining more accurate strength properties is more complicated because they will be a mixture of the weld and base metal properties. The mixed properties are a function of the weld geometry (weld joint thickness and bevel angle), crack location and difference between the base and weld metal properties. These mixture properties can be determined through either analytical or finite element analysis (FEA) evaluation.

Assessing crack growth effects is another more realistic consideration that is already required in several countries. There are various ways to incorporate crack growth into an LBB analysis. One approach is to postulate an initial surface-breaking flaw, which could reasonably be missed during inspection, and calculate the growth of this flaw over the life of the plant to ensure that it does not exceed a reduced value of the CCS. Another approach is to calculate the crack growth due to one operating cycle for the through-wall CCS and reduce the CCS by this amount to ensure that failure during an operating cycle is unlikely. Yet another approach is to calculate the time it takes for the LCS to grow into the CCS to ensure that there is sufficient time for operator action between leak detection and pipe rupture. Ideally, crack growth due to both fatigue and SCC mechanisms in any such analysis should be evaluated.

There are several aspects that can be refined in order to calculate more accurate LCS values. The first aspect is the selection of the leak rate detection limit (LRDL). Several countries now allow LRDL limits that are much lower than the 0.06 kg/s value that was used within

many historical US LBB applications. The second aspect is ensuring that this LRDL is acceptably conservative. Some countries have adopted a smaller LRDL margin than the value of 10 specified in the NRC SRP 3.6.3. Alternatively, a conservative computation of the leak rate without an additional margin has been used in Germany (i.e. KTA 3206). A single bounding LRDL value and margin could be determined within each country, which would recognise the operational improvements that have been achieved since the historical value was determined. It may also be more straightforward to allow LBB applicants to determine and justify a plant-specific LRDL rather than a single prescribed LRDL value, which would be dependent on their leak detection systems and requirements for identifying unexplained leakage.

However, as the LRDL and associated margin decreases, the LCS also decreases, along with the associated crack opening displacement (COD). As the COD decreases, the uncertainty in the leak rate (LR) calculations increases, so that either explicit or implicit (i.e. through a margin) consideration of the phenomena affecting the LR becomes more important in an accurate LCS calculation. There are several phenomena that were evaluated as part of this benchmark that can significantly affect the LCS calculation. These include the accuracy of the COD model, selection of the crack morphology, inclusion of weld residual stress (WRS) effects and consideration of crack face pressure (CFP).

The accurate determination of COD is an important consideration for accurately calculating the LCS. As seen in this benchmark, differences in the COD predictions caused much of the variability among the participants' benchmark results. This finding illustrates the need to better understand how the load vs. COD relationship is modelled within commonly used computational codes such as those used in this benchmark. These models can be benchmarked using finite element or experimental results to assess their accuracy for CODs associated with a range of applicable crack sizes, piping systems and loads. It would also be valuable to continue to develop methods that consider the entire through-thickness COD profile when determining the LR and not just a single point or average value. Furthermore, the contribution of additional displacement sources or constraints to the COD should be carefully evaluated. This benchmark explicitly considered the WRS and CFP effects on the COD, but many other phenomena (for example, pipe end restraint and system compliance) may be equally or even more important.

As mentioned previously, the effects of the crack morphology and two-phase flow models on the LCS calculation did not appear to be as significant as the COD model in this benchmark. However, this observation may largely be driven by similarities in the crack morphology and two-phase flow models contained within the participants' LR codes. Additional LR code validation is needed to better benchmark these codes, especially for tight cracks, before the accuracy and importance of these models can be fully assessed.

WRS prediction and codification has made great strides and is ripe for more explicit consideration within deterministic LBB evaluations. The fact that most approaches do not even address WRS is a glaring deficiency given its potential impact on the calculated LR and ultimately the LCS. Weld joints could be explicitly modelled or bounding solutions that are appropriate for classes of weld joint configurations could be used. This would be consistent with the direction of many current structural standards such as R6 and the American Society of Mechanical Engineers (ASME). Some care and specification may be needed on the best approach for coupling these effects to other COD contributions because, as evidenced in this benchmark, there are several methods for combining WRS contributions to COD.

The consideration of CFP, as illustrated in this benchmark, can be especially important for tight and tortuous cracks. Although the importance of considering CFP is well known, there appears to be little guidance or consensus on how CFP should be applied. Frequently, either

full, half or no CFP is considered as part of sensitivity analyses. It seems more intuitive that the CFP will likely vary through the piping thickness and be a function of both the COD and crack morphology. However, little work has been undertaken to develop refined models.

Finally, the selection and modelling of the crack morphology and accurately assessing its effect on two-phase flow are important considerations in calculating the LR associated with the LCS and ultimately determining if LBB is acceptable in a system. Although crack morphology and LR modelling differences did not appear to significantly contribute to the differences among the benchmark participants' results in this study, this outcome may have been due to greater commonality in the crack morphology and two-phase flow models used by the participants (in comparison to the wider variety of COD models that were used).

Choosing a crack morphology that is consistent with the expected degradation mechanism(s) is a logical first step in any more accurate analysis. However, the expected morphology of corrosion-assisted cracking degradation mechanism can be complex. This complexity raises doubt about the correctness of existing simplified methods used to characterise crack morphology, as well as the relationship between this morphology and the LRs. Much of the work in this area is dated (i.e. over 20 years old) and there is precious little LR verification data for realistic crack morphologies. This is the area that needs further study and additional insights are anticipated as part of a companion Committee on the Safety of Nuclear Installations (CSNI) benchmark activity.

There are additional aspects that lead to more accurate CCS predictions. As demonstrated within the benchmark, the material properties used in the analysis can significantly impact the calculated CCS and are probably the single most important consideration in obtaining more accurate estimates. The choice of the failure model is a secondary consideration. While elastic-plastic fracture mechanics-based failure models should be more realistic, net-section collapse models are often easier to apply and may offer some additional conservatism.

The benchmark results highlighted the potential impact of incorporating WRS within the CCS prediction. Although most participants in this benchmark did not explicitly consider these effects, two of the participants predicted a considerable decrease (≈ 30%) in the critical bending moment (CBM) using established methods such as the R6 code. Such a significant effect of WRS would appear to be conservative for the ductile materials evaluated in the benchmark. There has been significant progress over the last decade or more in both WRS prediction and the understanding of the influence of these effects on crack stability. This knowledge could perhaps provide valuable insights for more accurate consideration of WRS effects. One possible follow-on effort would be to compare various standardised approaches for incorporating WRS in crack stability analyses with existing experimental results in order to identify the most accurate approaches.

There are several issues related to the loading applied at the crack plane in a LBB analysis that were not evaluated within the benchmark. Firstly, loading scenarios that are associated with rare and accident loading events can be complicated in order to accurately model and the applied loads are frequently overly conservative. Furthermore, normal operation and accident loads are often conservatively applied as primary loads at the crack plane without any consideration of the system and material influences. In reality, system compliance, piping end restraints, material plasticity and the system configuration can significantly alter the loads applied at the crack plane, especially for the large (relative to the piping diameter) flaw sizes that are typically required for instability. These, and similar related phenomena, can be refined to obtain more accurate crack plane load profiles in a LBB evaluation.

The variety and potential importance of the issues discussed above for achieving a more accurate LBB evaluation also highlight the importance of considering sensitivity analyses either as part of, or to support, the required LBB analyses. Sensitivity analyses can elucidate the important variables associated with the specific piping configuration, materials and loading combination to provide a clearer indication of the analysis margins. Although this practice is common and was used by many of the participants in this benchmark, it is not clear if this practice is clearly specified within each country's existing requirements, or if any countries provide guidance for performing such analyses. Guidance on and use of sensitivity studies could improve the consistency and rigour of a LBB analysis.

This benchmark was intended to be the first phase of an effort to explore some of the differences in existing LBB requirements and explicitly consider WRS and crack morphology effects. There are other refined LBB considerations that were not addressed in this study that may be equally or even more important in developing a more accurate LBB approach. Participants have been solicited to provide follow-on topics to consider in the next phase of the benchmark. The following preliminary topics have been identified:

- predicting the effect of primary water stress corrosion cracking (PWSCC) morphology at small LRs;
- considering additional pipe geometries;
- evaluating weld overlay effects;
- using LBB analysis during the design of piping systems;
- evaluating thermal stratification effects;
- incorporating piping end restraint and compliance effects;
- considering additional weld residual stress (WRS) distributions;
- evaluating non-linear and/or plastic reduction effects;
- considering LBB in lower operating pressure and temperature applications;
- analysis of LBB for surface cracks, including a consideration of fatigue crack growth.

The Phase I participants, as well as any other interested parties, will consider these and possibly additional topics for a follow-on study. Those topics garnering enough interest, if any, will be selected. A plan to conduct the benchmark will be developed once the topics are selected.

References

[1] NEA (2016), "Leak Before Break (LBB) Status Report", Working Group on Integrity and Ageing of Components and Structures, Committee for the Safety of Nuclear Installations, ADAMS Number ML20195A089.

[2] NRC (2007), "Standard Review Plan for the Review of Safety Analysis Reports for Nuclear Power Plants: LWR Edition — Design of Structures, Components, Equipment, and Systems", Leak-Before-Break Evaluation Procedures, Standard Review Plan 3.6.3, Revision 1, US NRC, No. NUREG-0800.

[3] European Commission (2000), "Comparison of National Leak-Before-Break Procedures and Practices - Summary of Results and Potential for Greater Harmonisation", Revision 2, EU Study Contract B7-5200/97/000782/ MAR/C2 of DG XI, Final report.

[4] Scott, P.M., P.M., R.J. Olson and G.M. Wilkowski (2002), "Development of Technical Basis for Leak-Before-Break Evaluation Procedures", US NRC, US Nuclear Regulatory Commission Washington, DC 20555, No. NUREG/CR-6765.

[5] Wilkowski, G.M. (2009), "Future Directions for Using the Leak-Before-Break Concept in Regulatory Assessments", RSP-0250, Canadian Nuclear Safety Commission, Ottawa, Canada.

[6] NRC, "Guidance on Monitoring and Responding to Reactor Coolant System Leakage", Regulatory Guide 1.45, Revision 1, US NRC, Office of Nuclear Regulatory Research.

[7] NRC (1984), "Report of the U.S. Nuclear Regulatory Commission Piping Review Committee Evaluation of Potential for Pipe Breaks", 3, US NRC, No. NUREG-1061.

[8] Lafaille, L.P. and G. Roussel (1995), "Additional Requirements for the Application of the Leak Before Break Concept in Belgium", Specialists Meeting on LBB in Reactor Piping and Vessels, 9-11 October, Lyon.

[9] Gérard, R., Ch. Malekian and O. Meessen (`995), "Belgian Experience in Applying the Leak Before Break Concept to the Primary Loop Piping", Specialists Meeting on LBB in Reactor Piping and Vessels, 9-11 October, Lyon.

[10] Canadian Nuclear Safety Commission (2014), "Design of Reactor Facilities: Nuclear Power Plants", CNSC, Ottawa, Canada, Regulatory Document No. REGDOC 2.5.2.

[11] Duan, X., M. Li and M. Wang (2015), "Risk-Informed Assessment of PWSCC Issue in CANDU Feeder Piping", *Proceedings of the 17th International Conference on Environmental Degradation of Materials in Nuclear Power Systems-Water Reactors*, 9-13 August, Fairmont Chateau Laurier, Ottawa, Canada.

[12] Carroll, B. (2019), "Regulatory Considerations for the Adoption of Probabilistic Assessment Methodologies for Pressure Boundary Component Aging Evaluations", *Proceedings of the 1st International Conference on Materials, Chemistry, and Fitness-for-Service Solutions for Nuclear Systems*, 15-17 May, Toronto, Canada.

[13] CANDU Owners Group (2012), "Fitness-for-Service Guidelines for Feeders in CANDU Reactors", Revision 3, No. COG-JP-4107-V06, CANDU Owners Group, Toronto, ON, Canada.

[14] Former Czechoslovak Commission for Atomic Energy (1991), "Requirements for Preparation and Contents of Safety Reports and their Amendments: Guide for Application of LBB Method", Former Czechoslovak Commission for Atomic Energy, Zbraslav, Uranová.

[15] State Office for Nuclear Safety (1998), "Requirements for Leak Detection Systems for LBB Application", State Office for Nuclear Safety, Prague.

[16] Radiation and Nuclear Safety Authority (2014), "Strength Analyses of Nuclear Power Plant Pressure Equipment, 15.11.2013," First edition, within Regulatory Guides on Nuclear Safety, Structures and Equipment of a Nuclear Facility, Guide YVL E.4, STUK, Helsinki.

[17] Nuclear Safety Standards Commission (KTA) (2014), "Break Preclusion Verifications for Pressure-Retaining Components in Nuclear Power Plants", Safety Standard KTA 3206 (2014-11), KTA-Geschaeftsstelle, Salzgitter, Germany.

[18] IAEA (1994), "Guidance for the Application of the Leak-Before-Break Concept: Report of the IAEA Extra-Budgetary Programme on the Safety of WWER-440 Model 230 Nuclear Power Plants", IAEA-TECDOC-774, International Atomic Energy Agency, Vienna.

[19] Japan Society of Mechanical Engineers (2002), "Codes for Nuclear Power Generation Facilities - Rules on Protection Design Against Postulated Pipe Rupture for Nuclear Power Plants", JSME S ND1-2002, Japan.

[20] Korea Institute of Nuclear Safety, "Regulations on Technical Standards for Nuclear Reactor Facilities, Etc", Article 15 (Environmental Effects Design bases, etc.), KINS, Republic of Korea.

[21] KINS (2015), Korean Safety Review Guide, Section 3.6.3 "Safety Review Guidelines for Light water reactors", KINS, Republic of Korea.

[22] Dillström, P., J. Gunnars, P. von Unge and D. Mångård (2018), "2018:18 Procedure for Safety Assessment of Components with Defects", Swedish Radiation Safety Authority (SSM), Stockholm.

[23] Swiss Federal Nuclear Safety Inspectorate (2018), "Periodic Safety Review for Nuclear Power Plants", Guideline for Swiss Nuclear Installations ENSI-A03, ESNI, Switzerland.

[24] Swiss Federal Nuclear Safety Inspectorate (2018), "Probabilistic Safety Analyses (PSA): Quality and Scope", Guideline for Swiss Nuclear Installations ENSI-A05, ESNI, Switzerland.

[25] Swiss Federal Nuclear Safety Inspectorate (2019), "Design Basis for Operating Nuclear Power Plants", Guideline for Swiss Nuclear Installations ENSI-G02, ESNI, Switzerland.

[26] American Society of Mechanical Engineers (2015), "Rules for Inservice Inspection of Nuclear Power Plant Components", Boiler and Pressure Vessel Code, Section XI, Appendix C, ASME, New York.

[27] White, G.A., J.E. Broussard, J.E. Collin, M.T. Klug, D.J. Gross and V.D. Moroney (2007), "Materials Reliability Program: Advanced FEA Evaluation of Growth of Postulated Circumferential PWSCC Flaws in Pressurizer Nozzle Dissimilar Metal Welds (MRP-216, Rev. 1)", Electric Power Research Institute (EPRI), Palo Alto, California.

[28] Rahman, S., N. Ghadiali, D. Paul and G. Wilkowski (1995), "Probabilistic pipe fracture evaluations for leak-rate-detection applications" No. NUREG/CR-6004; BMI-2174, US Nuclear Regulatory Commission (NRC), Washington, DC.

[29] Williams, P., and S. Yin (2013), "Prediction of the Leakage rate for Cracked Pipes in Nuclear Power Plants," The 22nd International Conference on Structural Mechanics in Reactor Technology, 18-23 August, San Francisco.

[30] Brust, F.W., T. Zhang, D-J. Shim, S. Kalyanam, G. Wilkowski and M. Smith (2010), "Summary of Weld Residual Stress Analyses for Dissimilar Metal Weld Nozzles", The ASME 2010 Pressure Vessels and Piping Conference, 18-22 July, Bellevue, Washington.

[31] Cox, A., B.A. Young and P.M. Scott (2013), "Advances in COD Modeling: Validation of an Analytical Model to Experimental Results", The 22nd International Conference on Structural Mechanics in Reactor Technology, 18-23 August, San Francisco.

[32] Brust, F.W., and P. Gilles (1994), "Approximate Methods for Fracture Analysis of Tubular Members Subjected to Combined Tensile and Bending Loads", *Journal of Offshore Mechanics and Arctic Engineering*, Vol. 116, pp. 221-227.

[33] Olson, R., S. Kalyanam, J. Soon Park and F.W. Brust (2016), "Improvement of the LBB.ENG2 Circumferential Through-Wall Crack J Estimation Scheme", The ASME 2016 Pressure Vessels and Piping Conference, 17-21 July, Vancouver.

[34] Paul, D., N. Ghadiali, S. Rahman, P. Krishnaswamy and G. Wilkowski (1994), "SQUIRT, Seepage Quantification of Upsets in Reactor Tubes", No. ESTSC/NRC-001052IBMPC00, Battelle Memorial Inst., Columbus.

[35] Cenaero (2019), "Morfeo/Crack, Version 3.0.2, User Manual", Cenaero, Morfeo/Crack, Version 3.0.2, User Manual.

[36] Norris, D., A. Okamoto, B. Chexal and T. Griesbach (1987), "PICEP: Pipe Crack Evaluation Program (Revision 1)", Report EPRI NP-3596-SR, Electric Power Research Institute, Palo Alto.

[37] Scott, P., R. Kurth, A. Cox, R. Olson and D. Rudland (2010), "Development of the PRO-LOCA Probabilistic Fracture Mechanics (PFM) Code", MERIT Final Report.

[38] Kanninen, M.F. and C.H. Popelar (1985), "Elastic Plastic Fracture Mechanics", *Advanced Fracture Mechanics*, Oxford University press, New York.

[39] Kumar, V., M.D. German and C.F. Shih (1981), "Engineering Approach for Elastic-Plastic Fracture Analysis", Report EPRI NP1931, Electric Power Research Institute, Palo Alto.

[40] Zahoor, A. (1989), "Ductile Fracture Handbook, Volume 1, Circumferential Through Wall Cracks", No. EPRI NP 6301-D, Electric Power Research Institute, Palo Alto.

[41] Ross, E., K.H. Herter, P. Julisch, G. Bartolomé and G. Senski (1989), "Assessment of Large Scale Pipe Tests by Fracture Mechanics Approximation Procedure with Regard to Leak-Before-Break", *Nuclear Engineering and Design*, Vol. 112, pp. 183-195.

[42] G. Bartholomé, R. Steinbuch and R. Wellein (1981), "Ausschluss des doppelendigen Rundabrisses der Hauptkühlmittelleitung", 7. MPA Seminar, "Zähbruchkonzepte", 8-9 October Stuttgart.

[43] Milne, I., R.A. Ainsworth, A.R. Dowling and A.T. Steward (1988), "Assessment of the Integrity of Structures Containing Defects", CEGB Report R/H/R6 - Rev. 3 1986, *Int. J. Pres. Ves. and Piping*, Vol. 32, pp. 3-104.

[44] Klecker, R., F. Brust and G. Wilkowski (1986), "NRC Leak-Before-Break (LBB.NRC) Analysis for Circumferentially Through-Walled Cracked Under Axial Plus Bending Loads", NUREG/CR-4572, US Nuclear Regulatory Commission.

[45] Young, B.A., R. Olson and M. Kerr (2012), "Advances in COD Modeling: Circumferential Through-Wall Cracks", *ASME International*, PVP2012-78181, Toronto.

[46] Young, B.A., R.J. Olson and P. M. Scott (2013), "Advances in COD Modeling – Multiple Loading Modes: Concurrent Axial and Crack Face Pressure with a Subsequent Applied Bending Moment", Structural Mechanics in Reactor Technology (SMiRT) 22, 18-24 August, San Francisco.

[47] (2015), "Rules for Construction of Nuclear Facility Components", American Society of Mechanical Engineers, Boiler and Pressure Vessel Code, Section III, paragraph NB-3213.25.

[48] Bläsius, C., K. Heckmann and J. Sievers (2019), "Quality Management, Verification, and Validation of Structure Mechanical Computer Codes at GRS", Structural Mechanics in Reactor Technology (SMiRT) 25, 4-9 August, Charlotte, NC, United States.

[49] SINTAP, Final Prodecure (1999), "SINTAP Procedure – Structural Integrity Assessment Procedures for European Industry", Final Version, Brite-Euram project SINTAP.

[50] Wolfert, K. (1979), "Die Berücksichtigung thermodynamischer Nichtgleichgewichtszustände bei der Simulation von Druckabsenkungsvorgängen", Dissertation, TU München.

[51] Lerchl, G., H. Austregesilo, P. Schöffel, D. von der Cron and F. Weyermann (2012), "ATHLET User's Manual", GRS-P-1.

[52] Pana, P. and M. Müller (1978), "Subcooled and Two-Phase Critical Flow States and-Comparison with Data", *Nuclear Engineering Design*, Vol. 45, pp. 117–125.

[53] Henry, H.E. (1970), "The Two-Phase Flaw Critical Discharge of Initially Saturated or Subcooled Liquid", *Nuclear Science and Engineering*, Vol. 41, p. 336-342.

[54] AFCEN (2010), "Design and Construction Rules for Mechanical Components of Nuclear Installations", Association Française pour les Règles de Conception et de Construction des chaudières Electro-Nucléaires (AFCEN), RCC-MRx Appendix A16.

[55] Hishida, M., M. Saito, K. Hasegawa, K. Enomoto and Y. Matsuo (1986), "Experimental Study on Crack Growth Behavior for Austenitic Stainless Steel in High Temperature Pure Water", *J. Pressure Vessel Technol.*, Vol. 108, pp. 226-233.

[56] Nagasaki, T. and M. Tomimatsu (2002), "Fatigue Crack Growth Characteristics of Forged Stainless Steel", *Transactions of JSME*, *024-1*, pp. 8.

[57] Kanasaki, H., T. Funada, I. Morinaka and K. Koizumi (1991), "Fracture Toughness and Fatigue Crack growth of PWR Materials in Japan", The 1st JSME /ASME joint International Conference on Nuclear Engineering, pp. 527-531.

[58] Newman, J.C., Jr. and I.S. Raju. (1981), "An Empirical Stress Intensity Factor Equation for the Surface Crack", *Engineering Fracture Mechanics*, Vol. 15, Issues 1-2, pp. 185-192.

[59] Hasegawa, K., A. Okamoto, H. Yokota, Y. Yamamoto, K. Shibata, T. Oshibe and K. Matsumura (1989), "Crack Opening Area for LBB Assessment", *Journal of Japan Society of Mechanical Engineering*, Vol. 55, 514, pp.1269-1274.

[60] Moody, F.J. (1966), "Maximum Two-Phase Vessel Blowdown from Pipes", *Journal of Heat Transfer*, Vol. 88, p. 285-294.

[61] Rudland, D., P. Scott and G. Wilkowski (2001), "Importance of Using Proper Crack Morphology Parameters for Leak-rate Analyses in LBB Evaluations", Structural Mechanics in Reactor Technology (SMiRT) 16, 12-17 August, Washington DC.

[62] Battelle (2008), "SQUIRT: Seepage Quantification of Upsets In Reactor Tubes", Windows Version 1.3.

[63] Kiwa (2018), Kiwa Inspecta Technology AB, ISAAC-Integrity and Safety Assessment of Components, version 1.1 Rev. 0.

[64] NRC (2016), "xLPR Software Design Description for a Circumferential Through-Wall Crack Combined Tension and Bending COD Module", Version 3.1.

[65] Paul, D.D., J. Ahmad, P.M. Scott, F.F. Flanigan and G.M. Wilkowski (1994), "Evaluation and Refinement of Leak-Rate Estimation Models", NUREG/CR-5128, Rev.1, US Nuclear Regulatory Commission.

[66] Heckmann, K. and J. Sievers (2015), "Code Development for Integrity Assessment with Respect to New German Safety Standard", Structural Mechanics in Reactor Technology (SMiRT) 23, 10-14 August, Manchester.

[67] Heckmann, K. and J. Sievers (2016), "Analysis Methods for Leakage Rates in Pressurized Components", 42nd MPA-Seminar, 4-5 October, Stuttgart, pp.283-301.

[68] Olson, R. (2016), "A Simple Approach for Including Weld Residual Stresses in the Calculation of Pipe Circumferential Through-Wall Crack Opening Displacements", *Proceedings of the ASME 2016 Pressure Vessel and Piping Conference*, PVP2016-63169, American Society of Mechanical Engineers.

[69] Ansys® Academic Research, Ansys Mechanical, Release 19.1.

[70] Boley, B.A. and J.H. Weiner (1985), "Theory of Thermal Stresses", 2nd Edition, Kreiger, Melbourne, p.291.

[71] Park, J.H., Y.K. Cho, S.H. Kim and J.H. Lee (2015), "Estimation of Leak Rate Through Circumferential Cracks in Pipes in Nuclear Power Plants", *Nuclear Engineering and Technology*, Vol. 47, 3, pp. 332–339.

Annex A. Summary of the participants' results

Figure A.1. Summary of participants' evaluations: baseline problem

Task 0: Country LBB Evaluation

*** NSC = Net Section Collapse, EPFM = Elastic-Plastic Fracture Mechanics, FAD = Failure Assessment Diagram; [A] Please also indicate if different properties were used in leak rate (i.e., COD) and crack stability portions of analysis; [B] Please also indicate if crack face pressure was treated differently in leak rate (i.e., COD) and crack stability portions of analysis**

Please Provide Following Information Related to your Baseline Analysis

	BARC	CEI	EMCC	GRS	JAEA	KOREAa	KOREAb	KIWA	NRC	OPG	PSI-ENSI	Tractebel	UJV	VTT			
COD Code	In-house	In-house	SQUIRT4	WINLECK	N//A	In-house (EPRI Handbook)	In-house (EPRI Handbook)	In-house	xLPR circ_COD DLL	In-house (based on GE and handbook model)	LeakRate_Excel_ BetaR1 (Battelle COD model)	PICEP	PICEP	In-house			
Leak Rate Code	In-house	SQUIRT V2.1.3	SQUIRT4	WINLECK	N//A	PICEP	LEAPOR	WinSQUIRT V1.3	LEAPOR	SQUIRT V2.0	LeakRate_Excel_ BetaR1 (SQUIRT - NUREG/CR-5128, Rev1)	PICEP	LeakH	LEAPOR			
Crack Stability Code	In-house (based on RCCMR A-16 design code)	In-house	LBB.ENG2	PROST	N//A	In-house	LBB.ENG2 with psi correction	ISAAC	ENG2.DLL with psi correction	In-house (based on GE and handbook model)	In-house	Morfeo/Crack	BASLBB	In-house			
Crack Stability Method (NSC, EPFM, or FAD)*	EPFM	NSC*	EPFM	FAD	N//A	EPFM	EPFM	FAD	EPFM	EPFM	NSC	EPFM	NSC*	NSC*			
Strength Properties (Base, Weld, or Mixture)?[A]	W	W	B	B	N//A	COD: W Crack Stability: B	COD: W Crack Stability: B	COD: W Crack Stability: B	W	W	W	M	B	W			
Fracture Toughness Properties (Base, Weld, or Mixture)?[A]	W	W	W	B	N//A	W	W	W	W	W	-	W	W	W			
Crack Face Pressure Considered (Y/N)?[B]	N	Y	N	N	N/A	COD: N Crack Stability: Y	N	N	COD: Y Crack Stability: N	Y	Y	N	N	Y			
If Y, what pressure used? [MPa][B]		7.75			N//A	7.75			7.75	7.75	7.75			7.75			
Weld Residual Stress (WRS) Considered (Y/N)?	N	N	N	Y	N//A	N	N	Y	N	N	N	N		N			
If Y, how was WRS incorporated (FEM, Analytical, or Other)?				A				A		A (equivalent axial force and bending moment)							
LBB met?	No	No*	No	Yes	No*	Yes	No	No	Yes	Yes*	No*	Yes*	Yes	No			
Comments	Margin between critical crack and leakage crack size not met.	*Both EPFM and NSC used, but NSC provided smallest CCS; Under specified detectable leak rate, Weld properties used for both stability and COD calculations	If algebraic sum method is used, the critical crack size (360.22 mm) using SF=1.4 is larger than leakage crack size (256.84 mm) meeting the margin on load. However, the critical crack size (422.7 mm) using SF=1.0 is smaller than 2 times leakage crack size (513.68) and hence, does not meet the required margin on crack size.		*LBB cannot be applied to this problem in Japan because of the possibility of an active degradation mechanism, PWSCC, in the analyzed weld joint	Air-fatigue' morphology selected as the crack type in the PICEP code.		The safety margin of 2 on the size of the critical crack and the postulated leakage crack is not fulfilled.	Weld properties used for both COD and stability	50 kg/h (0.0139 kg/s) was set as station detection capability	*Under specified detectable leak rate	*Using Belgium detectable leak rate, as below	*For assessment of crack length at failure (cell O29), NSC was used as described in SRP 3.6.3. For assessment of crack stability margin for the leakage crack (cell O27) the R6 and LBB.NRC (NUREG/CR-457) methods were used. Crack instability moment was 770 kNm by R6 and 776 kNm by LBB.NRC. Therefore the lower value was considered. Two	*NSC found to be the limiting failure mode for detectable leaking cracks			
Comments		* Most Canadian plants have much smaller detectable leak rate limit.	Baseline analysis was performed to be consistent with 'traditional' LBB submittals					COD considered both base and weld properties in sensitivity analysis: R6, Option 2 analysis: No stable crack growth included in the analysis.		Leak rate calculations were based on 50% of critical crack length and 50% of COD under pressure. Calculated late rate is required to be larger than 500 kg/h (0.139 kg/s).	* Swiss plants are allowed a smaller analysis leak rate of 200 Kg/hr	* no using specified detectable leak rate		Didn't explicitly calculate critical crack length but just validated that it failed at 2 times the leakage size crack			
Baseline Results																	
A. Required leak rate for evaluation [kg/s]	0.61	0.61	0.61	0.061	N/A	0.61	0.61	0.61	0.63	0.14	0.63	0.3	0.61	0.63			
B. Total crack length at required leak rate: [mm]	250.84	286.32	256.84	202	N/A	175.44	275.74	320	283.6	177.0	335.32	211.6	184	283.6	corrected to mid-wall value		
C. For the crack length at required leak rate																	
a. Axial force at failure [kN]	1380.9	1337.64	1302.95	3000	N/A	1337.64	1337.64	1337.64	1337.7	1337.7	1337.64	1337.7	1337.64	1302.4			
b. Bending moment at failure [kN-m]	718.2	1084.43	732.14	553	N/A	852.7	693.85	361.3	1364	1620.3	1017.29	985	770	1097.5			
D. Total crack size at failure (under NO + SSE loading) [mm]	-	471	360.22	260	N/A	403.7	419.3	268	567.8	573	528.35	460	396.6	<567			
E. Crack Morphology Parameters																	
a. Global roughness (μ_G) [μm]	40	40.5	33.66	40	N/A	-	34	113.9	40	40.51	114	(*)	5	40			
b. Local Roughness (μ_L) [μm]	40	8.81	6.53	40	N/A	-	6.5	11.4	40	8.814	114		0	40			
c. Local path deviation (K_{G+L})	1.1	1.06	1.06	1.1	N/A	-	1	1.07	1.1	1.06	1.2		0	1.1			
d. Global path deviation (K_L)	1.1	1.02	1.02	1.1	N/A	-	1	1.33	1.1	1.017	1.2		0	1.1			
e. 45 degree turns / meter $\{n_{tl(45)}\}$ [m^{-1}]			N/A	0	N/A	-					N/A	0	0	0			
f. 90 degree turns / meter $\{n_{tl(90)}\}$ [m^{-1}]	0		201	0	N/A	-	2010	594		6730	N/A	0	0	6730			
g. 90 degree turns / meter $\{n_{t(90)}\}$ [m^{-1}]	0	6730	2010	0	N/A	-		5940	6730		5940	0	0	1730			
h. Loss discharge coefficient (C_d)	0.95	0.95	0.95	0.816	N/A	-		0.95	0.95	0.95	0.95 (believed to b	0.61	0.61	0.95			
		Using PRAISE-CANDU 2.0, the critical length is 476 mm and 586.6 mm based on NSC and EPFM, respectively.								573 mm is the pre-tearing total crack size. Post-tearing crack size is 583.896 mm		(*) a friction factor is used instead of a surface roughness (as per previous LBB studies). The friction factor is equal to 0.15					

Figure A.2. Summary of participants' evaluations: Task 1 problem (CF crack morphology without WRS)

Task 1: CF Crack Morphology without WRS (2c = 125 mm)

Task 1 Results
Under normal operation (NO) and loading conditions, report the following:

	BARC	CEI	EMCC	GRS	JAEA	KOREAa	KOREAb	KIWA	NRC	OPG	PSI-ENSI	Tractebel	UJV	VTT			
1. Total COD at inside pipe wall [mm]	0.08201	0.0888	0.0896877	0.071	0.112	0.073382776	0.073382776	0.0651	0.079	0.082	0.0699	0.063		0.0697			
2. Total COD at mid-wall [mm]	0.104812	0.0888	0.101902	0.071	0.121	0.073382776	0.073382776		0.096	0.0845	0.0836	0.074		0.0844			
3. Total COD at at outside pipe wall [mm]	0.130076	0.0888	0.124482	0.071	0.135	0.073382776	0.073382776	0.0973	0.116	0.087	0.0991	0.087		0.1014			
4. Leak rate [kg/s]	0.033	0.0276	0.039978	0.0153	0.0508	0.0208	0.0251	0.026	0.03343	0.0348	0.035	0.021		0.0278			
Comments		only COD at mid-wall is calculated using weld properties. The COD at ID/OD is assumed to be the same as mid-wall in SQUIRT. Applied pressure = 15.5 Mpa			Mid-wall COD was used in the leak rate analysis.	The global morphology parameters provided in the inputs tab were used in PICEP			Weld properties used for both COD and stability	Used SQUIRT default morphology parameters for Corrosion Fatigue (see above)	COD and Leak rate: calculated with the LeakRate_Excel code (PARTRIDGE-BATTELLE) by manual iteration because the code does not allow obtaining the requested results in a direct way. Input loads: P=15.5 MPa, applied Fax=13.34 kN, applied Mb=89.59 kN*m, crack face pressure hardcoded as P/2=7.75 Mpa					

Report the following values at crack instability

1. Axial Force [kN]	1337.64	1337.64	1337.64	1337.64	1337.64	1337.64	1337.64	1337.64	1337.7	1337.64	1337.64	1337.7		1337.64			
2. Bending Moment [kN-m]	1235	1768.09	1186.6	700	1685	1002.079528	1002.079528	732.7	1927.94	1841.7976	1842.4	1300		1701			
Comments		Both mG and mL = 0.0382 mm in stead of 0.04 mm, as ROUGHNmax in SQUIRT is 0.0382 mm, path loss coefficient = 272.31 VH. Number of turns = 6930/m, KG =KG+L = 1.1. COD effect is considered.	This analysis used FEA to calculate the COD due to internal pressure, axial force and crack face pressure. LEAPOR used the ID and OD COD values as input with the crack morphology parameters given in the problem statement inputs	SINTAP procedure level 3 for welds with strength mismatch is used				COD considered both base and weld properties in sensitivity analysis: R6, Option 2 analysis: No stable crack growth included in the analysis.		1908.3556 kN-m for post-tearing critical length 2c=150 mm	Crack instability: calculated with our in house code developed for this benchmark. Input loads: P=15.5 MPa, crack face pressure=7.75 MPa, applied Fax=48.04 kN. Calculations performed with weld material properties and failure stress Sf=(Sy+Su)/2=429.45 MPa						

Please Provide Following Information Related to your Task 1 Analysis

COD Code*	FEA	In-house	FEA	WINLECK	FEA	In-house (EPRI handbook)	In-house (EPRI handbook)	In-house	xLPR circ_COD DLL	In-house (based on GE and handbook model)	LeakRate_Excel_BetaR1 (Battelle COD model)	Morfeo/Crack	N/A	In-house			
Leak Rate Code*	In-house	SQUIRT V2.1.3	LEAPOR	WINLECK	LEAPOR	PICEP	LEAPOR	WinSQUIRT V1.3	LEAPOR	SQUIRT V2.0	LeakRate_Excel_BetaR1 (SQUIRT - NUREG/CR-5128, Rev1)	LEAPOR	N/A	LEAPOR			
Crack Stability Code*	In-house	In-house	NRCPIPE using LBB.ENG2	PROST	PASCAL-SP	In-house	In-house	ISAAC	ENG2.DLL with psi correction	In-house (based on GE and handbook model)	In-house	Morfeo/Crack	N/A	In-house			
Crack Stability Method (NSC, LEFM, or EPFM)*	EPFM	NSC	EPFM	EPFM (R6/SINTAP	NSC	EPFM	EPFM	e LEFM, EPFM and	EPFM	EPFM	NSC	EPFM	N/A	NSC			
Strength Properties (Base, Weld, or Mixture)?*[A]	M	W	B	B	W	COD: W Crack Stability: B	COD: W Crack Stability: B	COD: W Crack Stability: B	W	W	W	M	N/A	W			
Fracture Toughness Properties (Base, Weld, or Mixture)?*[A]	W	W	W	W	W	W	W	W	W	W	N/A	W	N/A	W			
Crack Face Pressure Considered (Y/N)?*[B]	Y	Y	COD: Y Crack Stability: N	N	Y	COD: N Crack Stability: Y	N	N	COD: Y Crack Stability: N	Y	Y	N	N/A	Y			
If Y, what pressure used?*[B]	7.75	7.75	7.75		7.75	7.75	0		7.75	7.75	7.75		N/A	7.75			

*** NSC = Net Section Collapse, EPFM = Elastic-Plastic Fracture Mechanics, FAD = Failure Assessment Diagram**
[A] Please also indicate if different properties were used in leak rate (i.e., COD) and crack stability portions of analysis
[B] Please also indicate if crack face pressure was treated differently in leak rate (i.e., COD) and crack stability portions of analysis

***Please identify any differences between baseline and Task 1 codes, properties, treatment of crack face pressure, and approaches. If no differences, exist you can leave that response blank**

Figure A.3. Summary of participants' evaluations: Task 2 problem (CF crack morphology with WRS)

Task 2: CF Crack Morphology with WRS (2c = 125 mm)

Weld Residual Stress (WRS) Evaluation

	BARC	CEI	EMCC	GRS	JAEA	KOREAa	KOREAb	KIWA	NRC	OPG	PSI-ENSI	Tractebel	UJV	VTT			
How was WRS incorporated (FEM, Analytical, or Other)?	F	F	F	A, stability only	F	F	F	A	A	A	Not Performed	F	N/A	F			
Task 2 Results																	
Under normal operation (NO) and loading conditions, report the following:																	
1. Total COD at inside pipe wall [mm]	0.0036	-0.047386	0.0529455	NA	0	0.017182776	0.017182776	0	0.064	0.068		0.055		-0.0272			
2. Total COD at mid-wall [mm]	0.142	0.067512	0.095787	NA	0.27	0.073782776	0.073782776		0.096	0.07		0.075		0.0989			
3. Total COD at outside pipe wall [mm]	0.356	0.27106	0.194492	NA	1.25	0.174482776	0.174482776	0.2374	0.131	0.072		0.12		0.315			
4. Leak rate [kg/s]	0.045	0.0194	0.0373	NA	0.17531	0.0113	0.009	0	0.032145	0.0274		0.021		0			
Comments		leak rate is calculated using mid-wall COD	ID and OD COD values were used as LEAPOR inputs	Reported COD and leak rate values did not account for WRS effects as specified for this problem which is why "NA" is reported for the task 2 values.	Mid-wall COD was used in the leak rate analysis.	* Delta-CODs by WRS were calculated by linear elastic FEA. * WRS was simulated by temperature that producing equivalent thermal expansion stress only in weld metal region.	* Delta-CODs by WRS were calculated by linear elastic FEA. * WRS was simulated by temperature that producing equivalent thermal expansion stress only in weld metal region.			Used SQUIRT default morphology parameters for Corrosion Fatigue (See above)		leak rate determined by Leapor using the total COD at midwall		0.0358 = leak rate using mid-wall COD			
Report the following values at crack instability																	
1. Axial Force [kN]	1337.64	1337.64	1337.64	1337.64	1337.64	48.04	48.04	1337.64	1337.7	891.824		1337.7		1337.64			
2. Bending Moment [kN-m]	1212	1768.1	1186.6	553	1685	1002.079528	1002.079528	549.8	1927.94	1862.943		1300		1701			
Comments			The bending moment did not change as the crack stability code does not account for WRS			The global morphology parameters provided in the inputs tab were used in PICEP		No stable crack growth included in the analysis.		1929.222 kN-m for post-tearing critical crack length 2c=125 mm				WRS found not to affect the limit load due to NSC failure mode			
Please identify any differences between Task 1 and Task 2 codes, properties, treatment of crack face pressure, and approaches.																	
Analysis Differences between Task 1 and Task 2		COD is calculated using FEM to incorporate residual stress.	Addition of WRS is the only difference.	Only crack instability is affected. Code is the same, WRS is used as additional load	Appling WRS loading to crack surface in COD analysis	None	None	None	None	Equivalent axial force due to weld residual stress of -445.816 kN was considered in Task 2.					Applied a temperature distribution to develop an equilibrium axial WRS that closely approximates the distribution supplied. This temperature distribution is then applied with the other loads to determine COD and crack stability.			

Figure A.4. Summary of participants' evaluations: Task 3 problem (PWSCC crack morphology without WRS)

Task 3: PWSCC Crack Morphology without WRS (2c = 125 mm)

Task 3 Results

	BARC	CEI	EMCC	GRS	JAEA	KOREAa	KOREAb	KIWA	NRC	OPG	PSI-ENSI	Tractebel	UJV	VTT			
1. Leak rate [kg/s]	0.029	0.0271	0.03281	0	0.04202	0.0109	0.0207	N/A	0.028304	0.0299	0.025	0.02		0.02652			
Comments		Both mG and mL = 0.0382 mm in stead of 0.04 mm, as ROUGHNmax in SQUIRT is 0.0382 mm, path loss coefficient = 272.31 VH. Number of turns = 6930/m, KG =KG+L = 1.1. COD effect is considered.	Used ID and OD COD from Task 1 as input to LEAPOR, used parameters given in problem statement inputs	Diverging flow resistance interpreted as 0 flow	Calculated using mid-wall COD	The global morphology parameters provided in the inputs tab were used in PICEP		*No results possible; very tight crack reported.		For SQUIRT, global roughness = 113.9 um, path loss coef. = 15.09 velocity heads, and discharge coef. = 0.95		leak rate determined by Leapor using the total COD at midwall					

Please identify any differences between Task 1 and Task 3 codes, properties, treatment of crack face pressure, and approaches.

Analysis Differences between Task 1 and Task 3		None	Crack morphology parameters were the only difference		Values of crack morphology parameters	None	None	None	None	The only difference is in choice of crack morphology parameters. SQUIRT default values for PWSCC were used for Task 3.	None			PWSCC parameters used instead of CF			

Figure A.5. Summary of participants' evaluations: Task 4 problem (PWSCC crack morphology with WRS)

Task 4: PWSCC Crack Morphology with WRS (2c = 125 mm)

Task 4 Results

	BARC	CEI	EMCC	GRS	JAEA	KOREAa	KOREAb	KIWA	NRC	OPG	PSI-ENSI	Tractebel	UJV	VTT			
1. Leak rate [kg/s]	0.041	0.019	0.029625	NA	0.11572	0.0077	0.0082	0	0.026563	0.0229	N/A	0.02		0			
Comments		leak rate is calculated using mid-wall COD	ID and OD COD from Task 2 were used as input to LEAPOR, used crack morphology from problem statement inputs	Reported COD and leak rate values did not account for WRS effects as specified for this problem which is why "NA" is reported for the task 2 values.	Calculated using mid-wall COD	The global morphology parameters provided in the inputs tab were used in PICEP		Because ICOD = 0, no leak is possible.		For SQUIRT, global roughness = 113.9 um, path loss coef. = 15.09 velocity heads, and discharge coef. = 0.95	Not Performed	leak rate determined by Leapor using the total COD at midwall		0.0325 = leak rate using mid-wall COD			
Please identify any differences between Task 2 and Task 4 codes, properties, treatment of crack face pressure, incorporation of weld residual stress and approaches.																	
Analysis Differences between Task 2 and Task 4		COD is calculated using FEM to incorporate residual stress.	None		Value of COD	None	None	None	None	The only difference is in choice of crack morphology parameters. SQUIRT default values for PWSCC were used for Task 4.				Applied a temperature distribution to develop an equilibrium axial WRS that closely approximates the distribution supplied. This temperature distribution is then applied with the other loads to determine COD and crack stability.			

Annex B. Summary of Tractebel's analysis and results

LBB requirements

Belgium

Leak-before-break (LBB) technology has not been applied in the first design of the seven pressurised water reactors (PWRs) currently being operated. The design basis of these plants required a consideration of the dynamic effects associated with the ruptures that are to be postulated in the high energy piping. The application of LBB technology to the existing plants was approved in the 1990s by the Belgian safety authorities but with a limitation to the primary coolant loop.

The analyses performed for the Belgian units are based on the United States' documents and methodologies; the requirements of the Standard Review Plan (SRP) 3.6.3 are followed. The US method is explained by other participants and therefore the following paragraph focuses on the Belgian practice.

The Belgian safety authorities impose additional requirements to the US regulatory requirements. The loads resulting from this accident are far from being the most severe for a low seismic region like Belgium and the steam line break (SLB), for example, may produce much higher loads in some specific locations of the primary coolant piping. The Belgian safety authorities require this loading be taken into account, which is more conservative than the usual US procedure. The rupture of the main auxiliary lines connected to the primary piping (pressuriser surge line and emergency core cooling system [ECCS] line from the accumulators and shutdown cooling line) was also considered.

Considering that some design basis events were not analysed in detail because they were enveloped by the postulated double-ended guillotine breaks of the primary loop piping, the Belgian safety authorities argued that LBB application might reduce the protection against these other unspecified events. The authorities therefore required a consideration of the following additional breaks in the design basis of the reactor core and internals, as well as for the steam generator tube bundle:

- rapid rupture (1 ms) of the steam generator manway cover (hot leg or cold leg);
- slow break (3 s) of one times the flow area, anywhere in the primary coolant piping.

Regarding the adequacy of the leak detection systems, there are several redundant systems in each unit, which enables the detection of a leakage of 1 gallon per minute (GPM) (226 litres/hour) in less than one hour. This fulfils the requirements of the Regulatory Guide 1.45. Some systems are much more sensitive if a longer detection period – of the order of a few hours or one day – is allowed. In this case, the detection capability could be as low as 0.2 to 0.3 GPM. Conservatively, the limit of 0.5 GPM (113 litre/hour) was justified and used in the previously performed LBB studies to determine the leakage crack size as under service conditions.

Baseline problem

Approach

The LBB studies that were performed in Belgium used the Pipe Crack Evaluation Program (PICEP) as a tool to calculate the leak rate and crack opening displacement (COD) under the applied loads while considering the material properties and geometry of the studied locations.

The crack stability of the cracks was determined using an in-house computation tool (JT crack). However, the stability of the critical crack and the bending moments calculation were determined using Morfeo-Crack for the current benchmark, which is a commercial computation tool that uses XFEM (eXtended Finite Element Method), because JT-crack cannot be applied to the geometry and material characteristics.

The leak crack size was determined under nominal loads using PICEP. Two detectable leaks were considered. The first leak was 1 GPM, which is the frequently used value. The second leak was 0.5 GPM, which corresponded to the justified detectable leak in Belgium, as explained above.

The leak crack size is the crack size allowing for ten times the detectable leak. Surface roughness can be input into PICEP or a friction factor. The latter is preferable because it accounts for other possible degradation mechanisms than fatigue. In Belgium LBB studies, a conservative value of 0.15 for the friction factor was used and the loss discharge coefficient was taken as equal to 0.61. These values were used for the baseline problem of the present benchmark.

Once both leak crack sizes have been calculated, the critical size should be at least equal to twice the leak crack size. As a result, the stability of crack sizes that were at least equal to twice the leak crack sizes was examined using the J-R curve of the weld material.

Results

$a_{q\text{-}1GPM}$ (= $2c_{leak\text{-}1GPM}$) will be the leak crack size allowing for ten times a detectable leak of 1 GPM (leak of 10 GPM) and $a_{q\text{-}0.5GPM}$ (= $2c_{leak\text{-}0.5GPM}$) will be the leak crack size allowing for tentimes a detectable leak of 0.5 GPM (a leak of 5 GPM).

A critical crack of $a_c = 2a_{q\text{-}1GPM}$ was found to not be stable. However, if the detectable leak rate is considered to be 0.5 GPM, the leak crack size is $a_{q\text{-}0.5GPM}$ = 211.6 mm. The critical crack size is a_c = 460 mm, thus the criterion is satisfied for 5 GPM:

$$\frac{a_c}{a_{q-0.5GPM}} = 2.17 \qquad \text{(B.1)}$$

The critical crack size was calculated by looking for the initial size a_0, so that J_{app} and the weld (A82) J-R are tangent as shown in the figure below:

Figure B.2. Determination of critical crack size

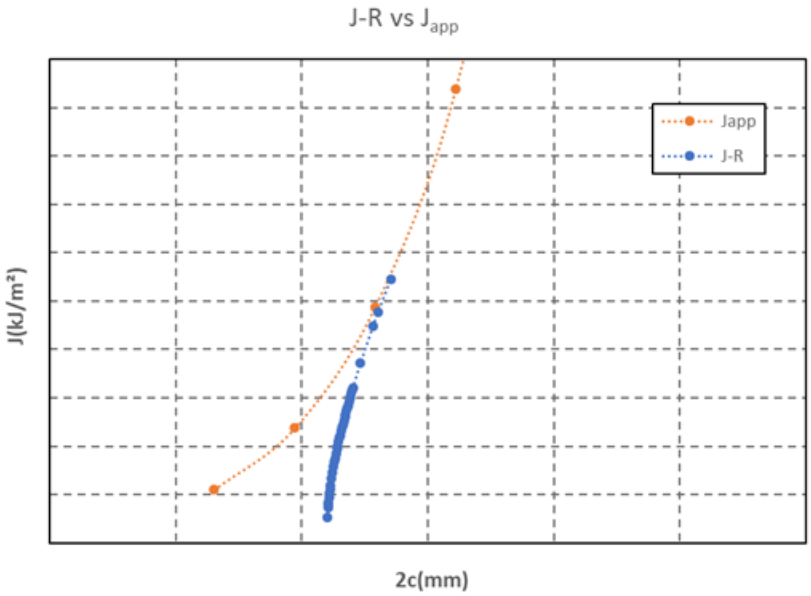

i. Failure moment calculation:

Considering a failure axial force of 1 337.7 kN, the failure bending moment was calculated using Morfeo-Crack for a crack size of $a_{leak\text{-}0.5GPM}$ = 211.6 mm. The bending failure moment was equal to 985 kNm.

The failure moment was determined by using the J-integral tearing modulus (J-T) graph method, which is explained below by comparing $(J\text{-}T)_{mat}$ to $(J\text{-}T)_{app}$.

a) Expression of $(J\text{-}T)_{mat}$:

Using the material J-R curve (see equations [B.2] and [B.3] below), the material $(J\text{-}T)_{mat}$ is expressed in equation (B.4) below.

$$J_{mat} = J_{IC} + C_1(\Delta a)^{C_2} \quad \text{(B.2)}$$

$$T_{mat} = \frac{E}{\sigma_f^2}\frac{dJ_{mat}}{da} \quad \text{(B.3)}$$

where E and σ_f are the material's Young Modulus and flow stress from Equations (B.2) and (B.3):

$$J_{mat} = J_{IC} + \left(\frac{\sigma_f^2}{E\,C_2}\,C_1^{-1/C_2}\,T_{mat}\right)^{C_2/C_2-1} \quad \text{(B.4)}$$

b) Expression of $(J\text{-}T)_{app}$

$$T_{app} = \frac{E}{\sigma_f^2}\frac{dJ_{app}}{da} \quad \text{(B.5)}$$

The $(J\text{-}T)_{app}$ curve, which represents the J-integral and the tearing modulus due to the applied loads, was determined by fixing the crack size and changing the applied bending moment.

The J-integral and T were calculated for each bending moment (according to equation [5]).

The term $\frac{dJ_{app}}{da}$ was then evaluated by estimating the influence of an increment *da* on the crack size of the J-integral.

c) Comparison

(J-T)app and (J-T)mat can then be drawn in the same graph.

The intersection of (J-T)mat and (J-T)app for a given value of the bending moment represents the failure bending moment as shown in the figure below:

Figure B.3. Determination of failure bending moment – J-T graph

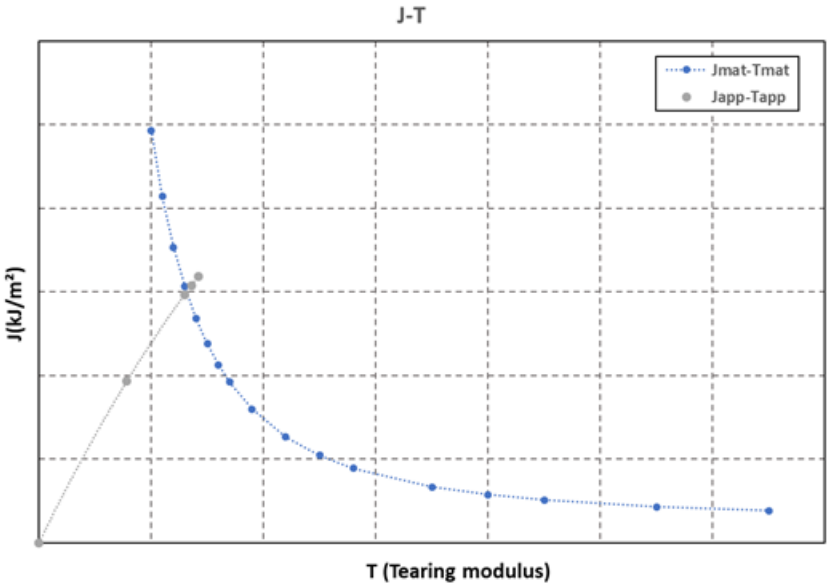

Supplementary information

The PICEP results giving the trend of the leak rate trend as a function of the crack size is given in the picture below:

Figure B.4. Crack size and flow rate

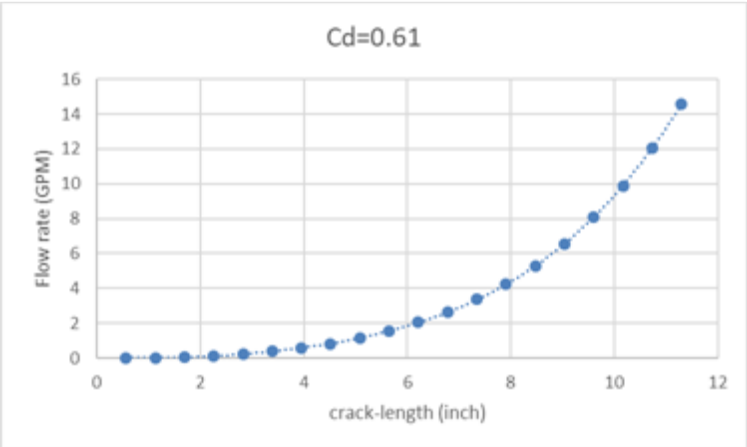

Source: Tasks 1-4

Approach

i. Tasks 1 and 3

Considering a crack size equal to 125 mm at mid-wall, the loadings at normal operation were applied in order to compute the COD by Morfeo-Crack. The leak rate was determined for a crack size of 125 mm at mid-wall using LEAPOR for each case of crack morphology parameters due to fatigue or primary water stress corrosion cracking (PWSCC).

ii. Tasks 2 and 4

The calculation is elastic plastic, and therefore a stress profile is auto-equilibrated when input. An iterative calculation using Morfeo-Crack was thus performed and the input profile gradually modified in order to obtain the intended residual stress profile. The final obtained profile is represented in the figure below.

Figure B.5. WRS vs axial stress along pipe thickness

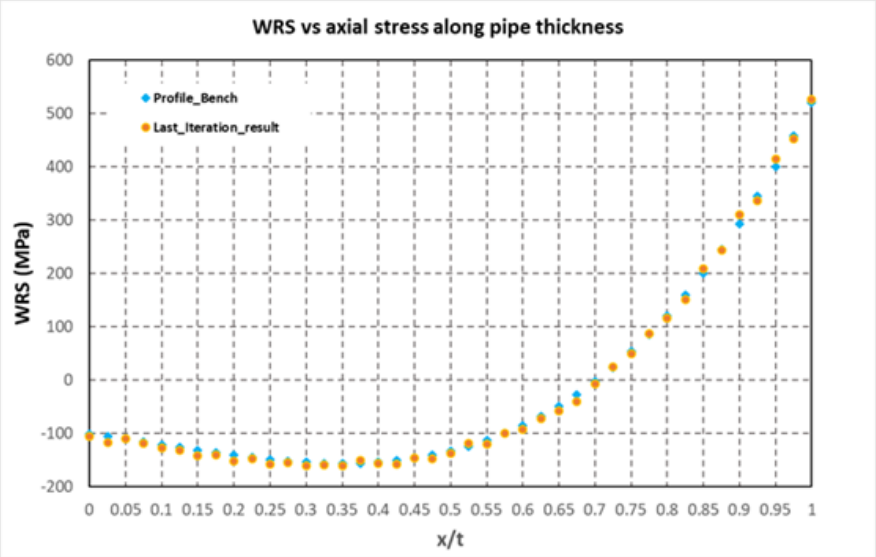

Results

The calculated COD with and without the weld residual stress (WRS) are summarised in the table below:

Table B.1. Calculated COD

	Without WRS	With WRS
At inside radius (mm)	0.063	0.055
At mid-wall radius (mm)	0.074	0.075
At outside radius (mm)	0.087	0.120

Using LEAPOR and the COD at mid-wall, the leak rate was calculated in the case of surface roughness due to fatigue and PWSCC. The results are presented in the table below:

Table B.2. Leak rate

	Leak rate without WRS (kg/s)	Leak rate with WRS (kg/s)
Fatigue	0.0208	0.0211
PWSCC	0.0199	0.0203

The failure bending moment for which the crack size 2c = 125 mm is calculated using the J-T method is explained above. The failure axial force was considered to be constant and equal to 1 337kN. The bending failure moment was equal to 1 300 kNm.

The resulting curves are shown in the figure below:

Figure B.6. Determination of failure bending moment– J-T graph

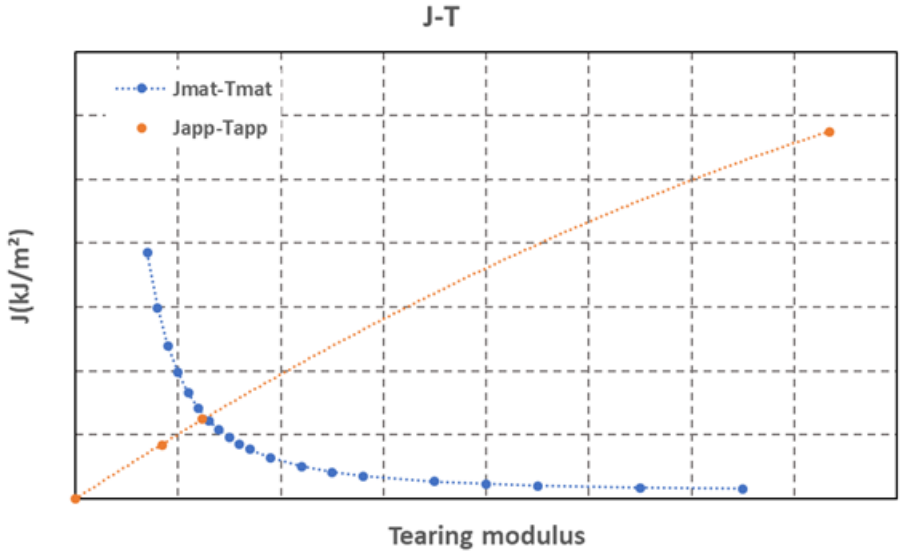

Annex C. Summary of KIWA's analysis and results

By P. Dillström, P. von Unge, A. Shipsha

Swedish LBB procedure

General requirements

1. Leak-before-break (LBB) should be applied to an entire piping segment (within class 1 or 2). Locations with both high and low stresses should be included in the analysis.
2. No active damage mechanism (or water hammer loading events) should be present in the piping segment.
3. A leakage detection system should be present (among other requirements fulfilling the Regulatory Guide [RG] 1.45).
4. The piping segment should have been inspected using a qualified non-destructive examination (NDE) procedure. A qualified NDE procedure should preferably also be used in all future inspections.

Leakage and critical crack size

1. Postulate a leaking through-wall crack (leakage crack size) at the chosen assessment location:

a) The leakage crack size should be chosen to produce a leakage which is ten times larger than the detection limit.
b) The leakage flow should be calculated using loads from the normal operation of the plant (including weld residual stresses if a weld is present at the chosen assessment location).
c) The leakage crack should be postulated at locations with both high and low stresses along the chosen piping segment.
d) Analyses should consider the contribution from the flexibility of the piping system, crack morphology on the leakage flow and dependence of the crack opening displacement (COD).

2. Calculate the critical crack size for the normal operating conditions and for the worst loading case/transient according to the design specification.

Acceptance/ safety margins

1. The margin between the calculated critical crack size and the postulated leakage crack size should be at least two.
2. The leakage crack should be stable using a load that is 1.4 times larger than the load used to calculate the critical crack size.

Baseline case

The baseline problem addresses LBB evaluation in a surge line pipe containing a circumferential crack located at the weld centreline. This case was analysed using the Swedish LBB procedure along with governing acceptance criteria, which is described in Section 1. The input data was taken from the excel-file provided by the US Nuclear Regulatory Commission (NRC).

Weld residual stresses

The LBB assessment used two weld residual stress (WRS) distributions. The first one was provided by NRC, while the second distribution was based on Swedish recommendations from the Swedish Regulatory Body (SSM) [SSM Report 2018:18]. A comparison of the NRC and the SSM WRS distributions is presented in Figure C.1.

Figure C.1. Weld residual stress distributions

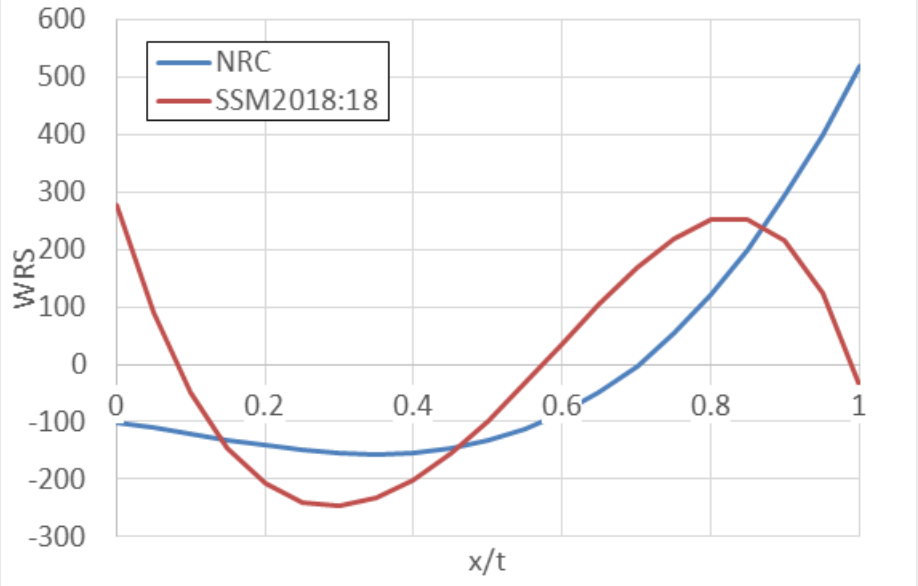

Leakage crack

The leak detection limit (LDL) was specified to be 0.0608 kg/s. According to the Swedish LBB procedure, a leakage crack should be postulated that provides a leak flow rate of 0.608 kg/s (10xLDL).

In-house software was used to calculate the COD values for a range of crack sizes. The used software enabled plastic correction of the COD. The COD values were calculated for normal operating conditions including WRS distributions in Figure C.1. The weld material properties at operating temperature were used for the plastic correction of COD values, see Figure C.2.

Figure C.2. Weld material properties used for the COD calculations

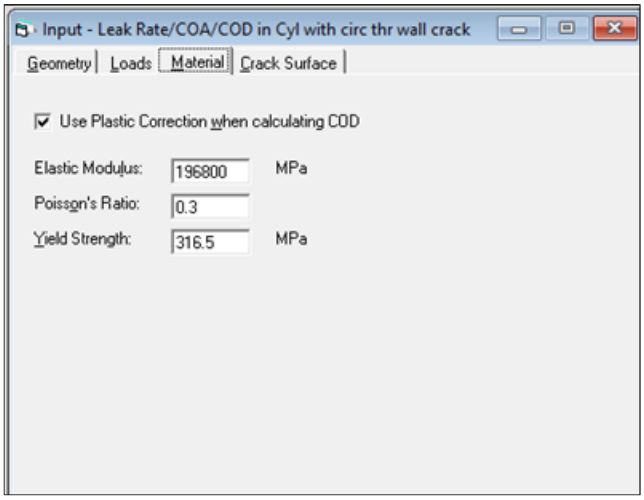

Sensitivity analyses were also conducted to study the impact of different assumptions in the analysis, i.e. the effect of elastic compared to plastic COD values and the effect of using base material properties.

Leak rate calculations were performed using WinSQUIRT Version 1.3. A built-in primary water stress corrosion cracking (PWSCC) crack morphology was used. The results from these analyses are presented in Table C.1.

Table C.1. COD values and leak rates for the baseline case

WRS NRC PWSCC morph	**Leakage flow rate (kg/s)**	**Interior COD (el-pl.) (mm)**	**Exterior COD (el-pl.) (mm)**	**Interior crack length (mm)**	**Exterior crack length (mm)**	**Mid-plane crack length (mm)**
	0	0.00	0.24	111.18	138.82	125.00
	0.153	0.04	0.39	200.00	249.73	224.86
	0.236	0.08	0.43	225.00	280.94	252.97
	0.36	0.13	0.50	250.00	312.16	281.08
	0.528	0.19	0.57	275.00	343.37	309.19
	0.568	0.20	0.59	280.00	349.62	314.81
Leak crack	0.61	0.21	0.60	285.00	355.86	320.43
	0.655	0.23	0.62	290.00	362.10	326.05
	0.753	0.25	0.65	300.00	374.59	337.29
WRS SSM PWSCC morph	**Leakage flow rate (kg/s)**	**Interior COD (el-pl.) (mm)**	**Exterior COD (el-pl.) (mm)**	**Interior crack length (mm)**	**Exterior crack length (mm)**	**Mid-plane crack length (mm)**
	0.21	0.13	0.38	200.00	249.73	224.86
	0.473	0.24	0.53	250.00	312.16	281.08
	0.556	0.27	0.56	260.00	324.64	292.32
Leak crack	0.602	0.29	0.58	265.00	330.89	297.94
	0.621	0.29	0.59	267.00	333.38	300.19
	0.652	0.30	0.60	270.00	337.13	303.57
	0.704	0.32	0.62	275.00	343.37	309.19

There had been the intention of carrying out analyses with LEAPOR (for comparison), but the version of the programme that Kiwa Inspecta could access had too many limitations and therefore it was not possible to use LEAPOR in this study (as an example, the COD at the inner diameter [ID] and outer diameter [OD] were assumed to be equal).

Leak rate as a function of the mid-wall crack length is shown in Figure C.3.

Figure C.3. Leak rate as a function of the mid-wall crack length

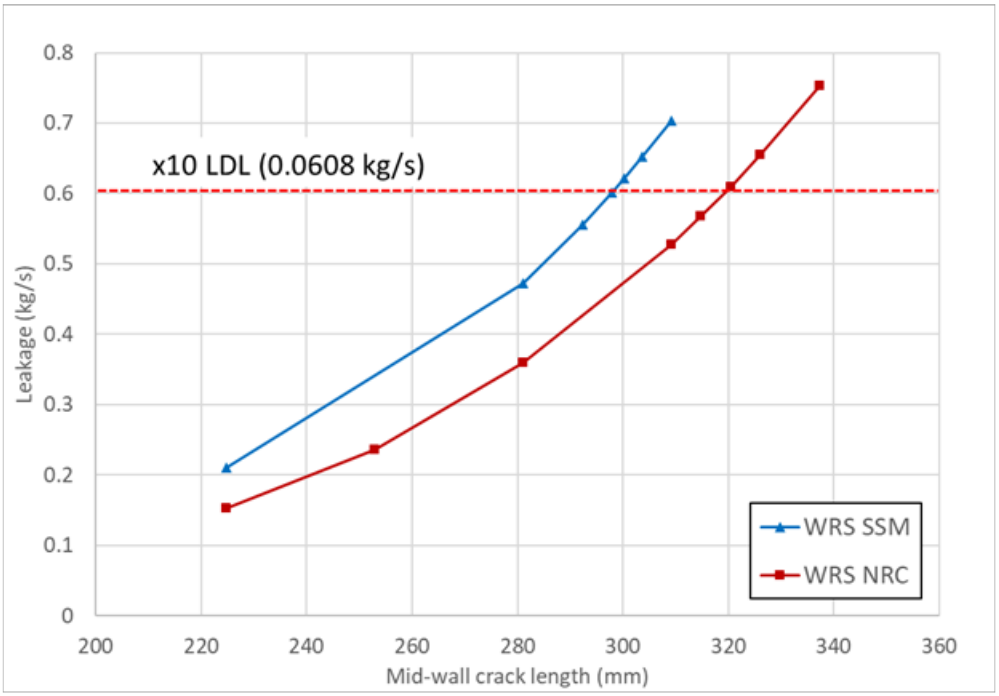

Critical crack size

A critical crack size for the normal operating conditions and safe shutdown earthquake (SSE) load was evaluated using the fracture mechanics code ISAAC, which is commonly used in the Swedish nuclear industry. Forces and moments for normal operating conditions and the SSE event were transferred into membrane and bending stresses. Figure C.4 illustrates the input of stresses (normal operation [NO] and NO+SSE) and material data.

Figure C.4. Stresses and material data used in the assessment of critical crack size

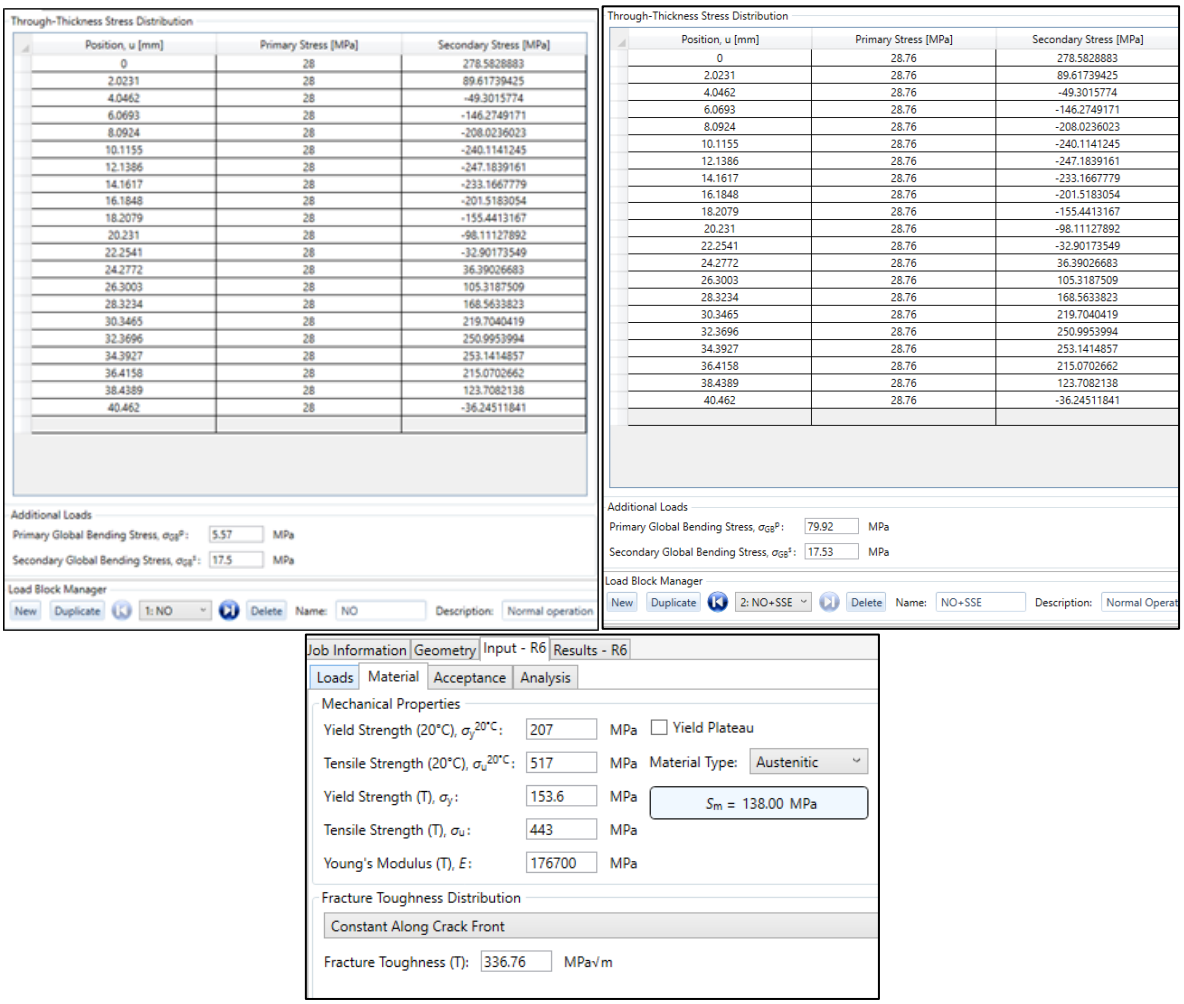

ISAAC (Integrity and SAfety Assessment of Components) has a module for the safety assessment of cracks by a procedure with a failure assessment diagram (FAD) that is based on a Swedish extension of the R6-method (as given in the SSM Report 2018:18). ISAAC also includes modules for assessment according to the American Society of Mechanical Engineers (ASME) Boiler and Pressure Vessel Code, Section XI, Appendices A and C (defects in ferritic components and in austenitic and ferritic piping). The software provides efficiency at practical analyses, for example by facilitating the following: analysis of limiting defect sizes; assessment of different types of defect in a component; analysis of crack growth; stresses from thermal transients; ductile tearing and sensitivity analyses. The implementation has been validated and verified over a long period since the first revisions of the programme were made. When conducting a LBB analysis, it must be based on the Swedish implementation of the R6 method.

When calculating a critical (or acceptable) crack size, the initiation values (K_{Ic} and J_{Ic}) should be used. However, it is considered acceptable when using the Swedish procedure to use higher fracture toughness values for very ductile materials (equivalent to a toughness value up to a maximum of 2 mm of stable crack growth, if possible). Initiation values were used in the benchmark because values including a small amount of stable crack growth was not included in the input data.

The results from this assessment are presented in Table C.2.

Table C.2. Calculated critical crack size (CCS) and comparison with the leakage crack size (LCS)

WRS	Mid-wall critical crack (mm)		Mid-wall leak crack (mm)
	NO	NO+SSE	
NRC	539.1	267.6	320.4
SSM	538.6	321.7	297.9

Acceptance check

According to the requirements in Section C.1, the margin between the calculated critical crack size and the postulated leakage crack size should be at least two. Comparing the results in Table C.2 shows how this requirement was apparently not met.

Sensitivity analysis

Most countries, including Sweden, require that CCS/LCS > 2 in order to meet the LBB requirements. When LCS = 320.4 mm, it is then necessary that CCS > 640.8 mm (given the results from KIWA). This crack is so large (more than half the circumference) that it will be difficult to meet the condition of CCS/LCS > 2.

In the baseline analysis, KIWA obtained CCS = 267.6 mm when using the tensile properties from the base material (as recommended when using the R6 method for similar problems). As a consequence, CCS/LCS = 0.835, which is the lowest value reported in this LBB benchmark study.

It may be interesting to conduct a sensitivity analysis using other tensile properties to evaluate these assumptions. KIWA's analysis used tensile properties from the base material (yield strength = 153.6 MPa and ultimate tensile strength = 443 MPa). In the sensitivity analysis presented in Figure C.5, KIWA used data up to those specified for the weld material (yield strength = 316.5 MPa and ultimate tensile strength = 542.4 MPa).

Figure C.5. Critical crack size (CCS) as a function of the tensile properties (yield strength)

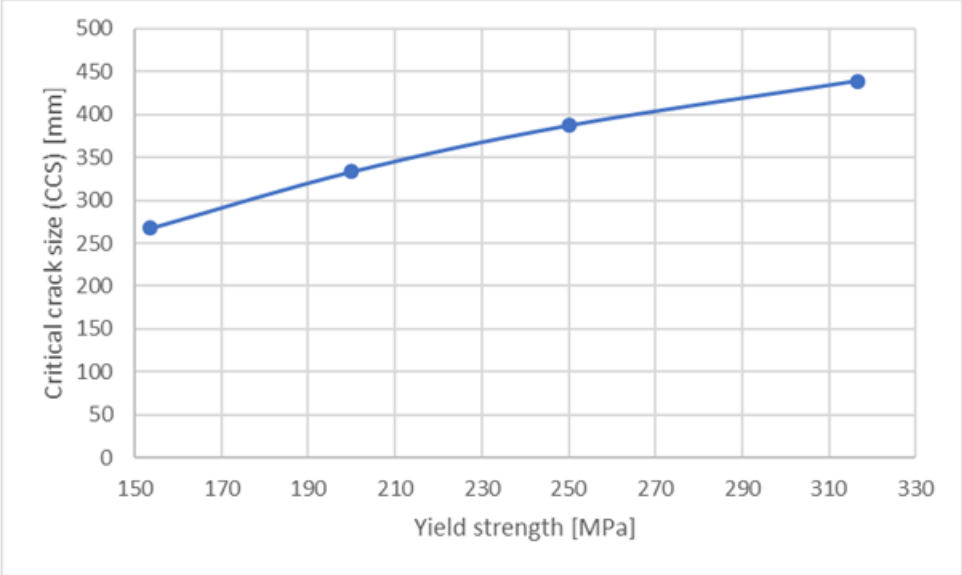

If the tensile properties from the weld material are used (which is not recommended in this case), the result is CCS = 438.5 mm and CCS/LCS = 1.37.

When calculating a critical (or acceptable) crack size, the initiation values (Kic and JIc) should be used. However, it is considered acceptable to use higher fracture toughness values when using the Swedish procedure for very ductile materials (equivalent to a toughness value up to a maximum of 2 mm of stable crack growth, if possible). Using the provided data for the baseline case, Jmat_2mm can be estimated to be 1 451 kN/m. As a result, CCS = 503.6 mm and CCS/LCS = 1.57. Finally, using a Jmat-value equivalent to 10 mm of stable crack growth produces CCS = 526.8 mm (CCS/LCS = 1.64).

This sensitivity analysis indicates that it is impossible to fulfil the LBB requirements, regardless of the material data used in the analysis (tensile properties and fracture toughness).

A similar problem arises in the analysis of the critical bending moment (CBM). For the baseline case, KIWA obtained CBM = 361 kNm, which is also the lowest value reported in this study. Using the tensile properties from the weld material (which is not recommended) results in CBM = 679 kNm. Using higher fracture toughness values (including 2 mm of stable crack growth) results in CBM = 756 kNm. An analysis must be carried out that considers the complete J-resistance curve in order to obtain CBM > 1 000 kNm (as reported by some participants). However, the instability point corresponds to such a large proportion of stable crack growth that the results end up being far beyond what is normally measured during J-R testing. This cannot be accepted in a LBB analysis when using the Swedish LBB procedure.

Task 1-4 analyses

Followed by the baseline problem, the analyses of Task 1-4 were conducted. The influence of WRS was again considered, as well as the distributions in Figure C.1. Two additional Tasks were therefore introduced: Task 2a for corrosion fatigue with the WRS SSM and Task 4a for PWSCC with the WRS SSM.

The calculation procedure was similar to the one used for the baseline problem. COD values with plastic correction were calculated for a mid-wall crack length of 125 mm. WinSQUIRT v. 1.3 was used for the leak rate calculations. The user-defined crack morphology was enabled to input the crack morphology parameters given by the NRC. The summary of all analyses is presented in Table C.3.

Table C.3. Summary of results for Task 1-4

Task	Degr. Mech.	WRS	Mid plane crack length [mm]	Interior COD [mm]	Exterior COD [mm]	Leakage flow rate [kg/s]
1	Corrosion fatigue	No WRS	125	0.0651	0.0973	0.026
2	Corrosion fatigue	NRC	125	0	0.2374	0
2a	Corrosion fatigue	SSM	125	0.0218	0.1985	0.037
3	PWSCC	No WRS	125	0.0651	0.0973	-
4	PWSCC	NRC	125	0	0.2374	0
4a	PWSCC	SSM	125	0.0218	0.1985	-

The COD value on the inside was zero for Task 2 and Task 4 (WRS according to NRC). In these cases, the leakage flow rate was assumed to be zero. The probable cause was the influence of compressive stresses (WRS) that can impact shorter cracks. A leakage flow greater than zero was obtained for longer cracks.

WinSQUIRT reported a very tight crack for Task 3, 4 and 4a (PWSCC). The activation of the option “Improved model for crack morphology parameters on COD” was required for the analyses to be carried out. However, this option should not be activated according to the prerequisites for this study and therefore no results can be reported.